SYNTHESIS, CHARACTERIZATION, ANTIMICROBIAL STUDIES AND CORROSION INHIBITION POTENTIAL OF 1,8-DIMETHYL-1,3,6,8,10,13-HEXAAZACYCLOTETRADECANE

by

HENRY UDOCHUKWU NWANKWO

B.Eng. (ESUT), B.Sc (Hons) (NWU)

A Dissertation submitted in fulfilment of the requirements for the Degree of

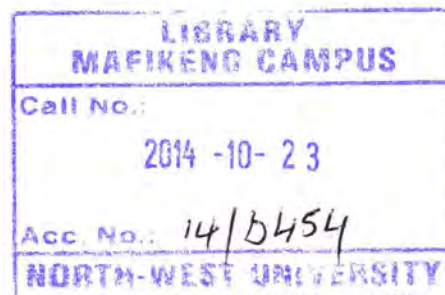Master of Science (Physical Chemistry)

in the

Department of Chemistry

Faculty of Agriculture, Science and Technology,

North-West University (Mafikeng Campus)

Supervisor: PROF. D.A. ISABIRYE

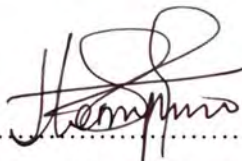**Co-Supervisor: PROF. E.E. EBENSO**

JULY 2014

DECLARATION

"I hereby declare that this Dissertation for the degree of Master of Science, at the North West University hereby submitted, has not been previously submitted by me for a degree at this or any other university.

The following research was compiled, collated and written by me. All the quotations are indicated by appropriate punctuation marks. Sources of my information are acknowledged in the reference pages".

....

HENRY UDOCHUKWU NWANKWO

ACKNOWLEDGEMENTS

ABSTRACT

The synthesis of 1,8-dimethyl-1,3,6,8,10,13-hexaazacyclotetradecane ligand was carried out by the demetallation of the prepared 1,8-dimethyl-1,3,6,8,10,13-hexaazacyclotetradecanenickel(II) complex. The characterization of the ligand and the nickel (II) complex was carried out using the UV-Vis, FT-IR, EDX, MS, NMR and TGA techniques. The structure was confirmed by the methods used and the TGA showed the mode of thermal stability and decomposition. The ligand displayed three steps losses upon dynamic heating at 1200 °C. The biological activity of the ligand against two bacterial strains namely *Staphylococcus aureus* and *Enterococcus* species was also studied. The result shows the ligand to be potentially active towards the bacterial strains. The corrosion inhibition potential of the ligand was studied using Potentiodynamic polarization (PDP), electrochemical impedance spectroscopy (EIS) and cyclic voltammetry (CV). The PDP and EIS showed that the %IE increases as the concentration increased. The CV provided insight into the kinetics and the effect of scan rate on peak currents. The ligand was found to be a mixed-type inhibitor. The phenomenon of chemisorption mechanism was proposed from the thermodynamic parameters obtained. The experimental result fits the Langmuir adsorption isotherm.

LIST OF ABBREVIATION

MS	Mild Steel or Mass spectrophotometry
RTIL	Room Temperature Ionic Liquids
SCC	Stress corrosion cracking
IE	Inhibition Efficiency
MIC	Microbial Corrosion
IL	Ionic Liquid
DS	Designer Solvents
XDR	Extensively Drug-Resistant
PDR	Pan Drug-Resistant
MDR	Multi-Drug Resistance
Kads	Adsorption equilibrium constant
SDFP	Salicylaldimine containing formaldehyde and piperazine moieties
EDX	Energy Dispersive X-ray
XRD	X-ray Diffraction
FT-IR	Fourier Transform Infrared
SEM	Scanning Electron Microscopy
UV-Vis	Ultraviolet Visible
ZPC	Zero Charge Potential
OCP	Open circuit potential
CPE	Constant phase element
FRA	Frequency Response Analyser
KPC	*Klebsiella Pneumoniae Carbapenemase*
SFP	*Staphylococcal* Food Poisoning
MBI	2-Mercapto Benzimidazole

MTAH	Tetramethyl-dithia-octaaza-cyclotetradeca-hexaene
KI	Potassium iodide
TGA	Thermo-gravimetrical analysis
PDP	Potentiodynamic polarization
CV	Cyclic voltammetry
PBS	Phosphate Buffer Solution
EIS	Electrochemical impedance spectroscopy
HCl	Hydrochloric acid
DNA	Deoxyribonucleic acid
RNA	Ribonucleic acid
S. aureus	*Staphylococcus aureus*
E.coli	*Escherichia coli*
B. subtilis	*Bacillus subtilis*
P. aeruginosa	*Pseudomonas aeruginosa*
S. typhi	*Salmonella typhi*

LIST OF FIGURES

LIST OF TABLES

TABLE OF CONTENTS

CHAPTER 1

INTRODUCTION

1.1   MACROCYCLIC COMPOUNDS

Gerbelue *et al*[1] defined macrocyclic compounds as cyclic molecules comprising of nine or more atoms in their ring of which at least three are electron pair donors. Macrocycles are very important and useful cyclic molecules mostly consisting organic frames into which heteroatoms, capable of chelating to substrates, have been interspersed.[2] They fall under one of the major categories of inorganic chemistry known as coordination chemistry that is concerned with the probing of the structures, properties and reactions of these macrocyclic ligands when coordinated to a transition metal centre.[2] Macrocyclic ligands have received reasonable attention for many years owing to some characteristic unique properties provided by the macrocyclic environment. These include extremely high thermodynamic stability, the ability of the central metal to exist in unusual oxidation states and their ability to mimic naturally occurring macrocyclic molecules in their structural and functional features.[3-4] Common examples of synthetic macrocycles are aza, oxa, thia, and phospha whereas few naturally occurring macrocycles include cyclodextrins, porphyrins, corrins, chlorins, corphins and phthalocyanins. Since the inception of the first synthetic macrocycle, 1,4,8,11-tetraazacyclotetradecane in 1936, development of macrocyclic chemistry has predominantly undertaken the following routes;[2]

1. As models to mimic the naturally occurring macrocycles containing mostly nitrogen donor atoms;

2. As receptors synthesized for significant recognition characteristics and supramolecular chemistry.

The following specific terms and expressions widely used in literature surveys and are relevant to this work include;[1]

- **Template centre**. The metal ion which can orientate and activate the ligand for their subsequent interaction.

- **Template bonds**. Forces by means of which the corresponding template orients and/ or activates the reacting ligands, organising their preparation for the reaction.

- **Ligand synthon or ligson.** A polyfunctional, usually chelating ligand that forms part of all the assemblage reactions at the template centre.
- **Chelant (chelator).** The open-chain ligand which occupies various coordination sites in the inner sphere of the template centre.
- **Template information.** The totality of coordinative-stereochemical characteristics of the template centre which prepares a definite spatial arrangement of ligsons.

Over the past decades, the scientific community has shown considerable interest in macrocyclic compounds due to their potential applications in biological systems, magnetochemistry, medicine, technology, chemical sensors, precursors to new conducting materials, ladder polymers, dyes and also as catalysts.[4,5-6] Transition metal macrocyclic complexes which usually contain nitrogen, sulphur or oxygen as donor ligand atoms are becoming increasingly important because these Schiff bases can bind with different metal centres involving various coordination sites[7-9] and allow for successful synthesis of metallic complexes with interesting stereochemistry.[5,7] Most nitrogen containing macrocyclic compounds make up an enormous part of chemical compounds which form part of many natural products, fine chemicals and biologically active pharmaceuticals needed to enhance the quality of life.[9] As a result, they have found usage in numerous biological activities. These include antifungal,[10-13] antibacterial,[5,12-13] hypolipidemic,[14] anticancer,[15] antihistaminic,[16] analgesic,[17-18] antitubercular,[19-20] anticonvulsant,[21] anti-inflammatory,[17-18,22] anti-tumour,[10] and anti HIV agents.[23]

Heterogenization of homogenous catalysts due to site isolation effect remains an interesting field of study.[24] Most homogenous transition metal complexes have been found to exhibit significant catalytic properties although their heterogenization has remained an environmental and toxicological challenge. Copper(II) complexes of 14-membered hexaaza macrocyclic ligands encapsulated in zeolite are among the newer heterogeneous oxidation catalysts attracting interest.[24]

Macrocyclic dicopper(II) compounds have been found to exhibit strong antiferromagnetic interactions and are capable of undergoing two-step redox couples.[25]

Three general methods of preparing macrocyclic compounds were given by Nelson,[26] and these include metal template synthesis, complexation method and synthesis involving modification of the macrocyclic ligand and/ or the metal ion.

1.1.1   Metal template synthesis and stability of macrocycles

Metal template effect came into limelight as a tool in the synthesis of new macrocyclic compounds by the pioneering work of Busch.[1] According to Gerbeleu *et al*,[1] template effects result when the metal ion serves as a pattern for forming, using appropriate building blocks, reaction products whose synthesis are often difficult or totally impossible under certain reaction conditions.

Metal template synthesis offers high-yielding and selective routes to new ligands and their complexes.[3] Template effect may arise from the stereochemistry imposed by metal ion coordination of some of the reactants, promoting a series of controlled steps which provides routes to products that do not form in the absence of metal ions.[3] Template effect is a term that suggests that the metal coordinates the ligand precursor fragments in its coordination sphere, thereby enhancing the process that gives rise to the macrocyclic ligand.[2] Template effect arose from the fact that most macrocyclic ligands can only be made in low yields, or not at all, in the absence of metal ions. One of the merits of metal template synthesis over other methods is that most often, it results to the appearance of additional metallocycles and may lead to the tailoring of these metallocycles.[1] The use of template synthesis offers a reliable and efficient strategy for the synthesis of macrocyclic compounds with nitrogen donor atoms, crown ethers and other useful cyclic systems that contain heteroatoms. In contrast to synthesizing macrocyclic compounds by non-template procedures, the probability of formation of the cyclic products is significantly lowered due to a decrease in entropy of the condensing fragments.[1]

Most complexes with chelating ligands are known to exhibit higher stability in relation to monodentate ligands, and even higher stability when the donor atoms are incorporated into a cyclic ligand that surrounds the metal ion.[2,8] Macrocyclic complexes are highly stable than their open-chain analogues with similar structure, and this stability is often referred as macrocyclic effect.[1] Most products of template transformations depend on the kinetic and thermodynamic stability of all the precursors participating in the equilibria. At each reaction step, either thermodynamic or kinetic parameters play the key role, however, it is only one of them that prevails in the overall reaction.

There has been significant development in two areas of complexation in recent years with regard to synthetic macrocycles.[3] Those containing heteroatoms such as arsenic, nitrogen, phosphorous and sulphur that form conventional covalent coordination complexes with transition metal ions. The second comprises of the recently evolving chemistry of polyammonium macrocycles that tend to form different complexes with anionic substrates.[2]

Most of the oxygen-derived macrocycles are well known for their complexation with organic cations, molecular substrates, alkalis and alkaline earth metal ions.[2]

1.1.2 The complexation method[26]

This method has been employed in the synthesis of complexes containing cyclic polyethers, cyclic tetramines and macrobicyclic ligands. The method involves a reaction between the metal ion and presynthesized ligand in solution. It is a useful technique as it allows the ligand to be isolated, purified and characterized before the complexation. The main disadvantage of complexation method is that it often results to in low yields of the desired product.

1.1.3 Modification of ligand and/ or metal ion[26]

In this method, either the metal ion or the ligand or both is modified during the synthesis. Since most macrocyclic complexes are kinetically inert to ligand substitution, the role the metal ion could play in coordinated ligand synthesis becomes important.

1.2 CLASSIFICATION OF MACROCYCLIC COMPOUNDS

Various classifications based on the unique features of macrocyclic compounds have been suggested in a number of surveys. For the purpose of this study, one given by Gerbeleu et al[1] would be exploited. This classification is based on the nature of donor atoms and the ability of the corresponding macrocyclic compounds to form complexes. In the light of this, the two classifications are discussed in detail under the following headlines;

1.2.1 **Denticity of the ligand**. This is further subdivided into the following classes;

1.2.1.1 Mononucleating macrocyclic ligands that form complexes with one metal ion. Examples include bidentate, tridentate, tetradentate, pentadentate and hexadentate macrocyclic ligands.

1.2.1.2 Bi-and polynucleating macrocycles which are capable of chelating to two or more ions within the macrocyclic systems. These include binucleating or compartmental (i.e. one with one common macrocycle), trinucleating (i.e. one with one common macrocycle), tetranucleating (i.e. one capable of forming a cubane core) and pentanucleating species.

1.2.2 **Nature of donor atoms**. This is further classified into:

1.2.2.1 Macrocycles consisting donors of one type. Examples include polyarsamacrocycles, cyclotriynes, polyazamacrocycles, polythiamacrocycles, polyoxamacrocycles and polyphoosphamacrocycles.

1.2.2.2 Macrocycles consisting two types of donor atoms such as polyazapolythiamacrocycles, polyazapolyphosphamacrocycles, polyazapolyoxamacrocycles and polyoxapolythiamacrocycles.

| (a) | (b) | (c) | (d) |
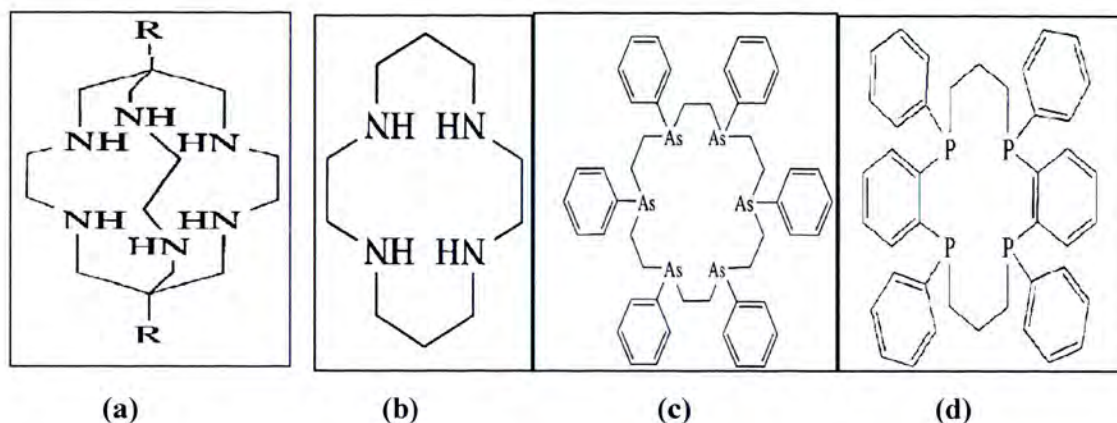
Figure 1.1. Common structures of some macrocyclic compounds

    a.   Sepulchrate

    b.   Cyclam

    c.   Polyarsa

    d.   Polyphospha

Fully saturated macrocyclic complexes consisting of six nitrogen atoms are considerably uncommon.[27,7] Attempts have been made to study the coordination geometry and characteristics of numerous transition metal complexes of 14-membered macrocyclic ligands, however, most of them were tetraaza macrocyclic ligands.[28] Few attempts have, however been made towards the application or use of a 14-membered hexaaza macrocyclic ligand in corrosion and anti-microbial studies. One way of achieving this is by demetallating metal complex to yield the ligand which can then be studied for its corrosion inhibitive and antibacterial characteristics against bacterial strains.

1.3   NOMENCLATURE OF MACROCYCLES[2,26]

Due to increase in number and complexity of macrocycles, a systematic method of abbreviations rather than lengthy names was developed by Busch.[29] Busch prescribed the following rules and guidelines for naming macrocycles;

1.3.1   The size of the macrocyclic ring is denoted by an Arabic number enclosed in square brackets e.g. [14], and [16].

1.3.2   This is preceded by a term denoting unsaturation (if any). If no unsaturation is present, the term 'ane' is used. When unsaturation occurs, the usual nomenclature terms e.g. 'ene', 'triene' etc are used.

1.3.3   Hetero or ligating atoms are identified after the unsaturation designation and expressed using their element symbols. In the presence of more than one heteroatom, the atoms are expressed alphabetically. The number of each kind of heteroatom is expressed by a subscript, whilst its position is shown as preceding locant. Non ligating heteroatoms are expressed in parenthesis after the ligating heteroatoms in the same manner as above.

1.3.4   The numbering scheme employed in naming macrocycles begins with a heteroatom of higher priority, namely, one that occurs earliest in the following list O, S, Se, N, P, As, Sb etc and proceeds in either direction so that;

- the lowest set of locants for heteroatoms is obtained e.g. 1,2,4 is lower than 1,4,6;
- the heteroatoms of highest priority have lowest locants and
- sites of unsaturation have lowest locants.

1.3.5   Common substituents attached to a simple macrocyclic compound are cited in front of the macrocycle in order conforming to the numbering order and preceded by standard abbreviations such as Me for methyl, Et for ethyl, Bzl for benzyl, Bz for benzoyl, Ph for phenyl. Other substituents may be expressed by usual formula names or representations, such as oxo, -COOH etc.

1.3.6   Stereoisomers of a macrocyclic compounds are cited by using the symbols 'ms', 'meso' and 'sac' for racemic; these symbols are applied to the orientation of substituents in equivalent positions and are identified using locants in parenthesis. Other substituents apart from hydrogen at these positions are identified using rule 1.3.5 above. It is a recognized fact that the definitions of such terms as meso and racemic is not in line with the IUPAC nomenclature rules, however, the practice of using them has continued.

1.3.7   Anionic macrocyclic ligands are cited by the addition of 'ato' to the abbreviation followed by the charge prescribed by Ewens-Basset number. Designation of charge is not used for metal complexes with metal in common oxidation states and where charge can easily be determined from the type and number of counter ions.

1.3.8   Rings of macrocyclic ligands fused to the macrocycle are cited as substituents to the macromonocycle even if attached at more than two points by using locant sets to describe the point of fusion. These substituents may be designated by abbreviations such as 'bzo' for

benzo, 'pyo' for pyridine etc., whereas unsaturation common to both the fused ring and macrocyclic ring is included in the abbreviations as described in rule 1.3.2.

1.4 ANTIMICROBIAL RESISTANCE IN MICROORGANISMS AND THE SEARCH FOR ALTERNATIVE AGENTS

Antibiotics are therapeutic agents that typically target structures and pathways that are unique and important to bacteria such as the cell wall, DNA, RNA and protein synthesis machinery, and also intermediary metabolism.[30] The treatment of infections caused by microorganisms is usually achieved through the administration of antibiotics. Some organisms tend to resist the action of particular antibiotics and are termed resistant strains.[31] French[31] described antibiotic resistance as the tendency for antibiotic use to promote the emergence of resistant pathogens. Therefore the emergence of drug resistant strains is known to complicate the management of infections in humans.[32] Different antimicrobial agents that are used for the treatment of infections in humans possess different modes of action against microorganisms.[30] In addition, different microorganisms display different strategies to escape destruction by the antimicrobial agents. The modes of action and resistance mechanisms for some selected antibiotics are shown in Table 1.1.

Table 1.1. Antibiotics, modes of action and mechanisms through which bacteria evade destruction.

Antibiotic Group	Examples	Target	Active against G+	Resistance mechanism
B-Lactams[a]	Ampicillin	[a]Cell wall synthesis. Inhibitor-act on penicillin binding proteins (PBP)	√	Penicillin-G impermeable to G- Mutation in PBPs. Produce ß-Lactamase
Aminoglycosides	Gentamycin Kanamycin Streptomycin	Bind to 30S subunit of ribosomes- inhibit protein synthesis	√	Aminoglycosides modifying enzymes. Fluz mechanisms RNA modifications
Tetracyclines	Tetracycline	Bind to 30S subunit of ribosomes- inhibit protein synthesis	√	Efflux mechanisms 16S mutations
Chloramphenicols	Chloramphenicols	Bind to 30S subunit of ribosomes- inhibit protein synthesis	√	Efflux mechanisms inactivation by enzymes
Quinolunes	Nalidixic acid	Inhibit DNA gyrase synthesis	√	Inhibit the microbial enzyme, DNA gyrase and thus blocks chromosomal replication
Glycopeptides	Vancomycin	Cell wall synthesis inhibitor	√	Binds to D-anyl-D-alanine, inhibit transfer of linear glycan acceptor to the N-acetylmuramypentapeptide-N-acetyglucosamine
Sulfamethoxazole	Sulfamethoxazole	Inhibit normal bacterial utilization of para-aminobezoic acid (PABA) for the synthesis of folic acid, an important metabolite in DNA	√	Over production of p-aminobenzoic acid by enzyme.

G+ = Gram positive: (Hitchings[f])[33] (Mingeot-Leclercq *et al*[b])[34] (Capitano *et al*[a-f])[35] (Kernodle[a])[36] (Connell *et al*[c])[37]

Faced with microbial resistance problems there is need to look for alternative agents that could have potential antimicrobial properties.[38] Macrocyclic ligands are attracting increasing attention due to the presence of nitrogen heteroatoms,[5,9] aromatic rings and large number of functional adsorption sites (e.g.–NH$_2$ group).[39] All these characteristics suggest an enormous role macrocyclic ligands could play as antimicrobial agents.

Drug resistance to the presently available classes of antibiotics has become a worldwide medical problem[40] and therefore the need to design novel antibiotic agents is pertinent. The danger posed by highly pathogenic microorganisms has remained a serious global problem in several areas such as food storage, water purification systems, hospitals, dental surgery equipments, medical devices, drugs, food packaging, textiles and hygienic applications.[40]

Staphylococcus aureus is considered the most pathogenic species within the genus *Staphylococcus* and isolates belonging to the species are widely distributed in the environment.[41-42] These organisms occur as normal flora in humans and animals.[40] Despite this, *S. aureus* strains have been reported to cause numerous syndromes and life threatening infections in humans and animals.[42-44] Infections caused by *S. aureus* range from mild skin infections, bacteraemia, systemic diseases, osteomyelitis to the more complicated toxic shock syndrome and staphylococcal food poisoning (SFP).[45] These syndromes account for a large proportion of morbidity and mortality reported worldwide.

Despite the fact that some of these infections are self-limiting, it is important to ensure that proper public health procedures are enforced to limit transmission to humans. Given the fact that the ability of this organism to develop resistance is mediated through mutation and by DNA transfer,[30,42] *S. aureus* strains may also acquire antibiotic resistance traits by changing the function of certain genes or obtaining new genes.[30] In addition, the ability to adapt to varying environmental conditions is known to also enhance its pathogenicity and multi-drug resistant potential.

Johnston *et al*[46] described *Enterococcus* species as ubiquitous, commensal inhabitants found in the gastrointestinal tract of humans and animals. They are mostly present in environment contaminated by human and animal faecal materials such as farmlands where animal dungs are used as fertilizers, urban sewage and in food products of animal origin.[47]

Over the past decades, *Enterococcus* species (*Enterococcus faecium* and *Enterococcus faecalis*) have grown in importance due to the emergence of multi-drug-resistant strains estimated to be responsible for twelve percent of all nosocomial infections in the United

States.[46] Although this figure keeps increasing substantially, trends in their resistance to key antibiotics remain sketchy.[45]

1.5   CORROSION STUDY

Fontana[48] defined corrosion as the deterioration of materials as a result of reaction with their environment. In iron, corrosion starts with the oxidation to ferrous (Fe^{2+}), followed by the oxidation of ferrous ions to ferric ions (Fe^{3+}), then the reduction of oxygen and finally the reaction of ferrous ions and oxygen. The corrosion of metals in acid solutions can be inhibited by a wide variety of substances, such as halide ions, carbon monoxide, and many organic compounds, particularly those containing elements of Groups V and VI of the periodic Table (i.e., nitrogen, phosphorous, arsenic, oxygen, sulphur, and selenium).[49-51] Studies have revealed that organic compounds containing nitrogen or sulphur atoms are superior corrosion inhibitors compared to those containing nitrogen or sulphur alone.[51] Presently, common inorganic corrosion inhibitors are mostly crystalline salts of sodium chromate, molybdate and phosphate, dyes and naturally occurring substances such as Azadirachta indica leaves extract.[52] It is only the anions of these compounds, however, that are involved in reducing corrosion in metals.[53]

Corrosion ultimately results in the formation of rust (ferric oxide), $2Fe_2O_3.\chi H_2O_{(S)}$[52] Metal oxide or rust poses a great threat to many industries in the world and is detrimental to the environment and a host of materials such as metals, polymers and ceramics. The common menace caused by corrosion can be seen on the bottle tops of most alcoholic and non-alcoholic beverages which constitute a serious health hazard to end users.[52]

Figure 1.2. Photo showing effect of corrosion

1.5.2 Effects of corrosion

In line with this, the following adverse effects of corrosion are worth mentioning;

- Loss of aesthetic properties and mechanical properties such as tensile strength of the corroding materials.
- Polluted environment due to corroding materials.
- High toxicity levels of natural resources such as water systems.
- Direct impact on the economies of countries since metallic materials are used in many industries like petrochemical and food processing industries. Lots of money is lost by the affected industries through replacement and maintenance of corroding materials. Many jobs may be put at risk.
- Foods security will be put at risk since metallic objects such as cups, plates and corrugated iron sheets are part of human lives. Corroded cups and plates may contaminate their contents, which may cause health associated problems.

As a result of these adverse effects, corrosion remains a serious global challenge and billions of dollars is lost annually to corrosion related problems.

1.5.3 Types of corrosion

For the purpose of this study, the following types of corrosion will be highlighted:

Pitting corrosion: This type of corrosion takes place as microscopic defects on a metal surface.

Inter-granular corrosion: Here, the grain boundaries of a substance are attacked perhaps by a strong acid.

Concentration cell corrosion: This is when two or more metals are allowed to come into contact with different concentrations of the same solution.

Uniform corrosion: Also referred to as general corrosion and connotes the corrosion resulting from direct chemical attack on the material.

Galvanic corrosion: Resulting from two different metals being in contact under electrochemical action.

Stress corrosion cracking: Abbreviated as SCC resulting from simultaneous effects of stress and the environment.

Refinery corrosion: This is the type of corrosion that results from the equipment surface that has been attacked by a strong acid.

Corrosion in concrete: Often occurring on concrete- steel reinforcements where the carbon steel corrodes.

Microbial corrosion: Also abbreviated as MIC is caused by the activities of microbes.

1.6   PROBLEM STATEMENT

In relation to studies done elsewhere, it is clear that providing a possible route for the demetallation of 1,8-dimethyl-1,3,6,8,10,13-hexaazacyclotetradecanenickel(II) would be a useful field of study.

Further developing viable antibiotics using a 14-membered hexaaza macrocyclic ligand that would replace the current drug resistance classes of antibiotics would be important.

The presence of six nitrogen atoms at the equatorial positions of 1,8-dimethyl-1,3,6,8,10,13-hexaazacyclotetradecane ligand and its inherent thermal and kinetic stability, point to their potential for use as corrosion inhibitors. Presently few attempts towards the use of a 14-membered hexaaza macrocyclic ligand in corrosion studies have being reported.[54]

Rust (ferric oxide), remains a serious global challenge affecting industries, environment, humans and host of materials such as metals, polymers and ceramics. Study on the possible use of a 14-membered hexaaza macrocyclic ligand as corrosion inhibitors would be necessary.

1.7   AIM AND OBJECTIVES OF THE STUDY

1.7.1   Aim of the study

The main aim of the study was to identify a possible route for the demetallation of Ni^{2+} from its hexaazacyclotetradecane complex, determine the effectiveness of the ligand to act as a corrosion inhibitor of mild steel in acidic medium and also study its antimicrobial activity.

1.7.2   Objectives

The objectives of the study were;

(a)   To synthesize 1,8-dimethyl-1,3,6,8,10,13-hexaazacyclotetradecanenickel(II) (by the template condensation of ethylenediamine, formaldehyde, and methylamine);

(b)   To characterize the metal complexes obtained using FTIR, EDX, MS, ^{1}H-NMR, ^{13}C-NMR and UV-Vis spectrophotometry;

(c)   To demetallate the metal complexes and to characterize the free ligand obtained using FTIR, EDX, MS, ^{1}H-NMR, ^{13}C-NMR and UV-Vis spectrophotometry; test thermal stability of the free ligand using thermogravimetric analysis (TGA);

(d) To test the free ligand ability to act as an antibacterial agent against bacteria isolates and as a corrosion inhibitor for mild steel;

(e) To evaluate the antibiotic resistance profiles of isolates using the selected free ligand;

(f) To employ electrochemical techniques such as potentiodynamic polarization, electrochemical impedance spectroscopy and cyclic voltammetry to study the synthesized ligand and

(g) To propose the possible type of adsorption and adsorption isotherm for corrosion inhibition of the ligand on mild steel.

1.8 SIGNIFICANCE OF THE RESEARCH PROJECT

The corrosion of metals in acid solutions can be inhibited by a wide variety of substances, such as halide ions, carbon monoxide, and many organic compounds, particularly those containing elements of Groups V and VI of the periodic Table (i.e., nitrogen, phosphorous, arsenic, oxygen, sulphur, and selenium).

Few attempts have been made towards the application or use of a 14-membered hexaaza macrocyclic ligand in corrosion studies. Furthermore, an attempt to separate this ligand from its metal complexes by treating the complexes with excess sodium cyanide, hydrogen sulphide gas, or strong acid was unsuccessful.

Providing a novel antibacterial agent that could replace the drug-resistant available class of antibiotics has remained an interesting field of study for decades.

Probing the role this novel macrocyclic ligand could play as an efficient, reliable and cost-effective solution for corrosion control would be more fascinating.

CHAPTER 2

LITERATURE REVIEW

2.1   LITERATURE REVIEW

Metal ions are essential for biological functions.[55] Nickel remains an important element in biological systems in that it is a building block of certain enzymes such as methyl-S-coenzyme M reductase, hydrogenase, urease and carbon monoxide dehydrogenase (CODH).[56]

The complex, 1,8-dimethyl-1,3,6,8,10,13-hexaazacyclotetradecane nickel(II) with molecular formula $[Ni(C_{10}H_{26}N_6)]$ is isostructural with its copper analogue.[57] The 14-membered hexaazacyclotetradecane macrocycle belonging to aza family binds in a chelating fashion to the Ni atom via its four secondary N atoms (Figure 2.1). The Ni(II) is coordinated by four N atoms at the equatorial positions, resulting in a square-planar geometry. The molecule has inversion symmetry with the Ni(II) ion located at the inversion centre.[7]
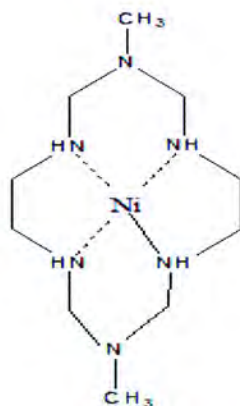
Figure 2.1. 1,8-dimethyl-1,3,6,8,10,13-hexaazacyclotetradecanenickel(II) complex

2.1.1   Synthesis and characterization of hexaaza macrocyclic complexes

Ballester *et al*[58] investigated hexaaza macrocyclic nickel and copper complexes and their reactivity with tetracyanoquinodimethane. Their study revealed that the macrocycle can host further two smaller metal ions due to the large cavity of the macrocycle.

Synthesis and characterization of 14-membered hexaaza macrocycle nickel(II) encapsulated complexes in zeolite was described by Niasari.[59] Studies on synthesis and characterisation of

a macrocyclic nickel complex with the molecular formula $Ni(C_{32}H_{26}N_4)$ and its macrocyclic ligand were done by Park et al.[60] The infrared spectra of the coordinated and free ligand revealed a major decrease in the C=N stretching mode. The decrease in frequency and in the intensity of these modes revealed that a metal atom is coordinated to nitrogen. The synthesis and spectra properties of nickel(II) complexes of 14-membered hexaaza macrocycles was reported by Suh et al.[7] A single absorption band was observed around $3200cm^{-1}$ on the IR spectra and was attributed to v(N-H) of the secondary amines. A single broad absorption band of $3200cm^{-1}$ on the IR spectra of a nickel(II) complexes of 16-membered hexaaza macrocycle was reported by Niasari et al.[28] Park et al[60] studied the reactions, synthesis and characterization of a macrocyclic nickel complex of the molecular formula $[Ni(C_{32}H_{26}N_4]$. The infrared spectrum of the nickel complex showed an absorption band at $3210cm^{-1}$ due to v(N-H) stretching.

Suh et al[7] synthesized, characterized and reported the Ni(II) and Cu(II) complexes of the 14-membered hexaaza macrocycles 1,8-dimethyl-1,3,6,8,10,13-hexaazacyclotetradecane and 1,8-diethyl-1,3,6,8,10,13-hexaazacyclotetradecane via template condensation of ethylenediamine, formaldehyde, and alkylamines. The infrared spectra of both the Cu(II) and Ni(II) complexes showed a single absorption around $3200cm^{-1}$. This was attributed to N-H stretching vibration of the coordinated secondary amines. The electronic spectra of the Ni(II) complex were comparable to those of square-planar Ni(II) complexes with saturated tetraaza macrocycles. ^{1}H NMR spectra of the Ni(II) complex revealed a very broad peaks in D_2O whilst ^{13}C NMR revealed three carbon peaks.

The work done by Niasari et al[24] on synthesis and characterization of Cu(II) complexes of 14-membered macrocyclic ligand in zeolite encapsulated nanocomposite materials suggested that the infrared bands of Cu(II) complex in zeolite shifted within $20cm^{-1}$ from the free complex. The infrared spectra of Cu(II) complex in zeolite was observed in the region of $3230cm^{-1}$ and was assigned due to N-H stretching vibration.

Wickenden et al[56] investigated the complexes of nickel(II) with acetonitrile and the coordination of perchlorate ion in these compounds. In their work, they established that perchlorate was observed to enter the coordination sphere.

2.1.2   Demetallation of macrocyclic complexes

Previous work on demetallation of cobalt(III) complexes of cage hexamines of the sarcophagine type was reported by Bottomley et al.[61] The demetallation mechanism suggested the reduction of cobalt(III) to cobalt(II) form that would enable the removal of the

ligand in concentrated acid, hot aqueous solution of excess cyanide ion and at a high temperature.

Another significant contribution in this regard was done by Kumar et al[62] who stressed the importance of reduction of Cu(II) in neutral and alkaline solutions to give the π-radical anions, Cu(II)P^{-} in their study on one-electron reduction and demetallation of copper porphyrins. This was followed by conversion of the radical into a metal-free porphyrin in the presence of moderately acidic medium. In the absence of reduction route, Cu(II) porphyrins at pH 1 are stable with the loss of Cu(II) only possible in HCl concentration above $4mol.L^{-1}$. The presence of acid (H^{+}) results into the formation of [HCu(II)P] and its rapid demetallation due to the low charge and large radius of Cu(I) in comparison to Cu(II).

2.1.3   Stability of Ni(II) complex

From a kinetic point of view, many macrocyclic complexes are extremely resistant against acid dissociation. This resistance may be attributed to the fact in a macrocyclic metal complex, it is not possible to dissociate and protonate one amino group after the other in a stepwise process.[63] However, it is necessary to dissociate two amino groups of the macrocycle at the same time, a process that is known for its higher activation energy than a stepwise dissociation.[63]

When a metal is incorporated into a macrocycle, the nucleophilicity of the nitrogen is reduced due to the involvement of the lone pair electrons on $-N=$ atoms in complex formation. Like the macrocyclic ligands, the electrophilic reactions of the transition metal complexes may occur at one of the three sites of the macrocyclic, i.e. nitrogen, meso-carbon or methyl-carbon atom.[63]

2.2   DEMETALLATION ATTEMPTS OF THE Ni(II) COMPLEX

Previous attempts to separate 1,8-dimethyl-1,3,6,8,10,13-hexaazacyclotetradecane ligand from its nickel complexes by treating the complexes with excess sodium cyanide, hydrogen sulphide gas, or strong acid have been unsucessful.[7] This enhanced stability is almost entirely due to a more favourable enthalpy. This results from the decreased ligand solvation of the macrocycle, which has less H-bonded water to be displaced in the complex-formation process.[63]

Macrocyclic ligands exhibit macrocyclic effects which can be categorized as thermodynamic and kinetic effects. The thermodynamic macrocyclic effect is a stronger binding constant (logβ) for a macrocyclic ligand compared to an analogous open-chain ligand equation (1).[63-64]

Macrocyclic effect $= \Delta \log\beta = \log\beta_{macrocycle} - \log\beta_{open-chain}$ (1)

Furthermore, stepwise removal of the donor atoms is practically impossible because the macrocyclic ring lacks a "free end", thus resulting into a relatively slow dissociation rate of macrocyclic ligands from their complexes (kinetic macrocyclic effect).[63]

2.3 ANTIMICROBIAL ACTIVITY OF METAL COMPLEXES

It is well documented that most drugs exhibit enhanced antimicrobial activity when prescribed as metal complexes.[65-71] A study that focused on the antimicrobial activity of Cu(II), Ni(II) and Co(II) complexes of polydentate Schiff base ligand and their metal complexes against *Escherichia coli, Pseudomonas aeruginosa, Staphylococcus aureus* and *Bacillus subtillis* revealed that the metal complexes were found to be more toxic than their parent Schiff base ligands.[72]

Zaky et al[73] synthesized, characterized and reported the antibacterial effect of Cu(II), Ni(II), Zn(II) complexes of *o*-hydroxyacetophenone [N-(3-hydroxy-2-naphthoyl)] hydrazone and their ligands against *E. coli* and *Clostridium species* at 1.0 and 2.0 mg/ml. The antibacterial results showed that the activities of the metal complexes and their ligands were greatly enhanced at higher concentrations. However, both the ligand and complexes showed a moderate activity against the two microorganisms when compared to a standard drug, Ampicillin.

Synthesis, characterization, and biocide properties of semicarbazide—formaldehyde resin and its polymer metal complexes was reported by Nishat *et al.*[40] The study revealed that the antibacterial activity and toxicity of the synthesized compounds were significant against four bacteria species viz *E. coli, S. typhi, S. aureus* and *B. subtilis* suggesting that these compounds could serve as anticancer agents in the future.

The work done by El-Sherif *et al*[68] focused on the synthesis, characterization, equilibrium study and biological activity of Cu(II), Ni(II) and Co(II) complexes of polydentate Schiff base ligand. Antimicrobial study was done using a modified Kirby-Bauer disc diffusion method against two Gram-positive organisms (*S. aureus* and *B. subtillis*), and two Gram-negative organisms (*E. coli* and *P. aeruginosa*). The result of antimicrobial activity indicated that copper chelates showed a better activity when compared to their analogous containing nickel(II) and cobalt(II) ions.

Antibacterial activity of the Fe(II) and Mn(II) complexes of 2-[4,6-di(tert-butyl)-2,3-dihydroxyphenysulfanyl] acetic acid and 2-[4,6-di(tert-butyl)-2,3-dihydroxyphenysulfinyl]

acetic acid was evaluated in comparison with Cu(II), Co(II) and Zn(II) complexes and three common standard antibiotics was performed by Loginova et al.[74] In general, the antimicrobial results revealed a lower inhibiting ability for the ligands than their metal complexes.

Manjunathan et al[75] conducted a study to investigate the antibacterial and antifungal activities of the ligand ambsalem and its metal complexes. Results obtained indicated that the compounds showed higher activity against the Gram negative bacteria E. coli, Klebsiella pneumoniae and P. aeruginosa when compared to Gram positive bacteria B. subtilis and S. aureus. On further examination, it was revealed that the metal complexes proved to be better antimicrobial agents than their parent ligands and this was as a result of an improved lipophilic nature of the metal complexes due to chelation.

Another significant contribution in this regard was the biological activity of complexes of 2-acetylthiophene benzoylhydrazone containing an SNO donor system with divalent metal ions, such as Co(II), Ni(II), Zn(II) and Cu(II) done by Saadeh.[76] The antibacterial activity was evaluated against three standard bacterial strains (E. coli, S. aureus and P. aeruginosa), however these complexes showed no biological activity. This biological inactivity was attributed to the exchange of a methyl group in place of hydrogen on the complexes. The study further suggested that the biological activity of a particular metal complex is a combination of complex factors such as steric, pharmacokinetic and electronic.

2.3.1 Antimicrobial resistance profiles of *Staphylococcus* and *Enterococcus* species

Globally, healthcare systems are encountering extended drug resistant (XDR) organisms that portray resistance to a large proportion of antibiotics except for colistin.[77] Colistin is a highly toxic agent which has questionable efficacy against microorganisms and was abandoned in the 1960s when safer and more effective therapies became available. Even worse than this, the global healthcare system is witnessing PDR organisms (e.g carbapenem-resistant bacteria such as KPC *Kebsiella and Acinetobacter*) both of which are resistant to all the available antibiotics including colistin. Given these resistance problems it is suggested that infections will continue to pose severe health problems to humans especially hospitalised patients[31] if new prevention and treatment methods are not made available. Gould[78] described the epidemic of antibiotic resistance as pandemic and referred to it as an ecological disaster of unknown consequences and no obvious solutions.

The inception of penicillin in 1944 increased the susceptibility of S. aureus isolates to over 94%, however, by1950 half were resistant.[78] This was evident in the outbreaks of virulent multi-drug resistant S. aureus in 1960. Between the 1960s to the 1980s, numerous

antimicrobial agents were introduced into the market to ease the emerging worldwide threat of the multi-drugs resistant *Staphylococcus* strains in hospitals. This threat was contained in the 1960s by the introduction of methicillin and penicillinase-stable penicillis.[79] The emergence of outbreaks caused by gentamicin-resistant *Klebsiella* and other Gram-negative organisms in the 1970s was eradicated with the use of newer aminoglycosides, cephalosporins and quinolones in the 1980s. This situation didn't last for long and outbreaks caused by MDR Gram-positive hospital pathogens such as multi-resistant *S. aureus* and coagulase-negative *staphylococci* and *enterococci* emerged. Pesavento *et al*[80] reported the first *S. aureus* resitance to penicillin occurred in 1941 only two years penicillin was introduced. In June 2002, a vancomycin resistant *S. aureus* and *E. faecalis* were isolated from a patient in the United States.[81] Methicillin resistant *S. aureus* became predominant in Europe in 2000. The resurgence of MRSA was attributed to its lack of potent therapeutic agents that have the ability to ultimately reduce the potential of the pathogen to kill the host cells and also able to eliminate MRSA strains from the patient's system.[78] Against this backdrop, vancomycin an antibiotic with proven weak cell-killing potency against the resurging MRSA strains was introduced as a potential agent for killing MRSA strains.[80] This marked the era of vancomycin resistance in MRSA.[80] Livermore[42] described *S. aureus* as a resilient bacteria that is capable of regaining its importance if antibiotics are used in an uncontrolled manner or if hygiene practices are not well implemented whereas Tajedor *et al*[81] described *Enterococci* species as organisms that serve as indicators of faecal pollution and are usually present in the faeces of humans and warm blooded animals. According to French,[31] the change from highly susceptible to more resistant isolates among *Staphylococcus* species can be attributed to an inevitable evolutionary response that is associated with the use of antibiotics and this has occurred rapidly due to the short generation time of bacteria. French[31] also indicated that the uncontrolled usage of antibiotics and lack of adequate infection control practices are mainly responsible for the increased occurrence of antibiotic resistant strains worldwide. Negligence in the usage of antibiotics was pointed out by the Standing Medical Advisory Committee of the UK Department of Health[82] where they advised that antibiotics must be treasured, protected and valued as non-renewable resources. The lack of consensus amongst microbiologists, infectious disease experts and other medical communities on issues regarding the usage of antimicrobial agents was also highlighted by McGowan.[83] The disagreements is also worsened by the lack of continuing research for the search of new antimicrobial agents. French[31] went on to point out that antimicrobial resistance has a major setback on the outcome of therapy and this may promote the risks of cross-infection in

hospitals. Moreover, antimicrobial resistance promotes inappropriate empirical therapy, delay in starting effective treatment and the use of less effective, more toxic and more expensive drugs. Ultimately, if the situation is left unattended it will result to a dramatic increase in mortality rates among humans, healthcare costs and length of hospital stay for patients infected with MDR bacteria compared to patients infected with susceptible strains of the same species.[31]

Threats posed by antibiotic resistant *S. aureus* strains and the extent of the spread amongst populations are directly linked to biological costs associated with resistant determinants.

Pesavento *et al*[80] in their study hinted on the nature of antibiotic resistance of *S. aureus* to methicillin and penicillin. Their views were that penicillin resistance is encoded by plasmids and therefore spreads out rapidly to other strains whereas methicillin-resistance is encoded by the bacteria chromosome which explains why it spreads slowly.

The extended use and misuse of antibiotics in stock-farming, agriculture and the treatment of diseases are few causes of increased bacteria resistance to antibiotics.[80] According to Gould,[84] antibiotic resistance is worsened by the economic gap between poorer and richer countries. In his view, many poorer nations have limited access to antibiotics resulting to a high mortality rate from infections such as pneumonia. This results in individuals relying highly on cheap and often low quality antibiotics produced in these countries.

Butler *et al*[85] indicated that the emergence of multi-drug-resistant bacteria results to economic and regulatory challenges which explains the need for the development of new antimicrobial agents. New antibiotics are necessary to treat microbial pathogens such as *S. aureus* that are becoming increasingly resistant to available treatment.[86] Despite the medical need, the number of newly approved drugs continues to decline.[84] Outterson *et al*[87] prescribed both short-term and long-term solutions for this global crisis caused by antibiotic resistance strains. In their short-term solutions, they suggested the urgent need to improve the quality and quantity of antibiotic use in order to minimize the resurgence and transmission of resistant determinants. Improved diagnosis before prescription, better socioeconomic conditions, improved sanitation, integration of antibacterial resistance into the existing health care system and alliances between industries and academia in the areas of drug discovery and production were all part of their long-term solutions. To achieve this, public and private partnership is crucial in gathering relevant diagnostic information, filling of gaps by increasing sustainable laboratory capacity and stimulating new antibiotic research.[84]

2.4   CORROSION STUDIES

The use of ionic liquids as potential corrosion inhibitors is common than inorganic ligands. Ashassi-Sorkhabi et al[88] studied the corrosion inhibition of mild steel in 1.0 M HCl by 1-butyl-3-methylimidazolium bromide [BMIM]Br ionic liquid. The results obtained showed that [BMIM]Br acts as a mixed type inhibitor. The effect of inhibitor concentration on zero charge potential (ZCP) of the mild steel in 1.0 M HCl was studied and its comparison with OCP has been made for evaluation of the mechanism of adsorption of [BMIM]$^+$cation. The effect of temperature on the corrosion behaviour of mild steel in 1.0 M HCl with addition of [BMIM]Br was studied under temperature range 25-45 ^{0}C. It was established that inhibition efficiency decreases with increase in temperature.

Zhang et al[89] investigated the corrosion inhibition of 2-mercapto benzimidazole and potassium iodide (KI) on copper in aerated sulphuric acid. The addition of KI was found to promote synergistic effect that enables the successful adsorption of MBI in acid environment. Corrosion inhibition was studied using electrochemical impedance spectroscopy and polarization curves. The result of inhibition efficiency was said to increase with increase in concentration of inhibitor.

The effect of ionic liquids with imidazolium cation (namely, 1,3-dioctadecylimidazolium bromide) and pyridinium cation (namely, N-octadecylpyridinium) on the corrosion inhibition of mild steel in acidic environment was studied by Likhanova et al.[90] In their work, ILs tested as corrosion inhibitors displayed corrosion protection efficiency within 82-88% at 100 ppm for mild steel in a 1.0 M aqueous solution of sulphuric acid. Chemical adsorption process was proposed from the calculated values of the standard free energy of adsorption (ΔG°_{ads}). The presence of carbon species pertaining to the inhibitor and corrosion products was indicated by surface analysis (SEM, EDX) completed by XRD and Mossbauer spectroscopy. This was also rationalized in their inhibition mechanism.

Onen et al[52] investigated the corrosion inhibitive properties of titanium(II)oxide against aluminium and mild steel in sulphuric acid solutions using the 'absorbance difference' technique at 303 K and 313 K. The results of activation energy, E_a and percentage inhibition efficiencies (%IE) calculated showed that both increased with concentration of titanium(IV)oxide. The values of activation energy for the inhibition suggested a physisorption mechanism. Evidence supporting that corrosion inhibition follows a physisorption mechanism was supported by Zhang et al[89] in their study on the synergistic effect of MBI and KI on copper corrosion inhibition in aerated sulphuric acid solution. On

analysis employing X-ray Photoelectron Spectroscopy (XPS), it was revealed that a (Cu$^+$MBI) complex film formed on the surface to inhibit the corrosion of copper.

Chemical cleaning and pickling at elevated temperatures remain valuable tools for many industries where mill scales pose a threat on the surface of metals. Qurashi et al[91] in their study revealed an important role tetramethyl-dithia-octaaza-cyclotetradeca-hexaene (MTAH) could play as a corrosion inhibitor of mild steel in hot 20% sulphuric acid. The result of corrosion inhibition of MTAH in synergy with iodide ions was compared to a commercial corrosion inhibitor (Metasave). Inhibition efficiency of MTAH was favoured up to 95°C in the presence of KI.

Another significant work in this regard was done by Torres et al[92] in their study of thiourea derivatives synthesized from a green route corrosion inhibitors for mild steel in HCl solution. Their work revealed inevitably the use of acidic medium in industries for purposes of acid pickling and acidification of petroleum wells which expose machineries to corrosion. Their choice of thioureas derivatives was based on the consideration that organic compounds containing N, O and S are considered to be effective corrosion inhibitors. The corrosion inhibitory ability of these compounds was attributed to the nature of the organic inhibitors, condition of the metallic surface, structure of the inhibitor and the adsorptive interaction of the inhibitor with the metal surface.

It has been proved by many studies such as Singh[93] that organic compounds containing heteroatoms with high electron density, such as oxygen, sulphur, nitrogen and phosphorous as well as those containing multiple bonds are effective corrosion inhibitors. This is attributed to reasonable adsorption centres offered by such class of organic compounds.

Gopiraman et al[94] employed potentiodynamic polarization, electrochemical impedance spectroscopy, ultraviolet−visible (UV−Vis), Fourier transform infrared (FTIR), Raman, scanning electron microscopy−energy-dispersive X-ray (SEM−EDS) spectroscopic methods, and adsorption isotherm measurements in studying the interactions of 1-benzoyl-3,3-disubstituted thiourea derivatives on MS surface. The use of UV-vis, SEM-EDS, FTIR and Raman spectroscopy in their study was to gain further insights into the nature of modification that has occurred on the mild steel surface after the inhibition process due to the observed film formation on the surface of the mild steel.

Aromatic compounds containing nitrogen atoms have been found to be efficient inhibitors for corrosion in acid media. Emregül et al[95] argued that adsorption of these organic molecules on the metal surface proceeds through the formation of bonds between the nitrogen electron pair

and π-electrons on the metal surface. According to them, this adsorption process depends upon;

(a)   the nature of medium

(b)   the chemical structure of the organic molecule

(c)   the nature and surface charge of the metal

(d)   the distribution of the charge in the molecule.

The present study is therefore an investigation into the corrosion inhibition potential of 1,8-dimethyl-1,3,6,8,10,13-hexaazacyclotetradecane using electrochemical impedance spectroscopy, potentiodynamic polarisation and cyclic voltammetry methods.

CHAPTER THREE

EXPERIMENTAL

3.1 MATERIALS

3.1.1 Reagents and strains

All solvents and chemicals used in the syntheses were of reagent grade and were used without further purification. Distilled or deionized water was used as solvent in some spectroscopic measurements. Methanol (CH_3OH), formaldehyde (CH_2O), ethylenediamine ($C_2H_8N_2$), methylamine (CH_3NH_2), acetonitrile (CH_3CN), sodium cyanide (NaCN), sodium hydroxide (NaOH) pellets and hydrochloric (HCl) acid were obtained from Sigma-Aldrich. Sodium dihydrogen orthophosphate dihydrate ($NaH_2PO_4.2H_2O$) and disodium hydrogen orthophosphate (Na_2HPO_4) were obtained from Saarchem. Potassium ferrocyanide(II) ($K_4Fe(CN)_6.3H_2O$) and potassium hexacyano-ferrate(III) ($C_6FeK_3N_6$) were obtained from Merck. Müller-Hinton Agar was obtained from Fluka analytical. Microorganisms (*Staphylococcus aureus* and *Enterococci)* were obtained from the culture collection of Department of biological sciences, NWU. Analytical reagent-grade disodium hydrogen orthophosphate, potassium ferrocyanide(II) and potassium hexacyano-ferrate(III) were utilized to prepare 0.1 mol L^{-1} Phosphate buffer solution and 5 mM $Fe(CN)_6{}^{3-/4-}$ respectively.

3.2 SYNTHESIS OF COMPOUNDS

3.2.1 Synthesis of 1,8-dimethyl-1,3,6,8,10,13-hexaazacyclotetradecanenickel(II) complex[7]

Nickel(II) chloride hexahydrate (11.5 g), ethylenediamine (6.8 ml), formaldehyde (20 mL), and methylamine (8.6 ml) were slowly added to a stirred methanol solution (50 mL). The mixture was heated at reflux for twenty- four hours until a dark orange solution formed. The solution was cooled in an ice-bath, followed by filtration of the solution to remove nickel hydroxide. To the filtrate, excess perchloric acid was added and the resulting mixture was kept in an ice-bath for 24 hours until yellow crystals formed. The yellow crystals were washed in a mixture of ether and methanol, and air dried. The crystals were further recrystallized from boiling water. Yield (37.65 g). The overall synthesis is shown in Figure 3.1.
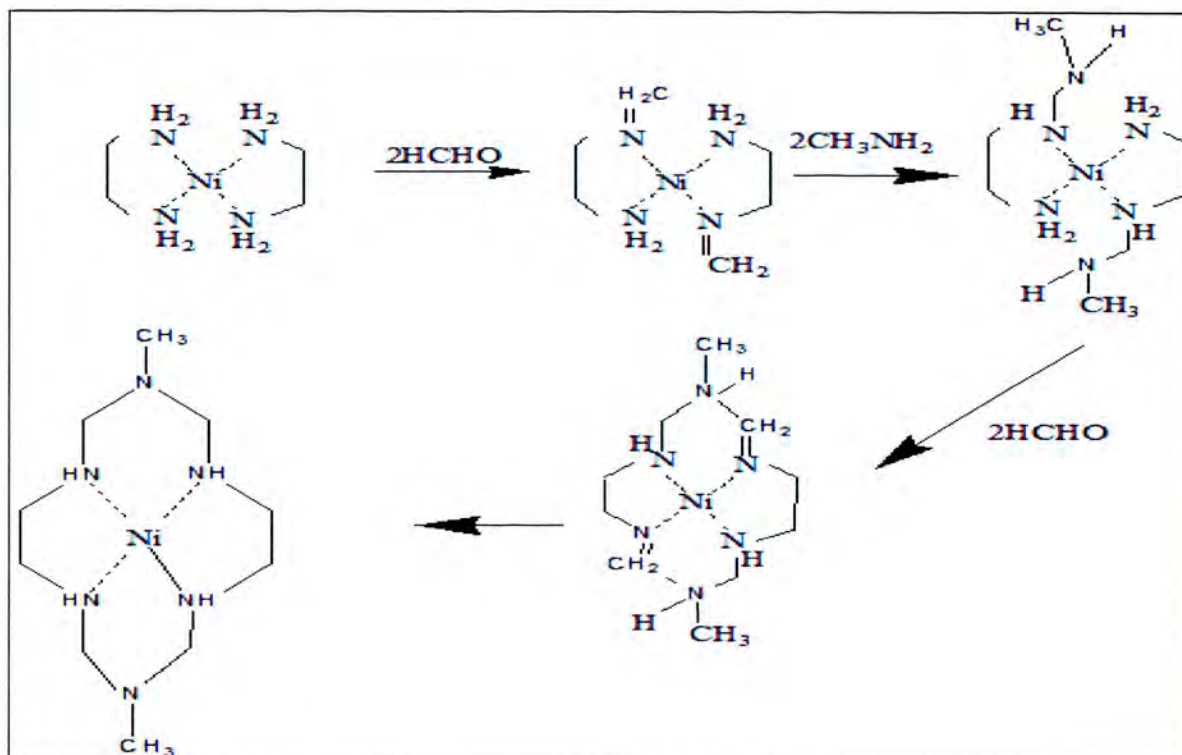
Figure 3.1. Synthesis of 1,8-dimethyl-1,3,6,8,10,13-hexaazacyclotetradecanenickel(II) complex.

3.2.2 Demetallation of 1,8-dimethyl-1,3,6,8,10,13-hexaazacyclotetradecanenickel(II) complex

Aqueous solution (10 ml each) of the nickel complex (5.64 g), sodium hydroxide pellets (6 g) and sodium cyanide (10 g) were added together and evaporated in a rotary evaporator until excess liquid was removed. The resulting crystalline solid was washed with acetonitrile and excess chloroform, followed by further evaporation to dryness. The white crystalline solid was collected and air-dried. Yield (4.24 g). The overall synthetic route is shown in Figure 3.2.
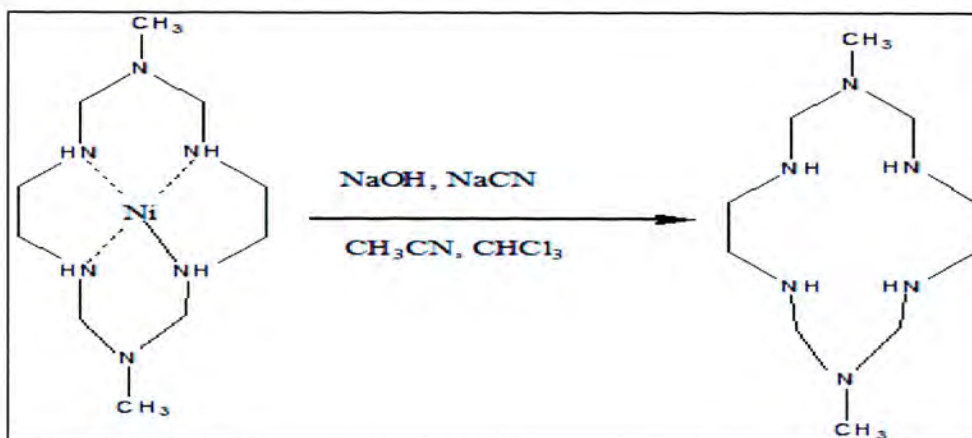
Figure 3.2. Demetallation of 1,8-dimethyl-1,3,6,8,10,13-hexaazacyclotetradecanenickel(II).

3.3   CHARACTERIZATION OF THE COMPOUNDS

3.3.1   Ultraviolet-Visible spectra

Ultraviolet-visible electronic absorption spectra of freshly prepared 1,8-dimethyl-1,3,6,8,10,13-hexaazacyclotetradecanenickel(II) complex and 1,8-dimethyl-1,3,6,8,10,13-hexaazacyclotetradecane ligand in appropriate solvents were recorded in a 1cm quartz cell using a Varian Cary 50 Conc UV-Vis spectrophotometer in the range of 200- 400 nm (λ_{max}). The relevant spectra of the compounds are recorded in Figures 4.1 and 4.2.

3.3.2   Infrared spectra

The infrared spectra of 1, 8-dimethyl-1,3,6,8,10,13-hexaazacyclotetradecanenickel(II) complex and 1,8-dimethyl-1,3,6,8,10,13-hexaazacyclotetradecane ligand were recorded on a Cary 670 Fourier Transform Infrared spectrophotometer. The range of interest was between 700 and 4000 cm^{-1}. The relevant spectra of the compounds are shown in Figures 4.3 and 4.4.

3.3.3   Energy Dispersive X-ray spectra (EDX)

Qualitative results indicating the percentages of analyte present in 1, 8-dimethyl-1,3,6,8,10,13-hexaazacyclotetradecanenickel(II) complex and 1,8-dimethyl-1,3,6,8,10,13-hexaazacyclotetradecane ligand was carried out with EDX-720. The results are presented in Figures 4.5 and 4.6.

26

3.3.4 NMR spectra

The proton and ^{13}C NMR spectra of the compounds were recorded on a Varian Gemini 300 Broadband NMR spectrometer at 300 MHz in CDCl$_3$/ D$_2$O. ^{13}C NMR data are listed in the order chemical shift (δ) in ppm. The coupling constant J (Hertz) was reported to the nearest 0.1 Hz and multiplicities were given as follows: s (singlet), d (doublet), t (triplet) and q (quartet). The data is presented in Figure 4.7 and 4.8.

^{1}H NMR data are listed in order of chemical shift (δ) reported in ppm. The coupling constant J (Hertz) was reported to the nearest 0.1 Hz and multiplicities were given as follows: s (singlet), d (doublet), t (triplet) and q (quartet). The data is presented in Figure 4.9 and 4.10 and Table 4.5.

3.3.5 Mass spectra

Mass spectra of the nickel(II) and free ligand were obtained on an Agilent 6890 chromatograph equipped with an Agilent 7683 autoinjector. The data is presented in Figure 4.11 and 4.12.

3.3.6 Thermo-gravimetric analysis (TGA)

The thermal behaviours of the synthesized ligand was evaluated using TA analyzer 2000. Figure 4.13 summarizes some results of thermal analysis of ligand.

3.4 BIOLOGICAL ACTIVITY

3.4.1 Antibiotics susceptibility test

The antibacterial activity of 1,8-dimethyl-1,3,6,8,10,13-hexaazacyclotetradecane ligand was studied against *Staphylococcus aureus* and *Enterococcus faecalis* isolated from milk and groundwater samples in the North West Province, South Africa. The identities of the isolates were confirmed using standard preliminary and confirmatory microbiology tests. The isolates were therefore obtained from the Molecular Microbiology Laboratory, Department of Biological Sciences, North-West University, Mafikeng Campus and used for the antimicrobial assay. The ligand to be investigated for antimicrobial properties was dissolved in sterile distilled water and concentrations of 1 µg/ml, 2 µg/ml, 3 µg/ml and 4 µg/ml were prepared separately. Sterilized paper discs of uniform diameter (6 mm) were cut and sterilized by autoclaving. The paper discs soaked in the different concentrations of the ligand solutions for 10 minutes. Bacterial suspensions of *S. aureus* and *Enterococci* were prepared,

and aliquots of 100 μl from each suspension were spread-plated on Muller Hinton agar. The paper discs were aseptically placed on inoculated plates and incubated at 37 °C for 24 hours. Isolates were also tested against ligands while a disc with no ligand concentration was included in each inoculated plate as a negative control. The inhibition zone diameter data of discs with different concentrations of the ligands were determined. Measurements were reported in mm. Figures 4.14 and 4.15 and Tables 4.6 and 4.7 describe biological screening of the free ligand against Gram-positive bacteria (*S. aureus* and *Enterococci*). Figure 4.16 is a photograph showing antibacterial study of the free ligand.

3.5   CORROSION STUDY

3.5.1   Material preparation

Mild steel (MS) strips (1 cm^2) of the composition 0.02 % Phosphorous (P), 0.37 % Manganese (Mn), 0.03 % Sulphur (S), 0.01 % Molybdenum (Mo), 0.039 % Nickel (Ni), 0.21 % Carbon (C) and the remaining part being iron (Fe) were prepared. Prior to running the experiment, the mild steel specimens were further abraded successively with different grades of emery papers (600 to 1200 grade), washed thoroughly with deionised water and degreased with acetone and finally air-dried. Each experiment was repeated at least four times to check the reproducibility.

3.5.2   Inhibitors

The synthesized ligand, 1,8-dimethyl-1,3,6,8,10,13-hexaazacyclotetradecane was utilized. Different concentrations in the range 10 ppm - 500 ppm were prepared for the ligand and the stock solutions were utilized throughout the electrochemical studies. The name and structure of the ligand used in this study is shown below in Figure 3.3.
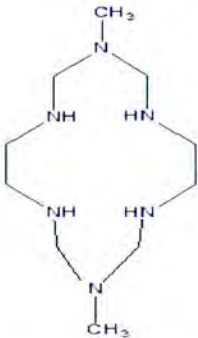
Name of Inhibitor	Molecular structure	Molecular weight (g.mol^{-1})
1,8-dimethyl-1,3,6,8,10,13-hexaazacyclotetradecane		230

Figure 3.3. Molecular structure of the ligand used in this study

3.6   ELECTROCHEMICAL MEASUREMENTS

Electrochemical experiments were carried out at room temperature (30 ^{0}C) using an Autolab Potentiostat PGSTAT 302 (Eco Chemie, Utrecht, and The Netherlands) driven by the GPES software version 4.9. Electrochemical impedance spectroscopy (EIS) measurements were performed with an Autolab Frequency Response Analyser (FRA) software between 10 kHz and 0.1 Hz using a 5 mV rms sinusoidal modulation in a particular test solution using a three electrode cell system. An Ag|AgCl in saturated KCl and platinum wire were used as reference and counter electrodes, respectively. Mild steel (MS) was used as the working electrode in the investigation.

A stabilization time of 30 minutes was allowed before the electrochemical measurements were performed and this time was deemed to be sufficient to attain a stable value of OCP (open circuit potential).

3.6.1   Cyclic Voltammetry (CV)

The electrochemical properties of the synthesised ligand was studied in 0.1 M phosphate buffer solution (pH 7.0) and 5 mM Fe(CN)$_6$ $^{3-/4-}$ redox probe using cyclic voltammetry technique. Sodium dihydrogen orthophosphate dihydrate, disodium hydrogen orthophosphate, potassium ferrocyanide(II) and potassium hexacyano-ferrate(III) were utilized to prepare 0.1 mol L^{-1} Phosphate buffer solution. This was done by weighing 3.05 g

Na$_2$HPO$_4$ salt and 4.45 g NaH$_2$PO$_4$ acid. The two was dissolved together in 500 ml standard flask with deionized water. The pH of the solution was checked and maintained at pH 7.5 mM Fe(CN)$_6$ $^{3-/4-}$ redox probe was prepared by weighing 0.211 g potassium ferrocyanide(II) and 0.165 g potassium hexacyano-ferrate(III) mixed together in 100 ml flask with the phosphate buffer solution. Figures 4.17 and 4.18 are the cyclic voltammograms obtained for platinum electrode in both the PBS alone and PBS containing 10^{-3} M 1,8-dimethyl-1,3,6,8,10,13-hexaazacyclotetradecane. Effect of scan rates (25 to 300 mVs^{-1}) on the electrochemical behaviour of the synthesized ligand was also studied.

3.6.2 Potentiodynamic polarization (PDP)

The electrochemical behaviour of mild steel sample in inhibited and non-inhibited solution was studied by recording anodic and cathodic potentiodynamic polarization curves. Measurements were performed in 1M HCl solution in the absence (blank) and presence of different concentrations of the tested inhibitor at potential window from −800 to -200 mV versus corrosion potential at a scan rate of 100 mVs^{-1}. The linear Tafel segments of anodic and cathodic curves were extrapolated to obtain the corrosion parameters such as corrosion potential, corrosion rate, corrosion current density, anodic and cathodic Tafel slopes. The measured corrosion current densities were used to calculate the percentage inhibition efficiency by making use of equation (2);

$$\%IE = \frac{i^0_{corr} - i^i_{corr}}{i^0_{corr}} \times 100 \tag{2}$$

where i^0_{corr} and i^i_{corr} are values of corrosion current in absence and in presence of inhibitor respectively.

3.6.3 Electrochemical Impedance Spectroscopy (EIS)

The EIS study was carried out at room temperature in a three electrode cell assembly already described above. The electrochemical impedance spectroscopy measurements were carried out using AC signal at E$_{corr}$ (vs Ag|AgCl in saturated KCl). The experiments were carried out after 30 minutes of immersion of the mild steel electrodes in solution containing different concentrations of 1,8-dimethyl-1,3,6,8,10,13-hexaazacyclotetradecane ligand. The inhibition

efficiency of the inhibitor was calculated from the charge transfer resistance values using the following equation (3):

$$\mu_{Rt} = \frac{(1/R_t^{\ 0}) - (1/R_t^{\ i})}{(1/Rt^o)} \times 100 \qquad (3)$$

where $R_t^{\ 0}$ and $R_t^{\ i}$ are the charge transfer resistances in the absence and in presence of inhibitor respectively. The AC impedance data of mild steel/HCl acid interface obtained in the absence and presence of various concentrations of macrocycle in the form of Nyquist plots.

CHAPTER 4

RESULTS AND DISCUSSION

4.1 SYNTHESIS AND DEMETALLATION OF 1,8-DIMETHYL-1,3,6,8,10,13-HEXAAZACYCLOTETRADECANENICKEL(II) COMPLEX

The synthetic route for the synthesis of 1,8-dimethyl-1,3,6,8,10,13-hexaazacyclotetradecanenickel(II) complex was carried out using the method described by Suh *et al*[7] whereas demetallation of 1,8-dimethyl-1,3,6,8,10,13-hexaazacyclotetradecanenickel(II) complex was achieved in an aqueous solution of Ni(II) complex, sodium hydroxide and sodium cyanide.

4.1.1 Synthesis of 1,8-dimethyl-1,3,6,8,10,13-hexaazacyclotetradecanenickel(II) complex

Synthesis of 1,8-dimethyl-1,3,6,8,10,13-hexaazacyclotetradecanenickel(II) complex was achieved by heating at reflux the nickel(II) salt in an ethylenediamine, formaldehyde, and methylamine solution for 24 hours. 1,8-dimethyl-1,3,6,8,10,13-hexaazacyclotetradecanenickel(II) complex was successfully prepared via template condensation of ethylenediamine, formaldehyde, and methylamine in the presence of nickel(II) chloride. Figure 3.1 summarises the overall reaction. Template condensation of ethylenediamine and formaldehyde was initiated by the formation of an imine which was subsequently coordinated to a nickel(II). The imine was attacked by the methylamine to yield a gem-diamine which was further condensed with a neighbouring imine group to produce a six-membered ring. This was further followed by the addition of excess perchloric acid to precipitate the crystals from the solution. The resulting crystals were recrystallized from boiling water to yield a yellow crude (37.65 g). Excess solvent was then slowly removed by rotary evaporation in order to avoid aggregation of the products mixtures. The yellow crystals were stored in a desiccator.

4.1.2 Demetallation of 1,8-dimethyl-1,3,6,8,10,13-hexaazacyclotetradecanenickel(II) Complex

The demetallation of 1,8-dimethyl-1,3,6,8,10,13-hexaazacyclotetradecanenickel(II) complex was cleanly achieved by the reaction of 1,8-dimethyl-1,3,6,8,10,13-hexaazacyclotetradecanenickel(II) complex, sodium hydroxide and sodium cyanide. This reaction was driven on one side by the highly thermodynamic stable nickel tetracyanonickelate ion and on the other hand the fact that the nucleophilic attack takes place at the centre Ni^{2+} centre. The resulting solution was evaporated in a rotary evaporator until excess solvent was removed. Acetonitrile and excess chloroform were added to precipitate out the resulting white crystalline solid followed by further evaporation in a rotary evaporator to dryness. The crystalline white sold was collected and stored in a desiccator. Yield (4.24 g). The free ligand was fairly soluble in acetonitrile. The overall synthetic route is shown in Figure 3.2.

4.2   CHARACTERIZATION OF COMPOUNDS

4.2.1   The ultraviolet-visible spectrum

A summary of the wavelengths of maximum absorption and the absorbance at these wavelengths for 1,8-dimethyl-1,3,6,8,10,13-hexaazacyclotetradecanenickel(II) complex and the free ligand are summarized in Table 4.1 while the spectra of these compounds are compiled in Figures 4.1 and 4.2 respectively.

Table   4.1.   Absorption   bands   of   1,8-dimethyl-1,3,6,8,10,13-hexaazacyclotetradecanenickel(II) complex and the free ligand.

Compound	Wavelength (λ_{max})(nm)	Absorbance
Nickel(II) complex	325.1	1.833
Free ligand	265.0	1.515
	285.1	1.413
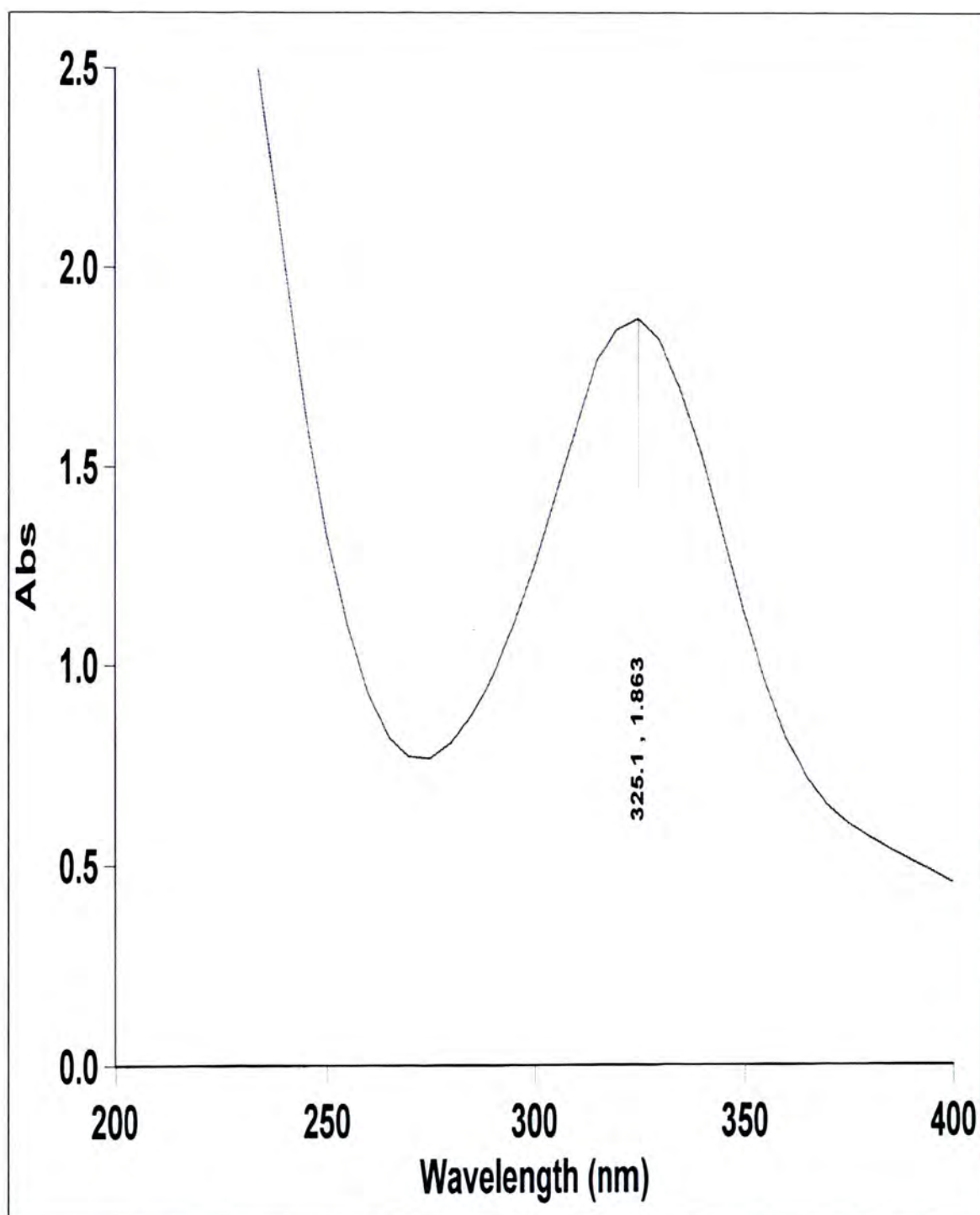
Figure 4.1. The ultraviolet-visible spectrum of 1,8-dimethyl-1,3,6,8,10,13-hexaazacyclotetradecanenickel(II).
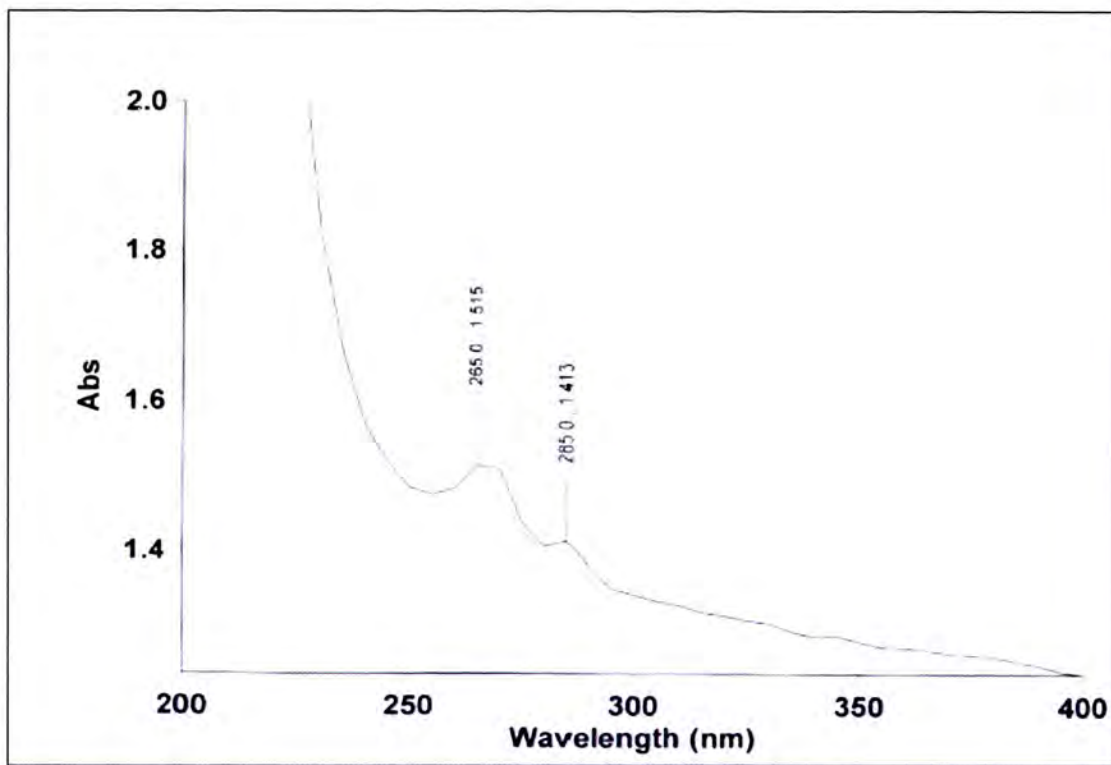
Figure 4.2. The ultraviolet-visible spectrum of 1,8-dimethyl-1,3,6,8,10,13-hexaazacyclotetradecane ligand

The ultraviolet-visible spectrum was utilized to confirm different electronic transitions within the compound. The ultraviolet-visible spectrum of 1,8-dimethyl-1,3,6,8,10,13-hexaazacyclotetradecanenickel(II) spectrum showed band peak at 325.1 nm due to the $^3A_{2g} \rightarrow ^3T_{1g}(P)$ transition, suggesting a square-planar environment.

The observed bands of the ligand showed no peak at 290-330 nm suggesting the disappearance of nickel(II) ion.

4.2.2 The infrared spectra

The summary of the relevant absorption peaks are presented in Table 4.2 and 4.3 while the spectra of the compounds are shown in Figures 4.3 and 4.4.

Table 4.2. Infrared spectra of 1,8-dimethyl-1,3,6,8,10,13-hexaazacyclotetradecanenickel(II) complex and their assignments.

Band (cm^{-1})	Assignment
3221.90	$v(NH)$
1502.56	$\delta(NH)$
1025.75	$v(CH)$
781.73	$\delta(CH)$

Figure 4.3. Infrared spectrum of 1,8-dimethyl-1,3,6,8,10,13-hexaazacyclotetradecanenickel(II) complex.

Table 4.3. Infrared spectra of 1,8-dimethyl-1,3,6,8,10,13-hexaazacyclotetradecane ligand and their assignments.

Band (cm^{-1})	Assignment
1421.15	δ(NH)
876.52	δ(NH)
766.98	δ(CH)

Figure 4.4. Infrared spectrum of 1,8-dimethyl-1,3,6,8,10,13-hexaazacyclotetradecane ligand.

The spectra of Nickel complex showed a broad medium intensity band in the region of 3221.90- 1502.56 cm^{-1} due to ν(N-H) stretching vibration of amine and amide groups.[28] These bands comprise of symmetric and asymmetric stretching of amine (-NH$_2$) and amide – NH- group. In most metal complexes, these bands undergo downward shift by 20- 25 cm^{-1} thus indicating that amide is coordinated to nickel ion. The disappearance of these prominent peaks of ν(H-N) between 4000- 1583 cm^{-1} however, may suggest the absence of coordinated nickel ion. Most peaks were present in both IR spectra of the nickel complex and its ligand (Figures 4.3 and 4.4 respectively) suggesting that all the functional groups didn't disappear. Nakamoto[96] assigned the stretching frequencies of Ni-N in the 410-380 cm^{-1} region for the [Ni(en)$_3$]$^{2+}$ which confirms that the Ni-N appears in far-infrared regions (Figure 4.3 Infrared spectra of complex). Ahamad et al[38] assigned Ni-N IR spectra of Poly-SDFP in the range 560- 540 cm^{-1}.

Table 4.4 summarizes the most important absorption band for the nickel(II) complex from two literature sources.

Table 4.4. Absorption band of the 1,8-dimethyl-1,3,6,8,10,13-hexaazacyclotetradecane complex.

Literature one[7] (cm^{-1})	3200
Literature two[27] (cm^{-1})	3200
Observed (cm^{-1})	3221

4.2.3 Energy Dispersive X-ray spectra

Figures 4.5 and 4.6 show the relevant EDX spectra for the 1,8-dimethyl-1,3,6,8,10,13-hexaazacyclotetradecanenickel(II) complex and 1,8-dimethyl-1,3,6,8,10,13-hexaazacyclotetradecane ligand.
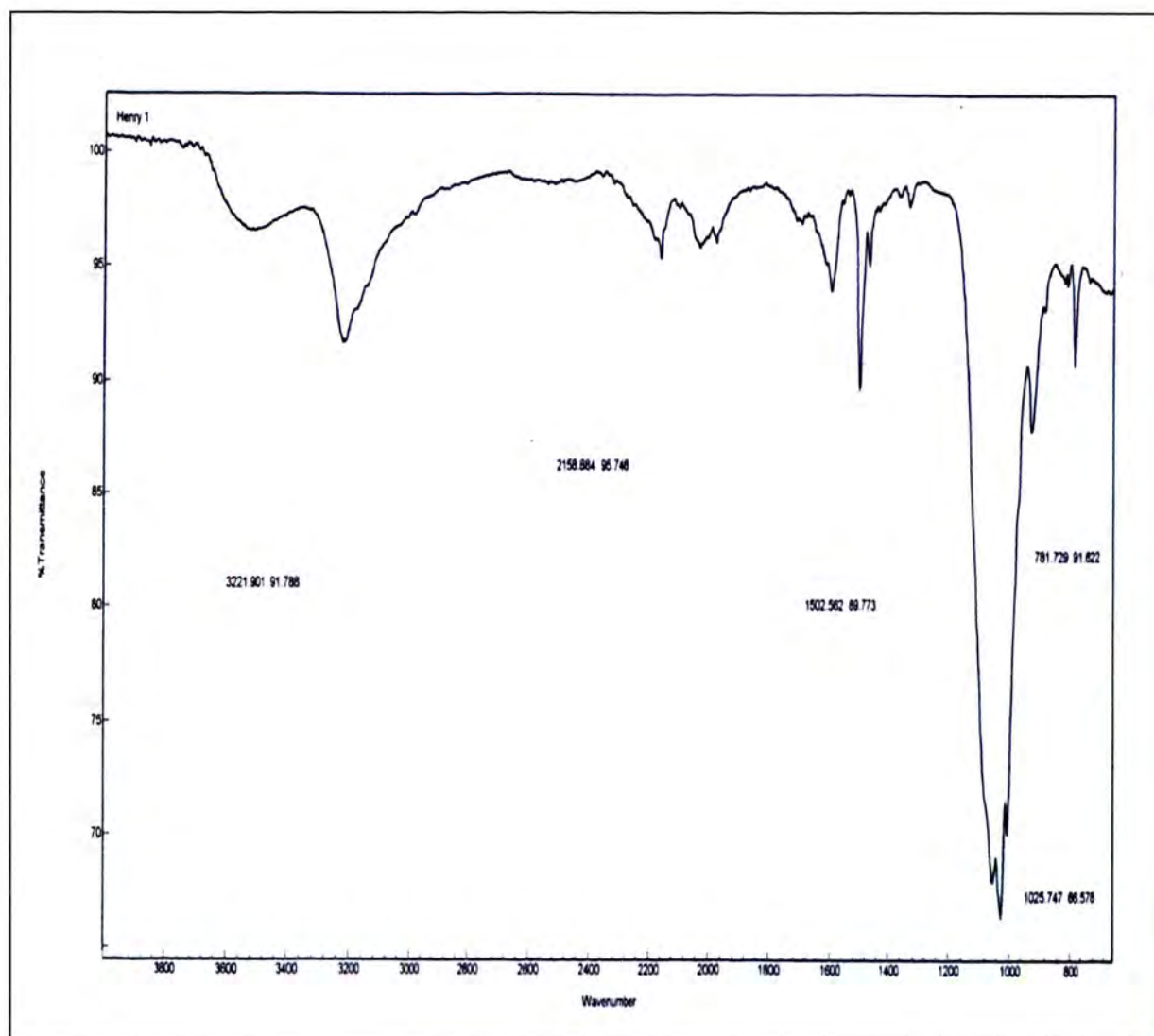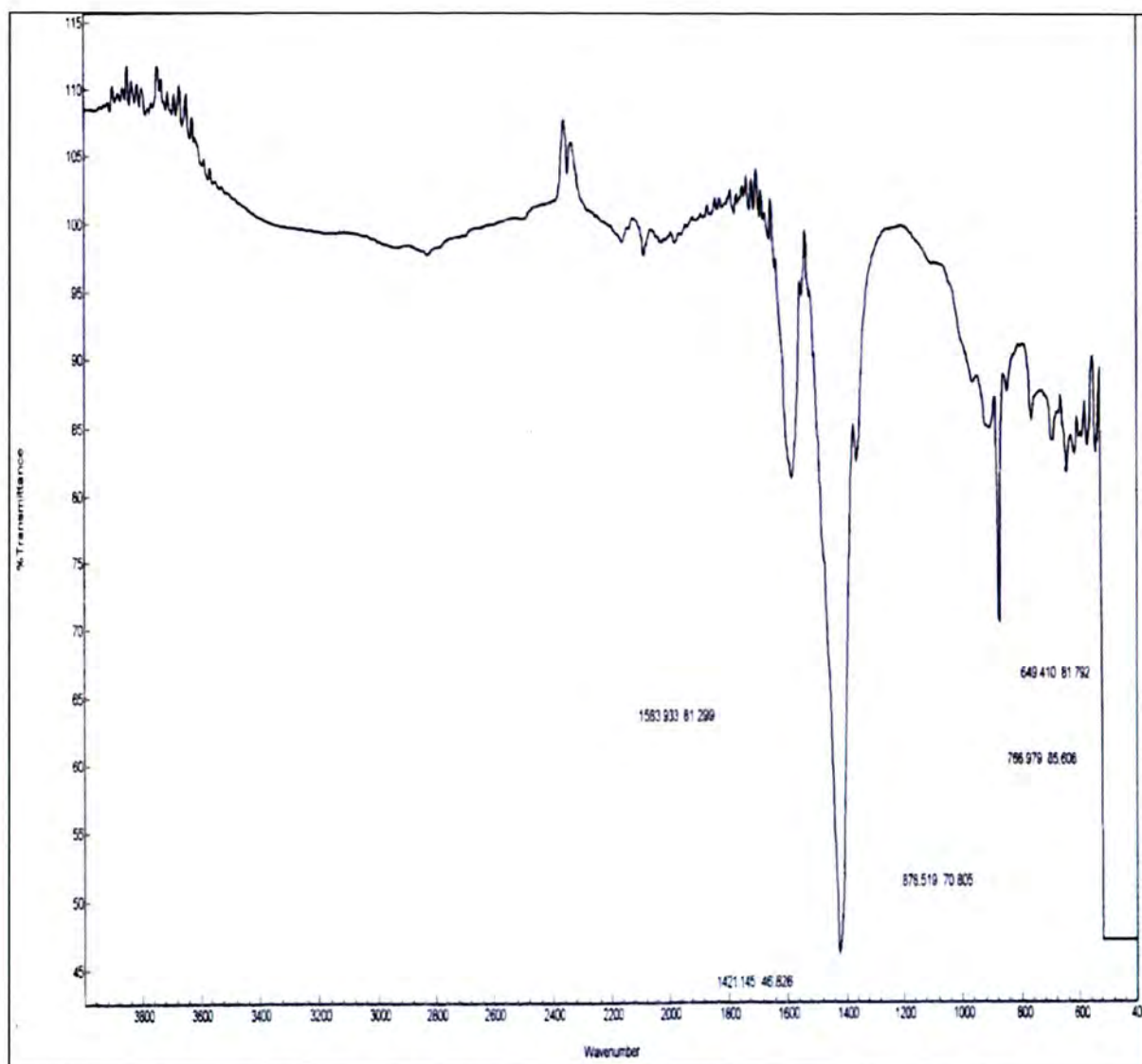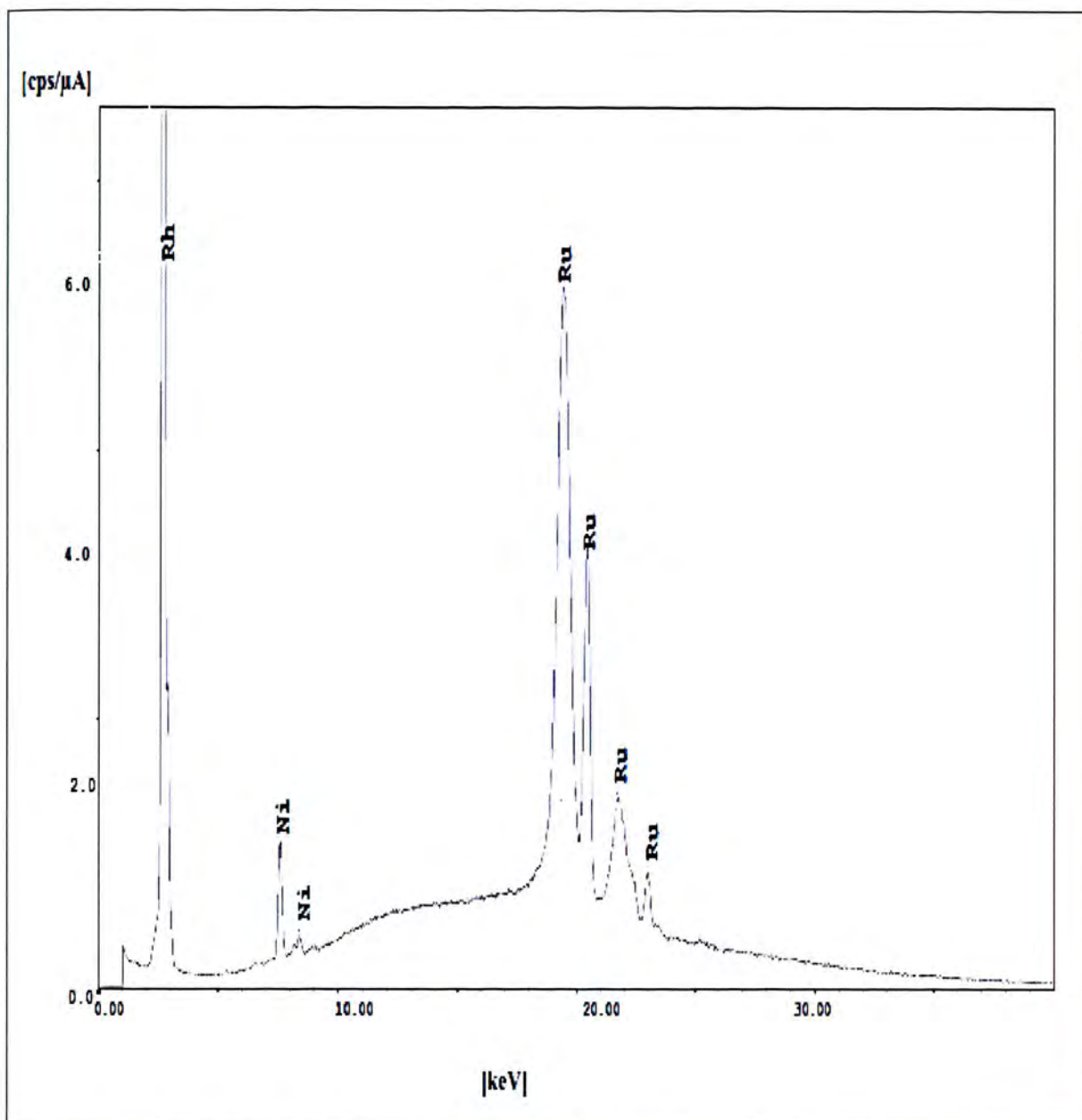
Figure 4.5. EDX spectra of 1,8-dimethyl-1,3,6,8,10,13-hexaazacyclotetradecanenickel(II) complex.

Figure 4.6. EDX spectra of 1,8-dimethyl-1,3,6,8,10,13-hexaazacyclotetradecane ligand.

EDX was carried out on the nickel(II) complex and its free ligand to probe the demetallation of 1,8-dimethyl-1,3,6,8,10,13-hexaazacyclotetradecanenickel(II) complex. The EDX profile (Figure 4.5) of the nickel(II) complex showed well-defined nickel and rhodium peaks. The occurrence of Ni peaks in the range of 7.4- 8.4 keV is in agreement with previous similar work done elsewhere.[97-98]

The disappearance of Ni(II) in Figure 4.6 suggests the successful demetallation of 1,8-dimethyl-1,3,6,8,10,13-hexaazacyclotetradecanenickel(II) complex.

Peaks representing rhodium (Rh) and Ruthenium (Ru) usually indicate radiation from the metal coatings and the specimen plug, hence can be ignored.[99]

4.2.4 ^{1}H and ^{13}C NMR spectra

The ^{1}H and ^{13}C NMR spectra of 1,8-dimethyl-1,3,6,8,10,13-hexaazacyclotetradecanenickel(II) complex and the free ligand are described below as they indicate the positions and different shifts for each molecule in a compound.

Table 4.5 summarizes the ^{1}H and ^{13}C NMR chemical shifts of 1,8-dimethyl-1,3,6,8,10,13-hexaazacyclotetradecanenickel(II) complex and the free ligand, while their spectra are shown in Figures 4.7- 4.10 respectively.

Table 4.5. Table showing proton and carbon shifts of 1,8-dimethyl-1,3,6,8,10,13-hexaazacyclotetradecanenickel(II) complex and the free ligand.

| Compound	^{1}H NMR (δ) CDCl$_3$	^{13}C NMR (δ) D$_2$O
Nickel(II) complex	1.55 (t, 4H) 3.54 (m, 4H) 7.24 (t, 6H)	28.56, 78.43, 174.60
Free ligand	1.19 (t, 4H) 3.75 (m, 4H) 7.16 (t, 6H)	39.90, 71.20, 172.60

Figure 4.7. ^{13}C NMR spectrum of 1,8-dimethyl-1,3,6,8,10,13-hexaazacyclotetradecanenickel(II) complex.

Figure 4.8. ^{13}C NMR spectrum of 1,8-dimethyl-1,3,6,8,10,13-hexaazacyclotetradecane ligand.

Figure 4.9. ^1H NMR spectrum of 1,8-dimethyl-1,3,6,8,10,13-hexaazacyclotetradecanenickel(II) complex.
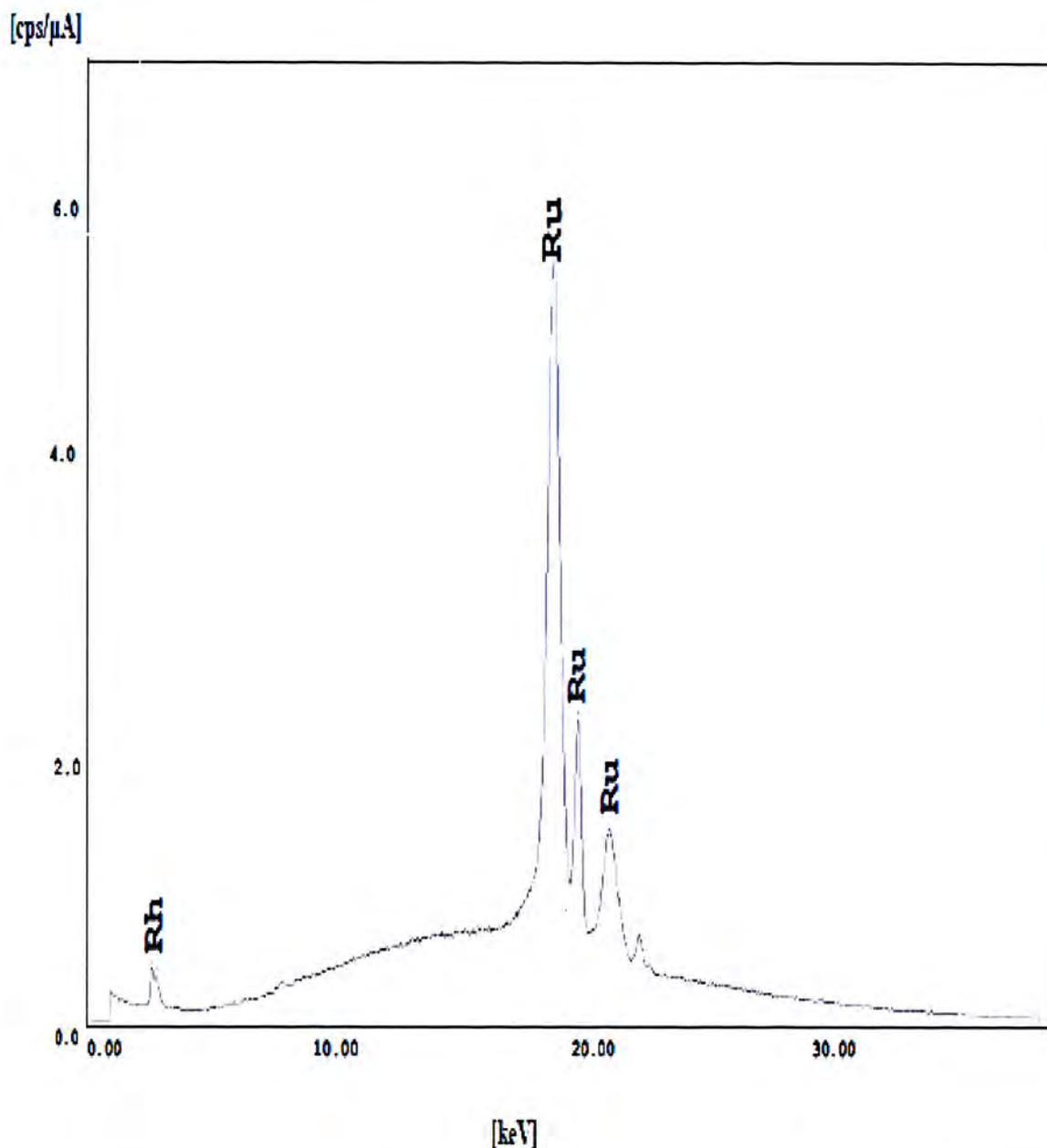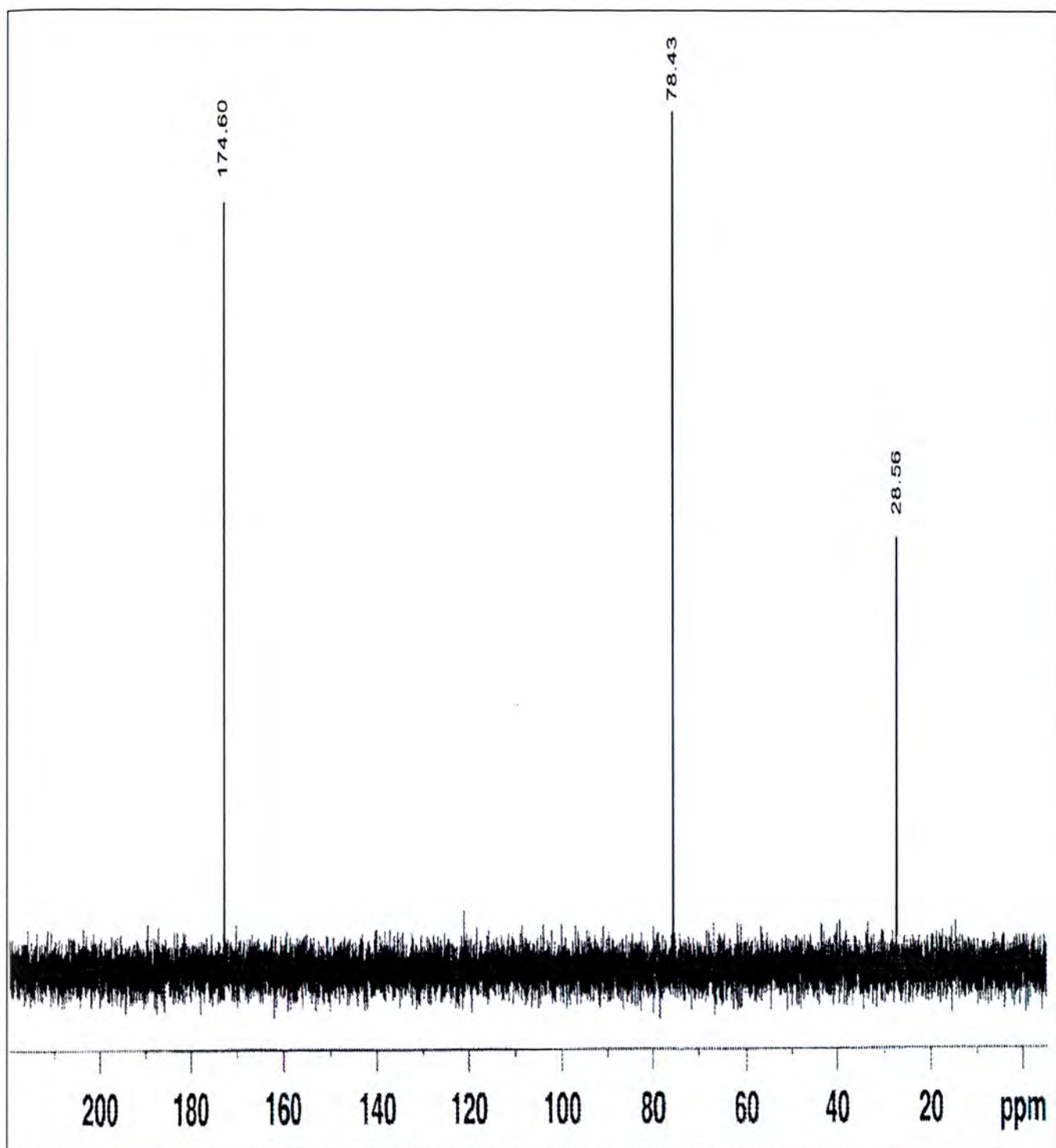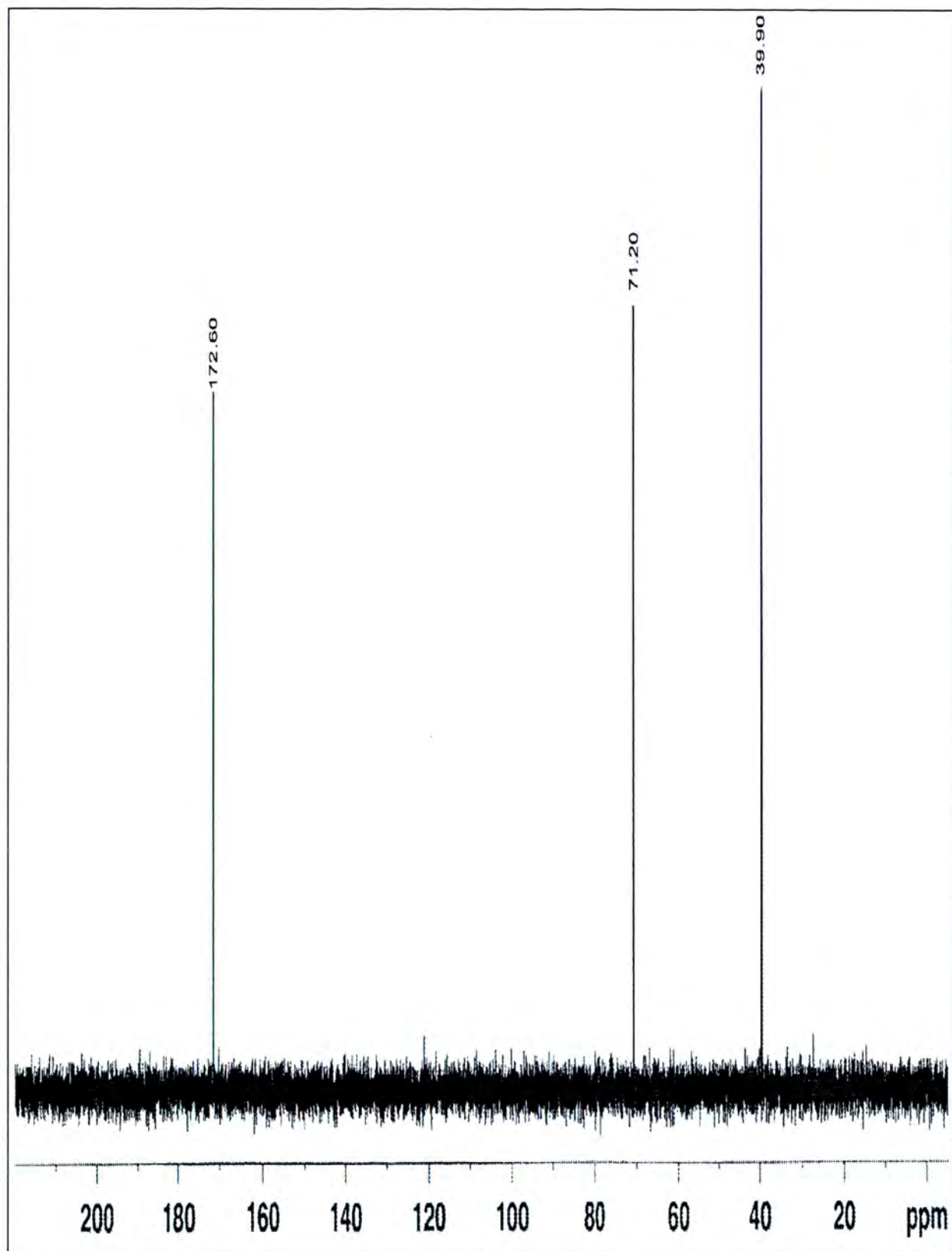
Figure 4.10. ^{1}H NMR spectrum 1,8-dimethyl-1,3,6,8,10,13-hexaazacyclotetradecane ligand.

The ^{1}H NMR of 1,8-dimethyl-1,3,6,8,10,13-hexaazacyclotetradecanenickel(II) complex indicates a triplet that appears in the up field position at 1.55 ppm, a singlet at 3.45 ppm and another singlet at 7.24 ppm in the downfield position. The triplet at the up field position is attributed to the aliphatic protons.

The ^{13}C spectra indicate three carbon peaks suggesting the nickel(II) complex exists as diamagnetic square-planar specie in D_2O. This result is in agreement with those found in literature.[7]

Nickel(II) exhibits very broad peaks in $CDCl_3$ and D_2O. This evidence supports complex exists primarily as diamagnetic square-planar species.[7] The secondary NH accounts for this broad peaks and appeared at almost the same location as found for the free ligand position.[5]

The ^{1}H NMR of 1,8-dimethyl-1,3,6,8,10,13-hexaazacyclotetradecane free ligand indicates a triplet that appears in the up field position at 1.19ppm, a singlet at 3.75 ppm and another singlet at 7.16 ppm in the downfield position. These results are closely related to the ^{1}H NMR of 1,8-dimethyl-1,3,6,8,10,13-hexaazacyclotetradecanenickel(II) complex and suggest that there is no major shifts in the compounds.

The ^{13}C spectra indicate three carbon peaks in the ligand which are similar to the ones found on the nickel(II) complex confirming the removal of the less electronegative nickel(II) ion from the complex has no major effect.

The NMR spectra were in agreement with the proposed structure.

4.2.5   The mass spectrum

The mass spectra of the complex 1,8-dimethyl-1,3,6,8,10,13-hexaazacyclotetradecanenickel(II) and its free ligand showing the molecular ion peaks are shown in Figures 4.11 and 4.12 respectively.
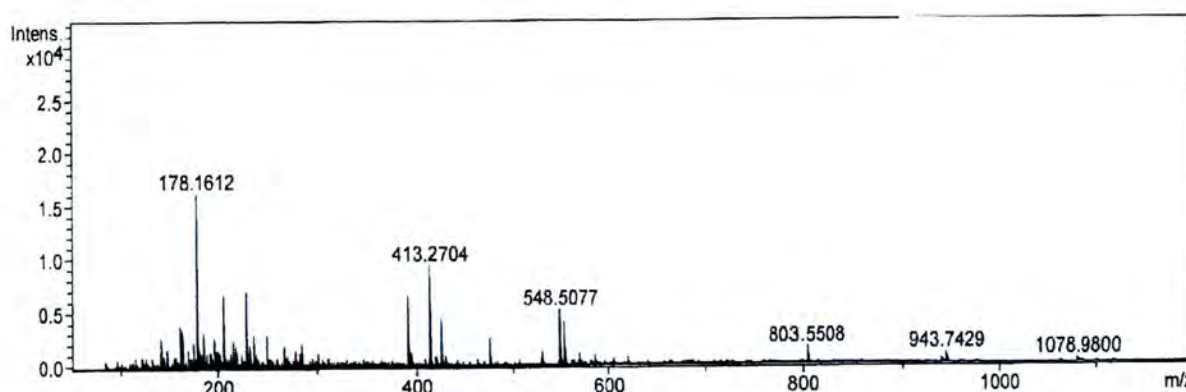
Figure 4.11. Mass spectrum of 1,8-dimethyl-1,3,6,8,10,13-hexaazacyclotetradecanenickel(II) complex.

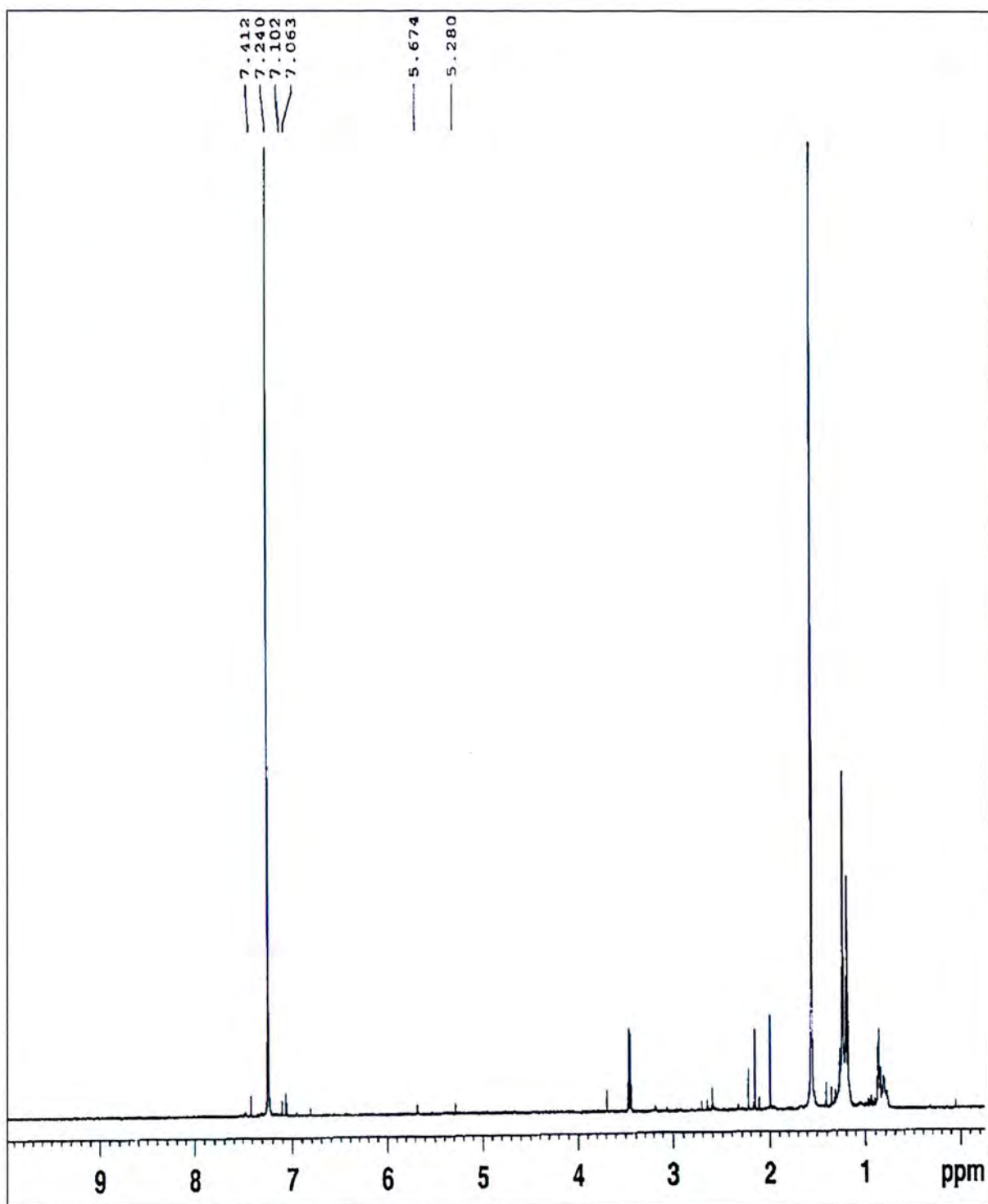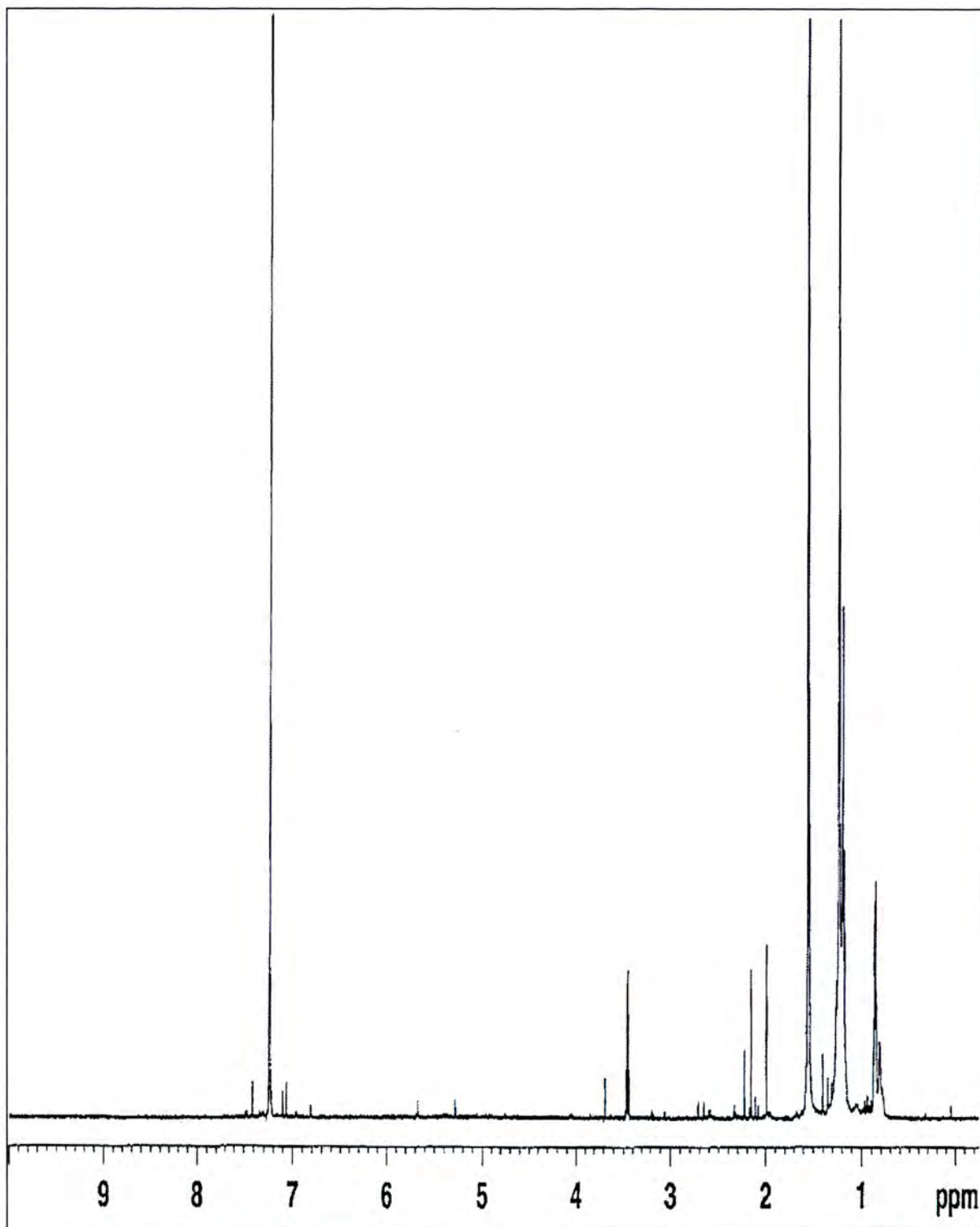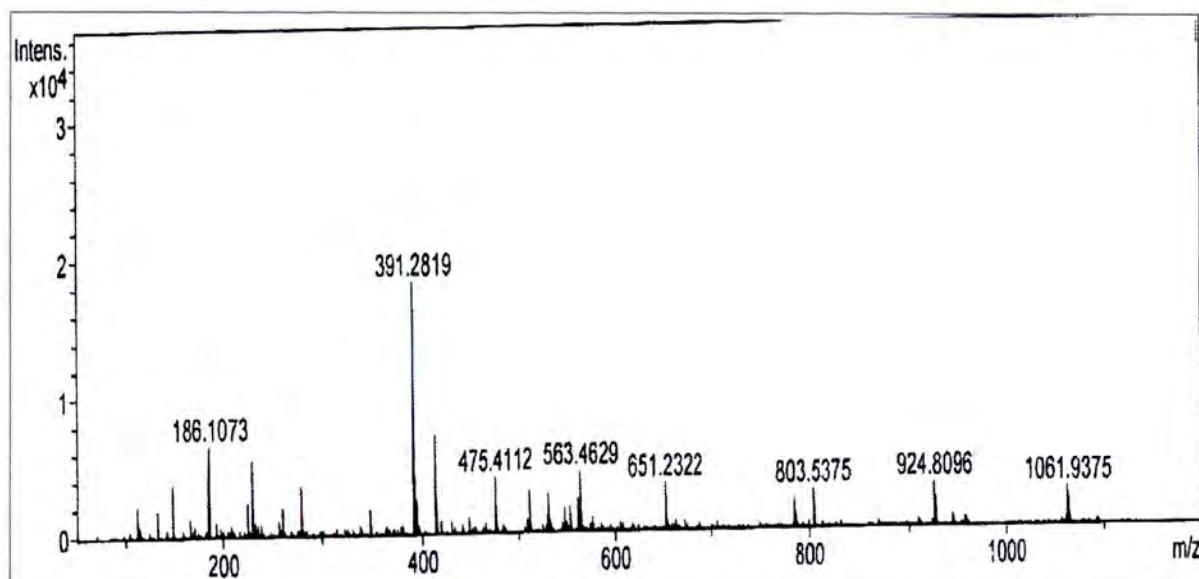**Figure 4.12.** Mass spectrum of 1,8-dimethyl-1,3,6,8,10,13-hexaazacyclotetradecane ligand.

The mass spectrum of nickel(II) complex shows the molecular ion peak at m/z 285 amu which confirms the proposed formula corresponding to the macrocyclic complex $[Ni(C_{10}H_{26}N_6)]$. The tallest line in the figure (at m/z = 178 amu $(C_{12}H_{20}N)^+$) is called the base peak. This is usually given an arbitrary height of 100, and the height of everything else is measured relative to this. The base peak is the tallest peak because it represents the commonest fragment ion to be formed. There is also other series of peaks, i.e. $206(C_{11}H_{18}N_4)^+$, $228(C_{15}H_{18}NO)^+$ and $285(C_{14}H_{27}NiO_2)^{+2}$ amu corresponding to different fragments.

The mass spectrum of free ligand shows the molecular ion peak at m/z 229 amu which confirms the proposed formula corresponding to the macrocyclic ligand $(C_{10}H_{26}N_6)$. The base peak occurs (at m/z = 391 amu $(C_{18}H_{26}N_6O_4)^+$. The other molecular ion peaks (475, 651, 803, 924 and 1061) that appeared in the mass spectrum are attributed to possible chelation due to an unstable ligand.[7] The mass spectrum of the free ligand was consistent with the proposed structural formula (Figure 3.12).

4.2.6   Thermal studies

The TGA curve of the macrocyclic ligand showing four stages of decomposition is compiled in Figure 4.13.
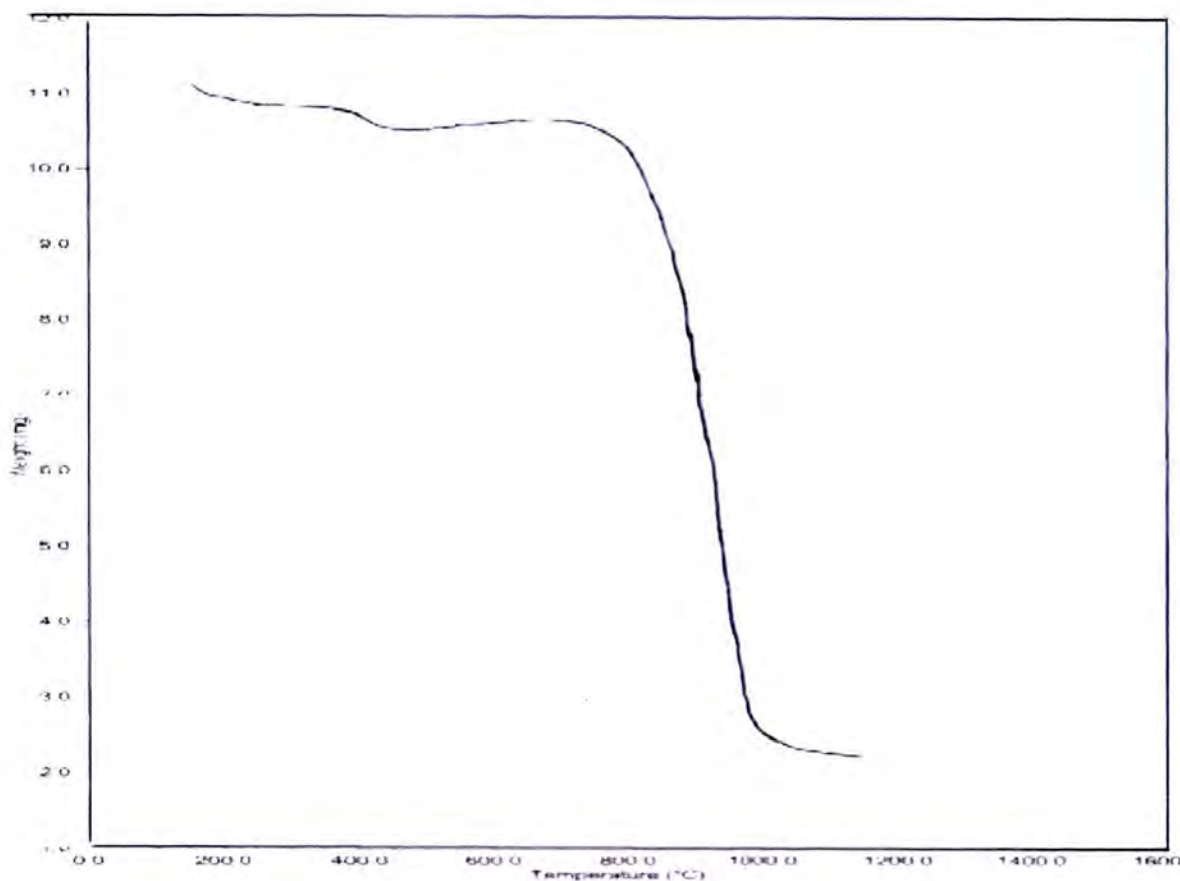
Figure 4.13.   Thermogravimetric   curve   of   1,8-dimethyl-1,3,6,8,10,13-hexaazacyclotetradecane ligand.

Interpreting the order of thermal stability in terms of the structure and nature of the ligand, often, could be complex. This order, to some extent can be made a lot easier from the basis of the steric factors such as the labile nature of ligand bonds, bulkiness of the groups attached to the ligating groups and the nature of chelate rings formed by ligand.[4]

TGA studies were carried out to illustrate the thermal stability of the free ligand and to investigate whether the water molecules are crystalline. The free ligand was thermally investigated by TGA analysis and its degradation scheme is presented in Figure 4.13. The presence of weight loss up to 300 ^{0}C shows that there is water molecule in the crystalline solid.[2] The thermogram of the free ligand ($C_{10}H_{26}N_6$) shows that it is thermally stable up to 787 ^{0}C, above which point partial decomposition of the free ligand begins. The sharp decomposition may be attributed to the loss of organic moiety and occurs in the range of 787-

48

998 ^{0}C. The final weight loss at 1173 ^{0}C, is attributed to complete decomposition of the remaining more tightly bound fragment of the organic molecules.[73] Quraishi *et al*[91] in their study of corrosion inhibiting action of MTAH on mild steel suggested that an effective corrosion inhibitor must remain effective at high temperatures.

4.3. ANTIBIOTIC RESISTANCE OF BACTERIA ISOLATES FROM MILK AND GROUNDWATER SAMPLES

S. aureus and *E. faecalis* isolates from milk and groundwater samples were obtained. These isolates were tested to evaluate their susceptibilities against 1,8-dimethyl-1,3,6,8,10,13-hexaazacyclotetradecane ligand. Data depicting the susceptibilities of the isolates were presented as diameters of inhibition zone (in mm) as shown in Tables 4.6 and 4.7 and Figures 4.14 and 4.15.

Table 4.6. Antibacterial activities data of ligand against *Staphylococcus aureus*.

Sample	Disc Conc. (μg/ml)	Inhibition diameter (mm)
1	1	6
	2	6
	3	7
	4	9

Ligand

■ LI

DIAMETER OF INHIBITION ZONE (MM)

1µg/ml   2µg/ml   3µg/ml   4µg/ml

1

CONCENTRATION
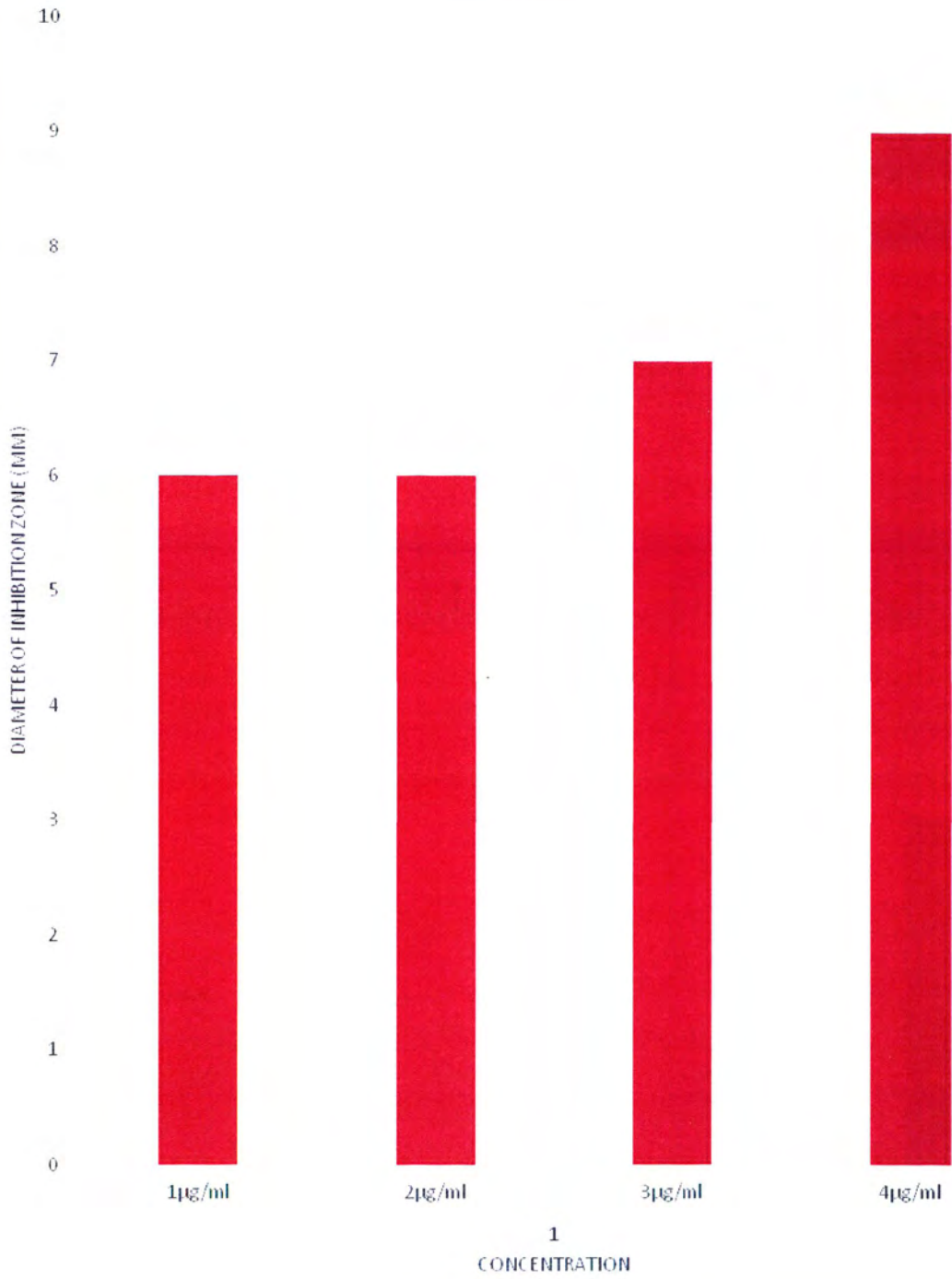
Figure 4.14. Comparison of diameter of inhibition zone of free ligand at 1-4µg/ml *Staphylococcus aureus*.

Table 4.7. Antibacterial activities data of ligand against *Enterococci species*.

Sample	Disc Conc.(µg/ml)	Inhibition diameter (mm)
1	1	6
	2	7
	3	10
	4	20

Ligand

■ LI

DIAMETER OF INHIBITION ZONE(MM)

1

CONCENTRATION
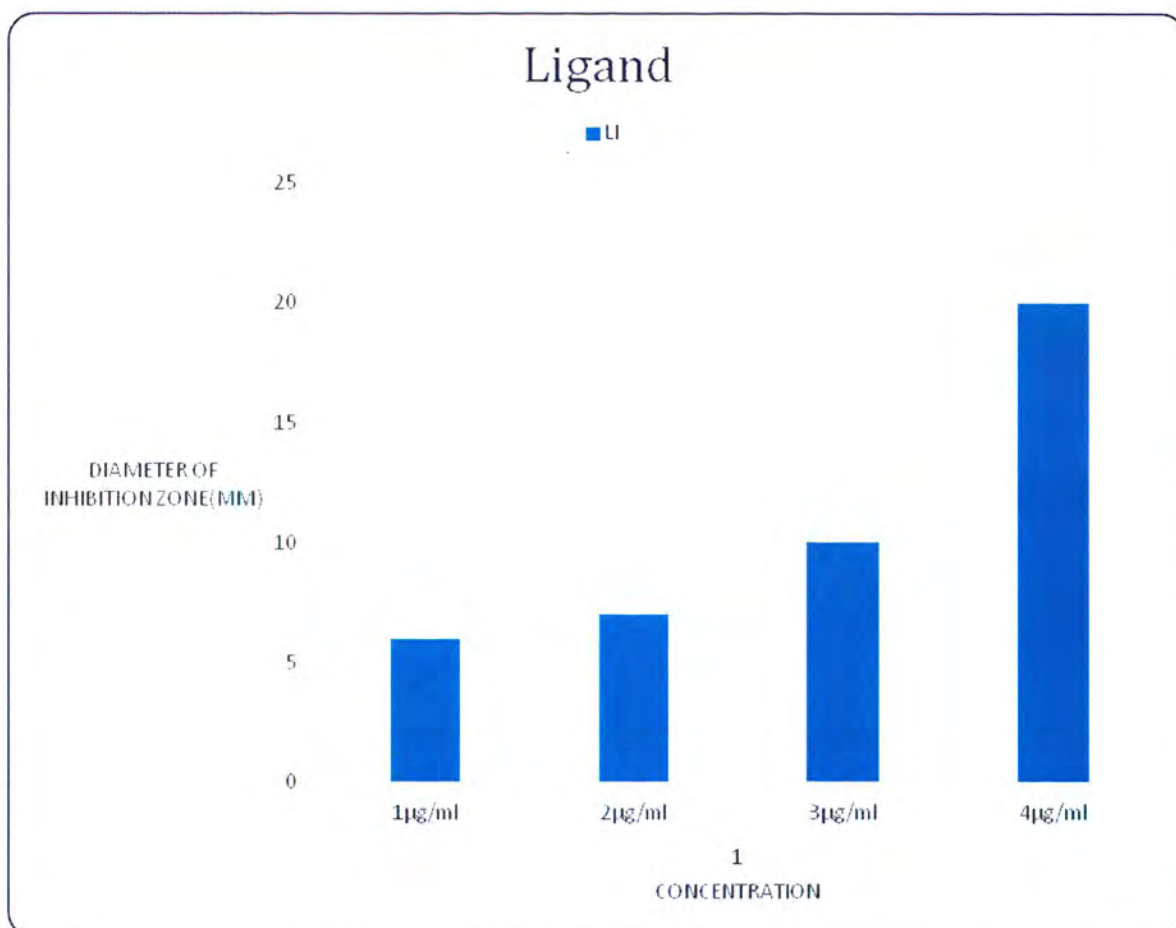
Figure 4.15. Comparison of diameter of inhibition zone of ligand at 1-4µg/ml against *Enterococcus* species.

To assess the antibacterial potential of the synthesized compounds, the macrocyclic ligand was tested against the selected bacteria.

Concentrations of 1-4 µg/ml 1,8-dimethyl-1,3,6,8,10,13-hexaazacyclotetradecane ligand were obtained and tested against *Staphylococcus aureus* and *Enterococci species* that were isolated from two sources in order to establish a reliable trend.

1,8-dimethyl-1,3,6,8,10,13-hexaazacyclotetradecane ligand is biologically active against the two bacteria strains (*Enterococci* and *Staphylococci* species) and its activity may be attributed to the presence of nitrogen donor groups and its large molecular size that offers a reasonable adsorption centres for inhibition process in many drug systems.[100-101] The ligand was found to be more toxic at higher concentration especially against *Enterococci species*.
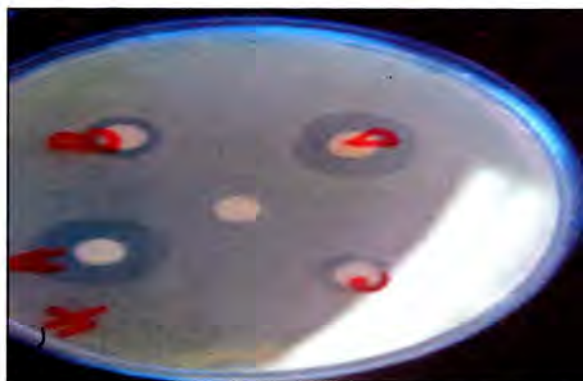
Figure 4.16. Photograph showing antimicrobial studies of free ligand at different concentrations (A=4; B=1; C= 2; D= 3 µg/ml; at the centre is control).

4.4   ELECTROCHEMICAL STUDIES

4.4.1   Cyclic voltammetric study

Figures 4.17 and 4.18 are the cyclic voltammogramms obtained for platinum electrode in both the phosphate buffer solution alone and phosphate buffer solution containing 10^{-3} M 1,8-dimethyl-1,3,6,8,10,13-hexaazacyclotetradecane ligand. Effect of scan rate (25 to 300 mVs^{-1}) on the electrochemical behaviour of the synthesised ligand was also studied and reported in Figure 4.19 (a).
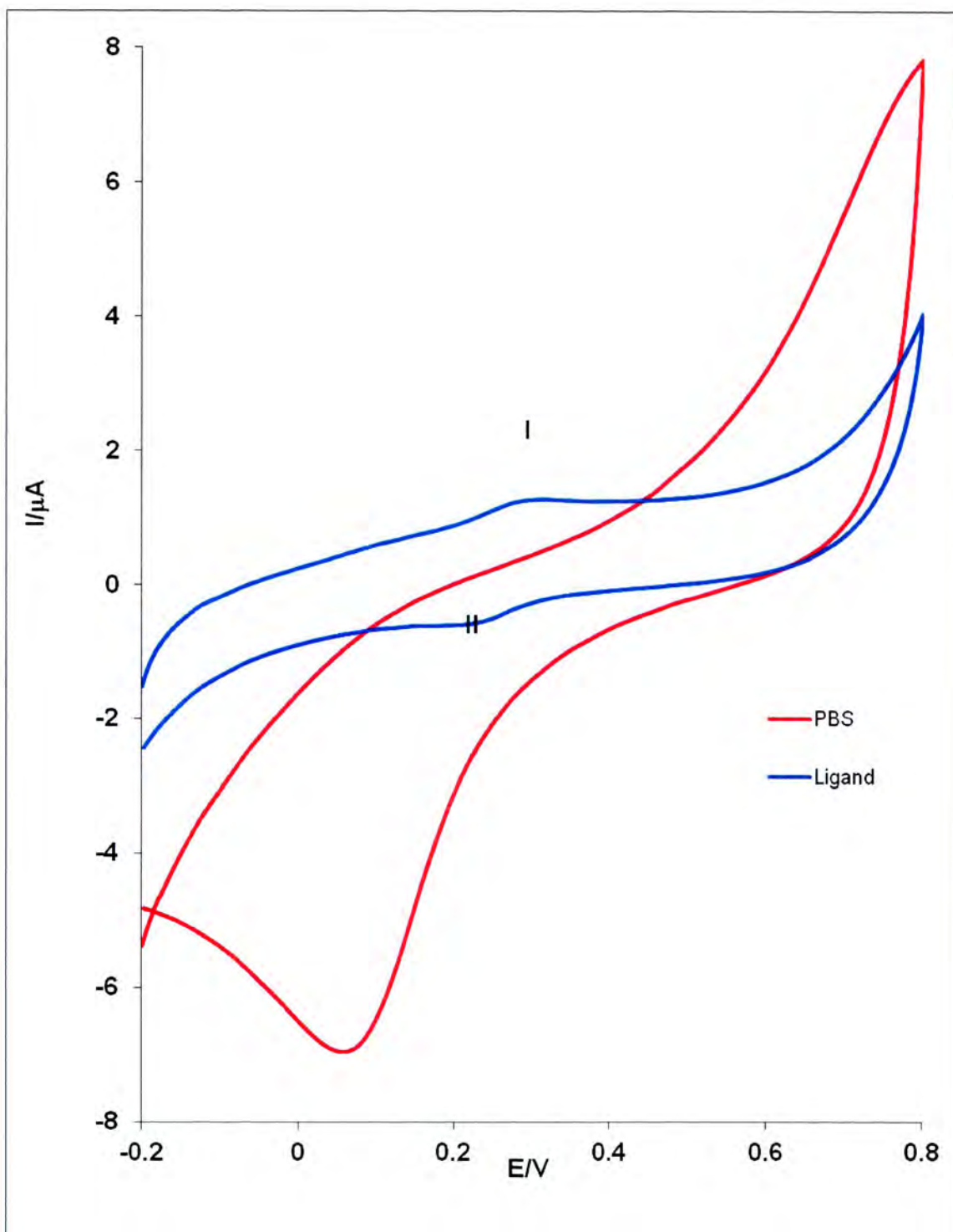
Figure 4.17. Cyclic voltammograms obtained for bare Pt electrode in 0.1 M PBS (pH 7.0) in the absence and presence of 10^{-3} M of 1,8-dimethyl-1,3,6,8,10,13-hexaazacyclotetradecane ligand (scan rate : 25 mVs^{-1}).
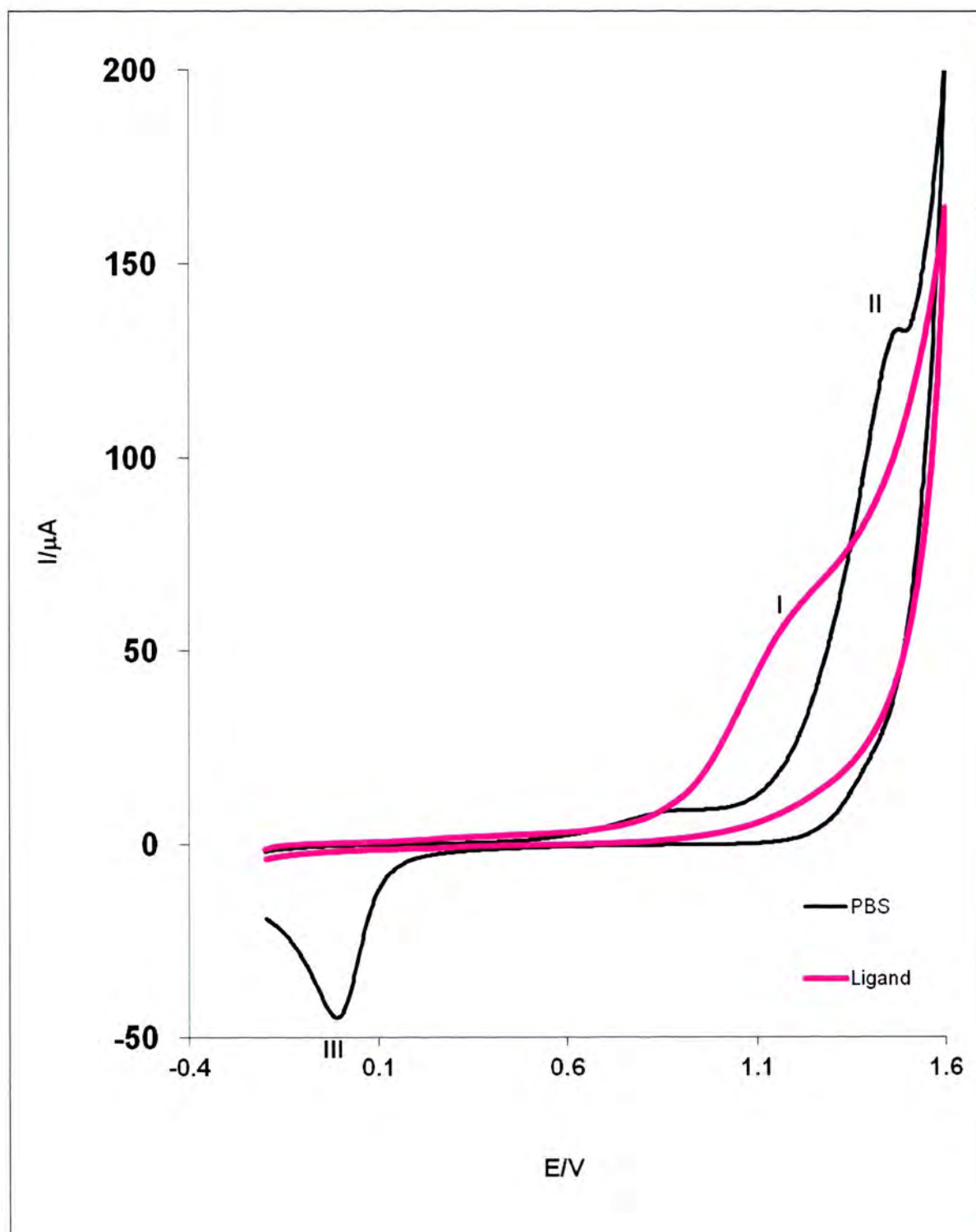
Figure 4.18. Cyclic voltammograms obtained for bare Pt electrode in 0.1 M PBS (pH 7.0) in the absence and presence of 10^{-3} M of 1,8-dimethyl-1,3,6,8,10,13-hexaazacyclotetradecane ligand (scan rate of : 25 mVs^{-1}).

The CV in Figure 4.17 showed a well-defined redox peaks at position (I) and (II) attributed to the ring redox process. The redox reversible process at 0.3 V (Figure 4.17) indicates that the ring in the ligand is electroactive.

Similar redox peaks have been observed and reported for thiol-derivatized porphyrins by Postlethwaite et al.[103] Another anodic peak around 1.3 V (I) (Fig. 4.18) not observed in the blank was attributed to the ligand oxidation process and also suggest that the synthesised ligand is electroactive and can act as catalyst in many electrochemical applications such as chemical and biochemical sensors, fuel cells etc.

The effect of scan rate on the electrocatalytic oxidation of 1,8-dimethyl-1,3,6,8,10,13-hexaazacyclotetradecane ligand at the platinum electrode was investigated by cyclic voltammetry (Figure 4.19 a). The oxidation peak potential shifted to more positive potentials with increasing scan rate which confirms diffusion kinetic limitation in the electrochemical reaction. It can be observed that when $v > 0.02 \, Dec$, the E_{pa} was significantly linearly dependent on the log v with the regression equation as follows;

$$E_{pa} = 0.0213 \log v + 0.122 \; (R^2 = 0.9907) \tag{4}$$

From (Fig. 4.19b) current is greatly enhanced with increasing the scan rate. Furthermore, plots of log of peak current (I_p) vs. log of scan rate (v); and peak potential (E_p) vs. log of scan rate (v) (Fig. 4.19c) were linear but with slight deviation from zero intercept expected for a true diffusion process[89,102] thus suggesting an interplay of an electrochemical and chemical process at the electrode. From the Tafel equation for a totally irreversible diffusion-controlled process,[104] plots of E_p versus log v gave a linear relationship and a slope (b/2 = $\partial E_p / \partial (\log v)$) of 0.0213, Vdec^{-1}, corresponding to Tafel value (b) of 42.6 mVdec^{-1} which is lower than the theoretical value of 118 mVdec^{-1} for a one-electron process in the rate-determining step, suggesting either adsorption or the involvement of reaction intermediates on the electrode surface.[105-106] The results therefore point to oxidation or chelation of the highly lipophilic ligand on the surface of the platinum electrode as indicated by the oxidation peak at around 1.3 V (Fig 4.18).
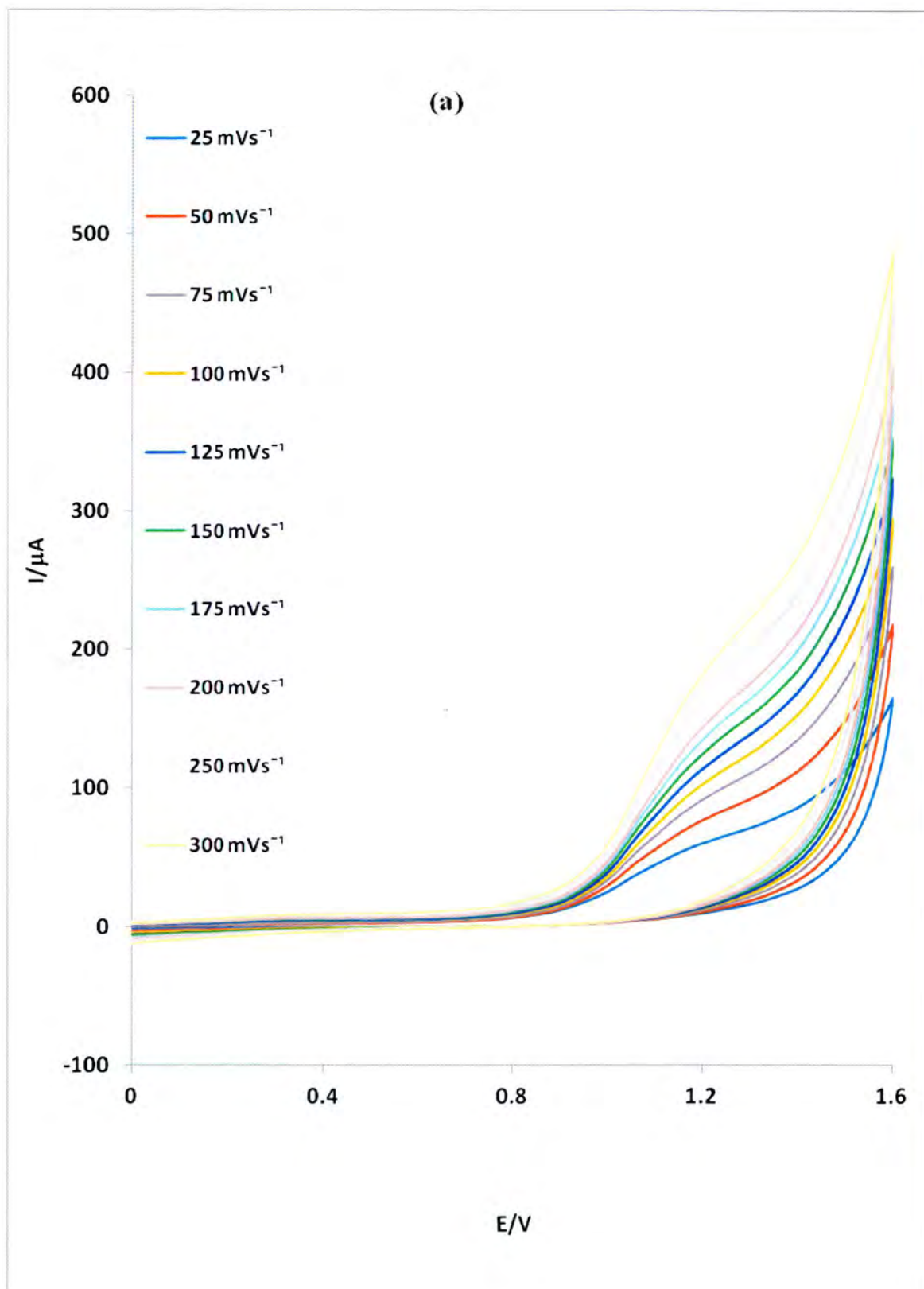
Figure 4.19 (a). Cyclic voltammograms of ligand in 0.1 M PBS (pH 7.0) at scan rates of 25, 50, 75, 100, 125, 150, 175, 200, 250 and 300 mVs⁻¹.
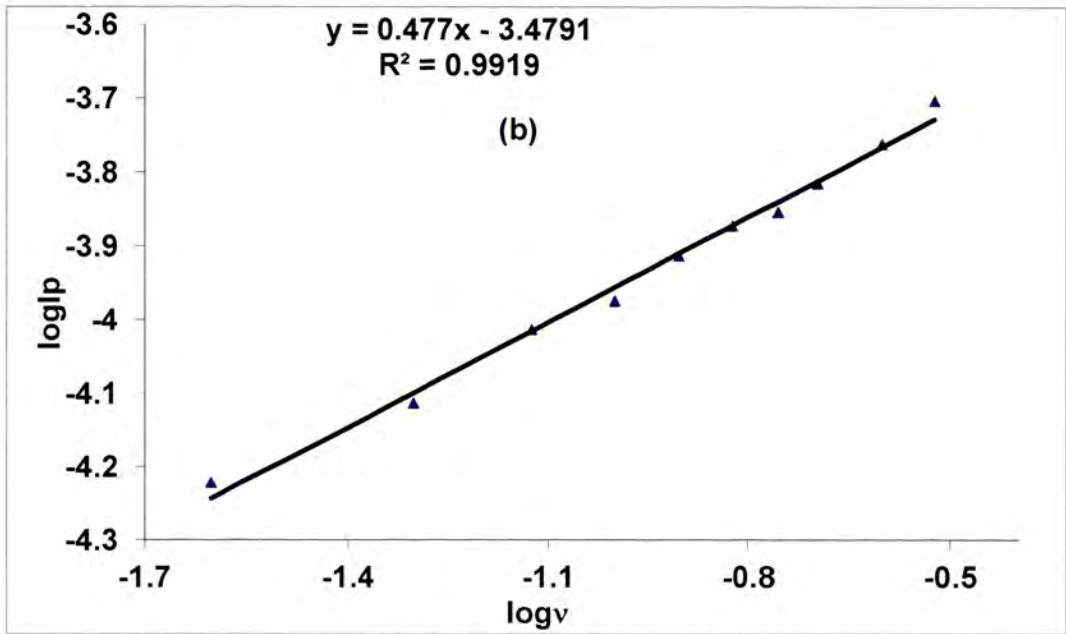
Figure 4.19 (b). Plot of log of I_p vs log v.
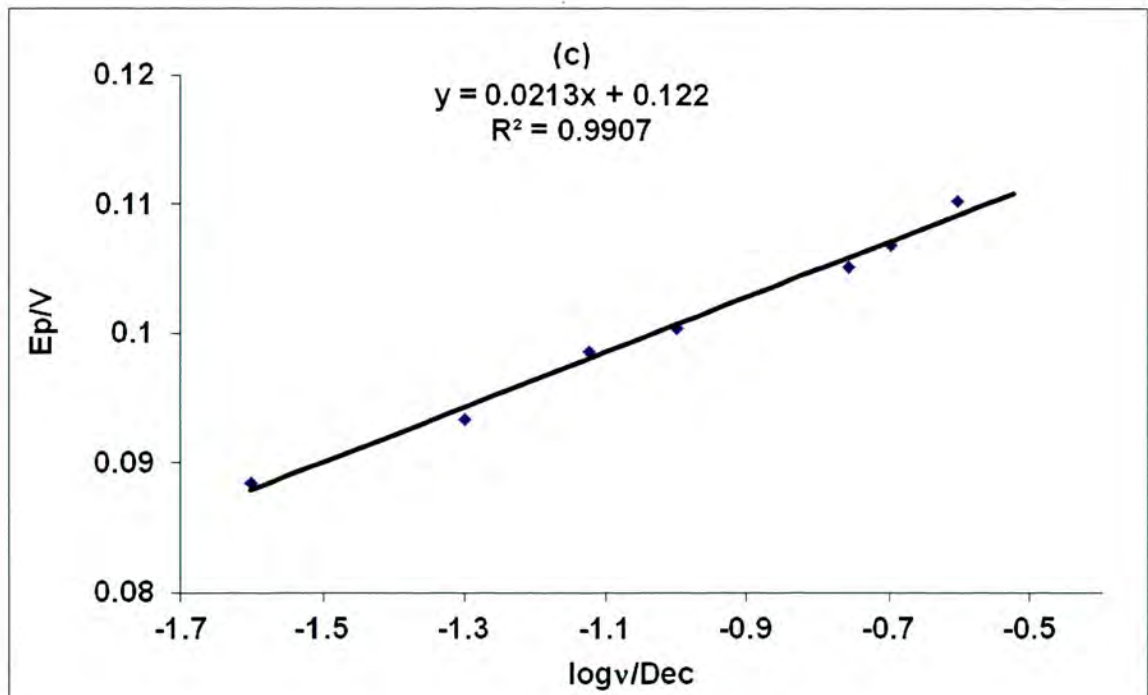
Figure 4.19 (c). Plot of E_p vs log v.

4.4.2 Potentiodynamic polarization measurement

Tafel plots was employed as a reliable tool to measure the corrosion potential (E_{corr}), corrosion current density (i_{corr}) and anodic and cathodic Tafel slopes (b_a and b_c). The linear Tafel segments of anodic and cathodic curves were extrapolated to corrosion potential to obtain corrosion current densities (i_{corr}). The Potentiodynamic polarization curves for the ligand is shown in Figure 4.20 while Table 4.8 summarizes the potentiodynamic polarization parameters for the synthesized ligand (1,8-dimethyl-1,3,6,8,10,13-hexaazacyclotetradecane).
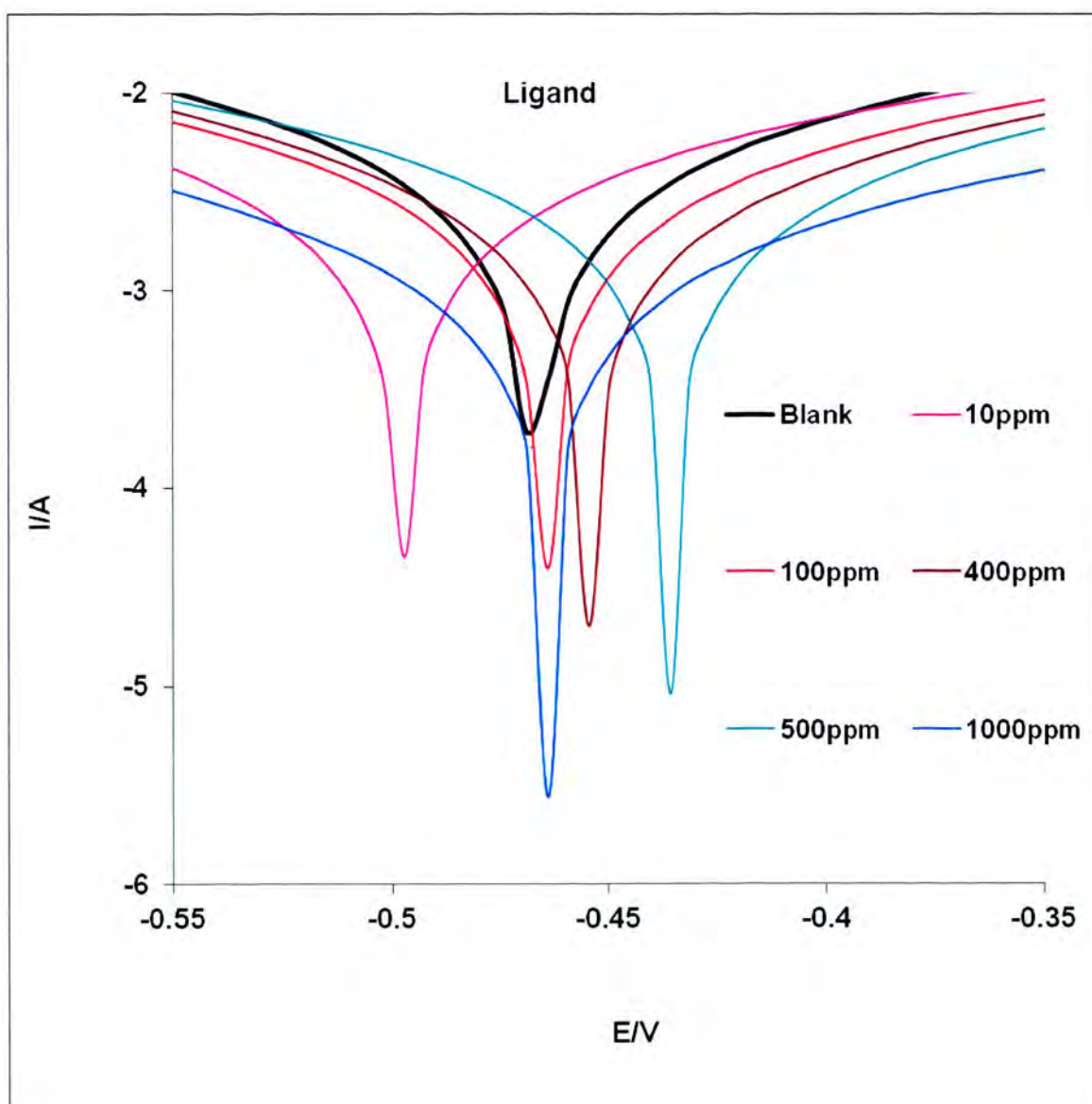
Figure 4.20. Potentiodynamic polarization curves for mild steel in 1 M HCl in the absence and presence of different concentrations for 1,8-dimethyl-1,3,6,8,10,13-hexaazacyclotetradecane ligand.

Table 4.8. Potentiodynamic polarization parameters such as corrosion potential (E_{corr}), corrosion current density (i_{corr}) and anodic and cathodic Tafel slopes (b_a and b_c) at different 1,8-dimethyl-1,3,6,8,10,13-hexaazacyclotetradecane ligand concentrations

Name of inhibitor	Conc. of Inhibitor (ppm)	$-E_{corr}$ (mV vs. Ag/AgCl, 3 M KCl)	i_{corr} ($\mu A\ cm^{-2}$)	b_a (mV dec^{-1})	b_c (mV dec^{-1})	E_{PDP} %
Blank	-	467	2838.0	134	185	-
1,8-dimethyl-1,3,6,8,10,13-hexaazacyclotetradecane ligand	10	498	2288.0	153	215	76.54
	100	465	1947.0	128	176	79.53
	400	445	1296.0	90	120	89.61
	500	436	1251.0	90	118	95.28
	1000	464	581.1	86	129	98.58

It is evident from Table 4.8 that the value of b_a and b_c changed or increased at 10 ppm concentration of the inhibitor which indicates the influence of the inhibitor on the hydrogen evolution reaction. However, after 10 ppm, the Tafel values (b_a and b_c) decreased with increasing concentration of the inhibitors, suggesting the adsorption of the ligand on the mild steel surface thus reducing its dissolution in the acid. This is also supported by the decrease I$_{corr}$ values with increasing inhibitor concentration suggesting adsorption on the mild steel surface. Similarly, Inhibition efficiency of the inhibitor increased with concentration with highest inhibition efficiency of 98.58% recorded at 1000 ppm (Table 4.8).

The efficiency of the inhibitor was evaluated from dc measurements by employing equation (2).

It was also observed that in the presence of the inhibitor, the curves shifted to the lower current regions. This trend supports the corrosion inhibitive property of the ligand utilized in this study. The shift or displacement in E_{corr} with respect to the blank is within 30-40 mV. It is reported by different workers that, if the displacement in corrosion potential is more than 85 mV with respect to blank solution, the inhibitor can be considered as a cathodic or anodic type.[107-108] Therefore E$_{corr}$ shift observed in this study suggest a mixed type inhibition mechanism which is in agreement with other mixed type mechanism reported in literature.[109-110] The utilized ligand is therefore a mixed type inhibitor, but significantly cathodic inhibitor.

4.4.3 Electrochemical impedance

Electrochemical impedance spectroscopy was employed to study the corrosion behaviour of mild steel in 1 M HCl in the absence and presence of different concentrations of the ligand at room temperature. The impedance technique is a very sensitive technique which gives insight into the mechanism of the electron transport between the electrode|electrolyte interface. The Nyquist and Bode plots of mild steel in uninhibited and inhibited acid solutions containing different concentrations of the ligand are presented in Figures 4.21-4.23.

Figure 4.21. Nyquist plots obtained for mild steel in 1 M HCl in the absence and presence of concentrations of ligand (10, 100, 300 and 500 ppm).
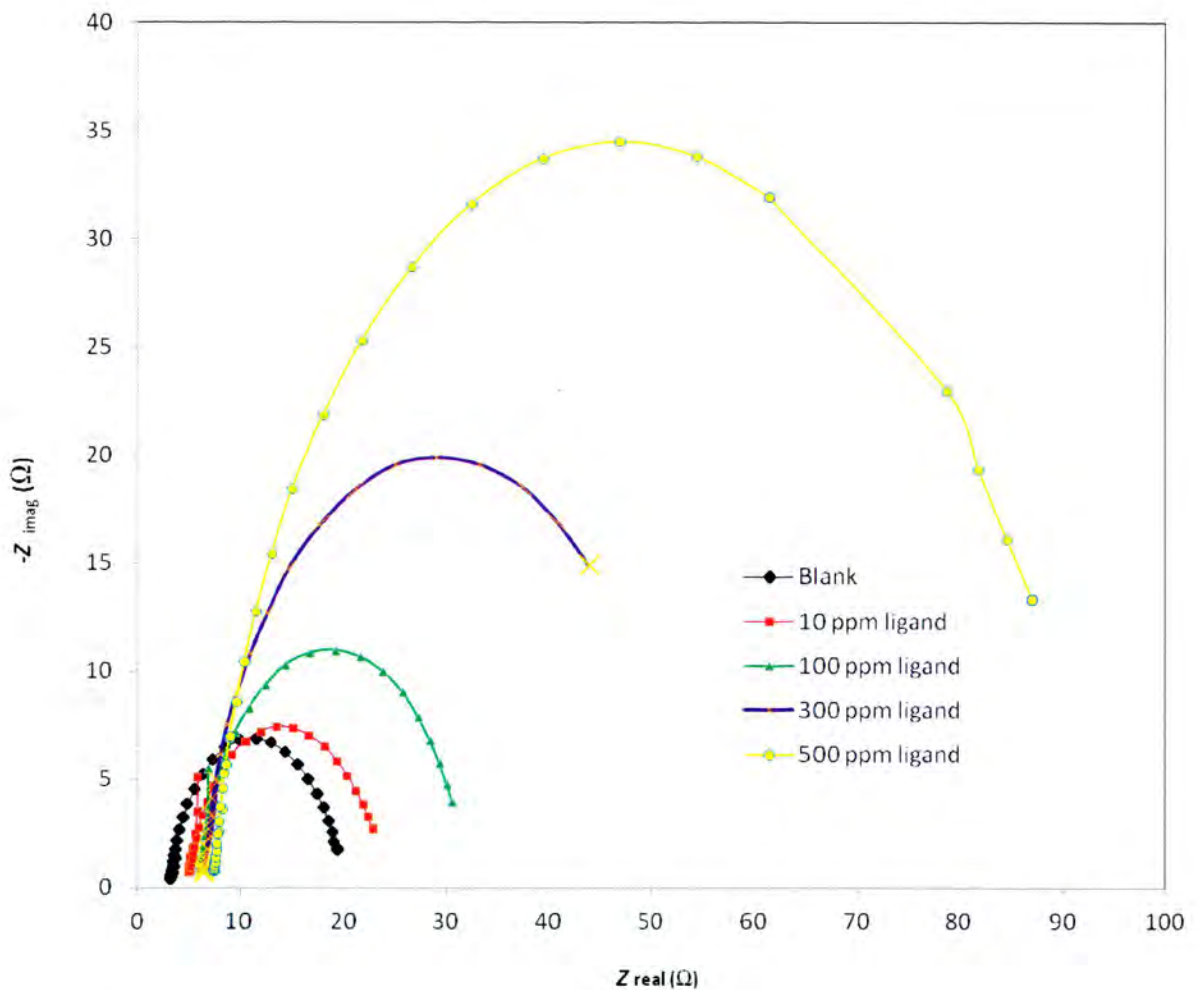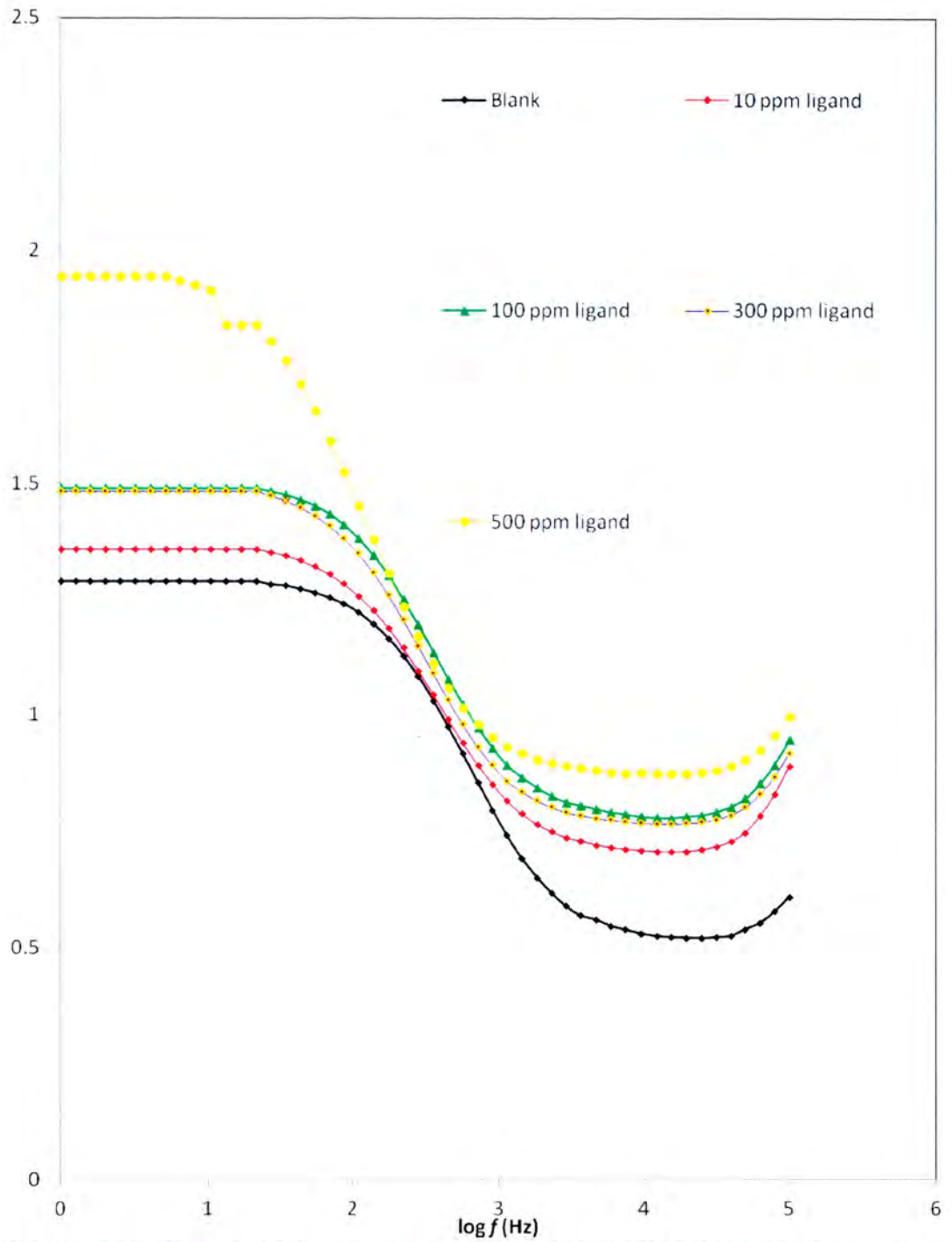
Figure 4.22. Bode-modulus plots for mild steel in 1 M HCl in the absence and presence of concentrations of ligand (10, 100, 300 and 500 ppm).
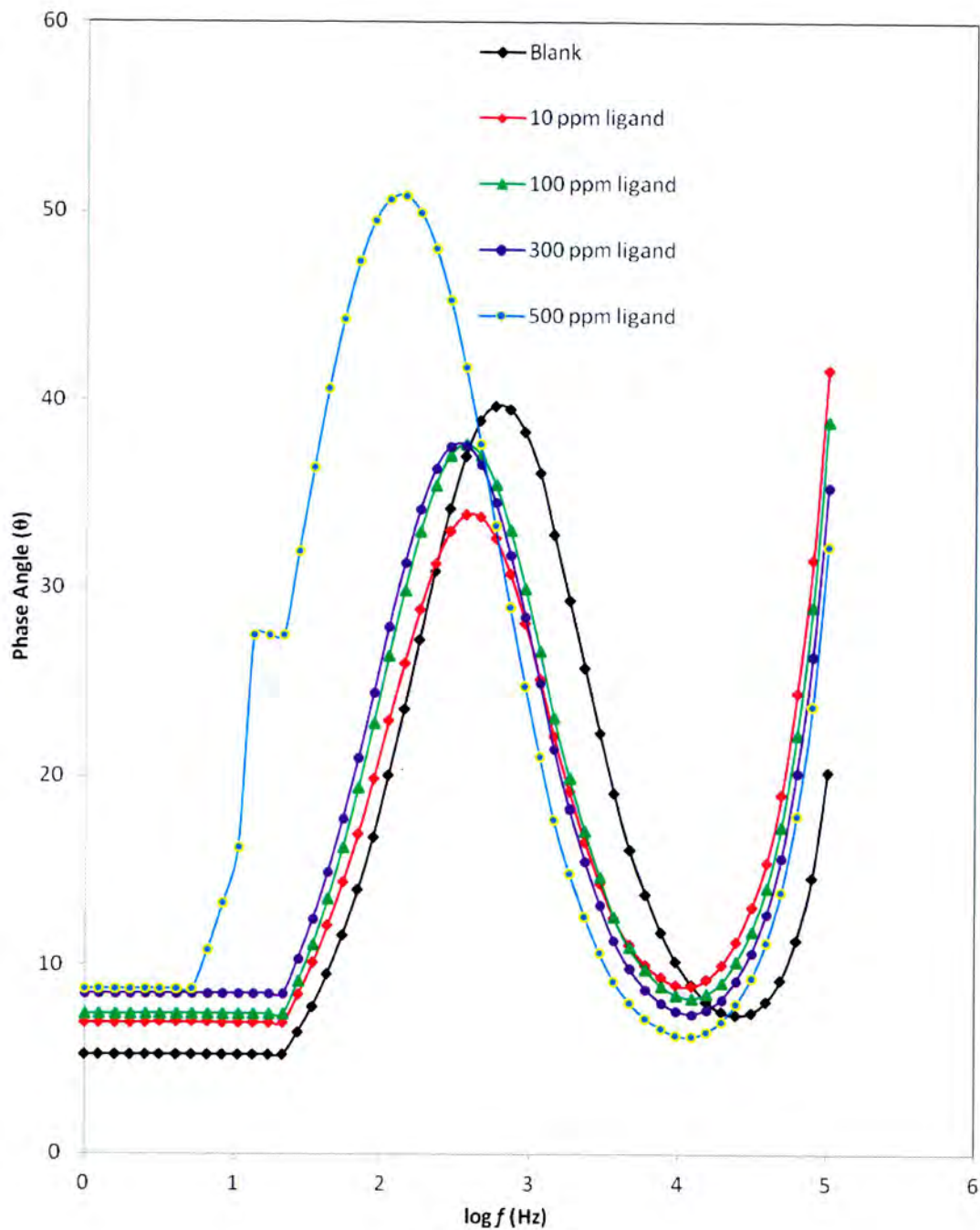
Figure 4.23. Bode-phase angle plots obtained in 1 M HCl in the absence and presence of ligand concentrations (10, 100, 300 and 500 ppm).

The EIS data was satisfactorily fitted with the equivalent circuit model (Figure 4.24), judged by the values of the pseudo Chi-square (χ^2) and relative % errors (Table 4.9) as well as the goodness of fit where C_{dl} is the true capacitance and Z_w is the Warburg impedance. In this model the R_s is the solution/electrolyte resistance, R_{ct} represents the charge transfer resistance, C_{film} describes the high pseudocapacitive nature of the system while CPE describes porous nature of the electrode. The semi-circle diameter at a higher frequency represents electron-transfer resistance (R_{ct}). The absence of the linear part at lower frequency confirms the absence of diffusion process. As shown in Figure 4.21, there is a remarkable increase in the semicircle diameter at higher concentrations of ligand which confirms that electron-transfer resistance is greatly enhanced. Related impedance behaviour was reported by Chen et al[89] and Adekunle et al[98,111] in their work on electrochemical impedance studies. The frequency dispersion which has been attributed to the roughness and other inhomogeneity of the electrode often result in the Nyquist impedance plots to exhibit imperfect semicircles.[93-95] The depression in Nyquist semicircles is a characteristics of solid electrodes and often referred to as frequency dispersion.

Table 4.9. Fitted impedance parameter of mild steel in HCl 1M solutions at 30 °C in absence and presence of 1,8-dimethyl-1,3,6,8,10,13-hexaazacyclotetradecane ligand in different concentrations. All values were obtained from the fitted impedance spectra after several iterations using the circuit. Values in parentheses are the percentage errors of data fitting

Concentration (ppm)	R_s (Ωcm^2)	C ($\mu F\ cm^{-2}$)	R_{ct} ($\Omega\ cm^2$)	Z_W ($\Omega\ cm^2$)	$E_{EIS}\%$
Blank	1.520 (1.969)	0.002 (4.801)	8.98 (6.563)	0.1313 (32.766)	-
10 ppm	5.20 (3.857)	49.4 (9.237)	17.76 (6.119)	8.323 (44.877)	49.44
100 ppm	6.20 (3.548)	39.9 (7.882)	24.35 (5.508)	6.293 (42.672)	63.12
300 ppm	6.64 (3.400)	56.5 (17.105)	34.8 (6.464)	1.868 (20.155)	74.20
500 ppm	7.74 (2.941)	53.1 (5.116)	71.4 (5.448)	1.859 (34.499)	87.35
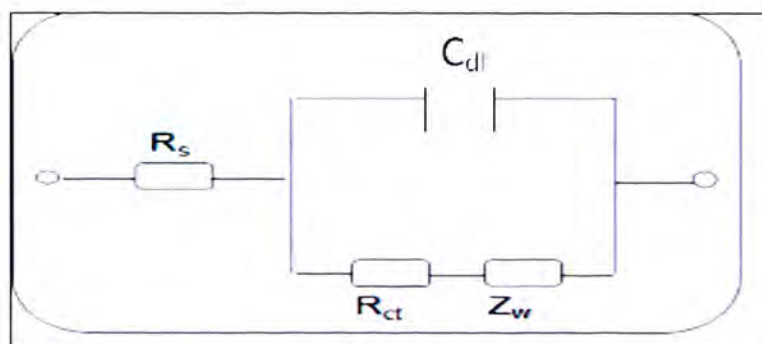
Figure 4.24. The equivalent circuit of the impedance spectra obtained for mild steel in the presence of 1,8-dimethyl-1,3,6,8,10,13-hexaazacyclotetradecane ligand.

The inhibition efficiency (E_{EIS} %) was calculated from the data obtained from the electrochemical impedance (Table 4.9) according to equation (3) above but now reduced to equation (5) below:

$$E_{EIS}\ \% = \left[1 - \frac{R_{ct}^{0}}{R_{ct}}\right] \times 100 \qquad (5)$$

where, R_{ct}^{0} is the charge transfer resistance in the absence of the inhibitor and R_{ct} is the charge transfer resistance in the presence of the inhibitor.

Charge transfer resistance (R_{ct}) was obtained from EIS measurement as described by Singh.[93] The high R_{ct} values support the formation of surface film and the observed properties of the inhibitor. It is apparent from Table 4.9 that the charge transfer resistance (R_{ct}) of the inhibited system increases with increasing inhibitor concentration and the W values decreased with increasing inhibitor concentration. This decrease in W is due to a decrease in local dielectric constant, and suggests that inhibitor molecules inhibit the mild steel corrosion by adsorption at the metal/acid interface. Similar findings was reported by Murulana et al.[112]

The data obtained for EIS measurements and the PDP were not very comparable. Differences in inhibition efficiency between polarisation and EIS experiments have been reported in the literature and some reasons have been advanced for this observation. For instance Pereira et al[113] reported that the differences in IE between these two techniques could be due to applied potential since in EIS experiments, the electrode was under the open-circuit potential whereas in polarization experiments, the working electrode was polarized and the electrochemical parameters was obtained by extrapolation of the Tafel lines. Also Oguzie et al[114] opined that

the differences could be attributed to predominant influence of the anodic dissolution process in determining the corrosion rate from polarization measurements.

4.5.1 Adsorption isotherm studies

Gomma et al[115] reported that the adsorption of an organic adsorbate on to metal-solution interface can be represented by a substitutional adsorption process between the organic molecules in the aqueous solution phase ($Org_{(sol)}$) and the water molecules on the metallic surface ($H_2O_{(ads)}$). This is given in equation (6) below:

$$Org_{(sol)} + xH_2O \rightarrow Org_{(ads)} + xH_2O_{(sol)} \qquad (6)$$
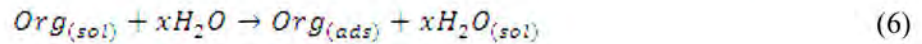
where x represents the size ratio of the number of water molecules replaced by one molecule of organic substrate.

Thermodynamic parameters have been reported to play an important role in understanding corrosion inhibition mechanism.[116] Further study on adsorption isotherms was done in order to gain more insights into the mechanism of corrosion inhibition, due to the fact that it describes the molecular interaction of the inhibitor molecule with the active sites on the metal surface.[92,95,115-117] Different adsorption isotherms were applied which include Langmuir, Temkin, Freundlich, Frumkin and Flory-Huggins adsorption isotherms. Overall, the free ligand was found to obey Langmuir adsorption isotherm. This was determined by plotting the concentration of the inhibitor/ surface coverage ($\frac{C_{inh}}{\theta}$) against concentration of the inhibitor (C_{inh}). This is represented in equation (7) below:

$$\frac{C_{inh}}{\theta} = \frac{1}{K_{ads}} + C_{inh} \qquad (7)$$

where θ is the degree of surface coverage, K_{ads} is the equilibrium constant of the adsorption process and C_{inh} is the concentration of the inhibitor. K_{ads} represents the degree of adsorption, i.e. the higher the value of K_{ads} signifies that the inhibitor is strongly adsorbed on the mild steel surface.[95,109,114,118-119] One of the Langmuir assumptions holds that a solid surface contains a fixed number of adsorption sites and each of these sites can only hold one adsorbed species. Figure 4.25 shows the Langmuir adsorption isotherm obtained for adsorption of the ligand at 30° C.
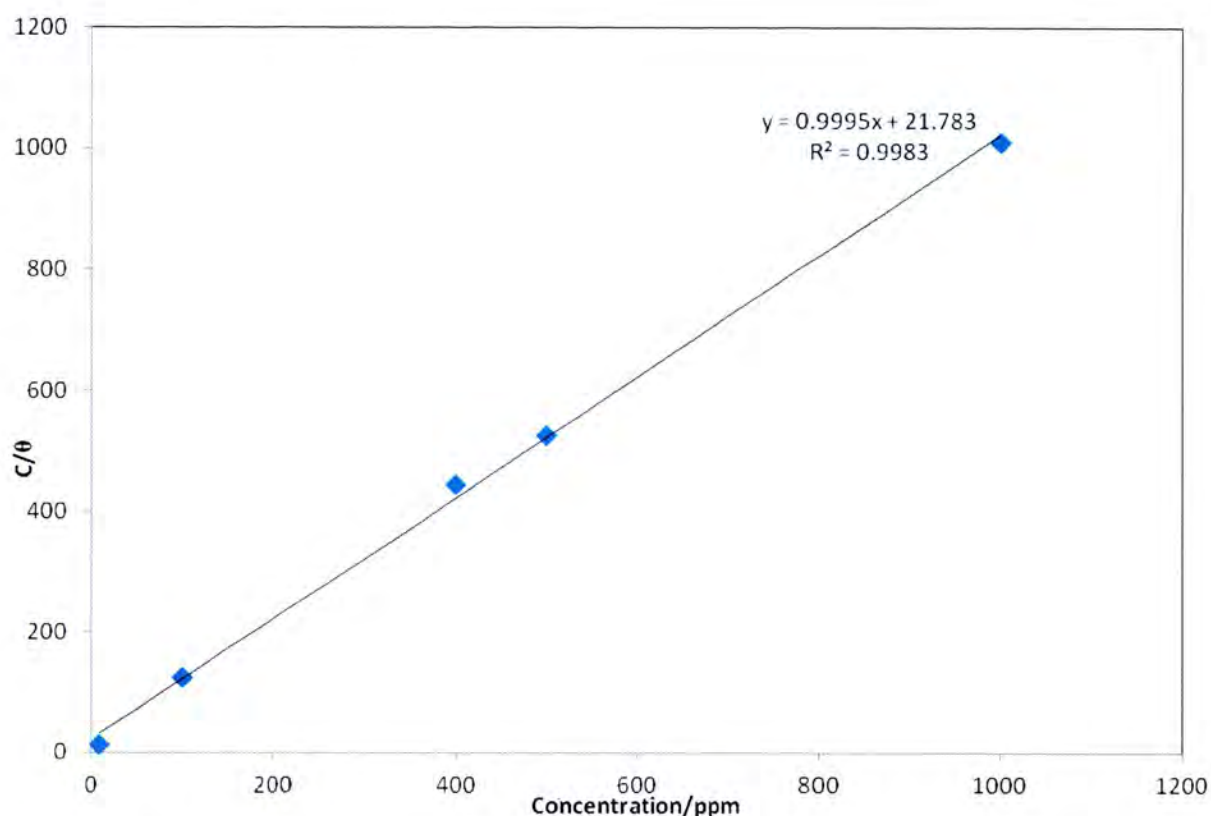
Figure 4.25. Langmuir adsorption isotherm plot for 1,8-dimethyl-1,3,6,8,10,13-hexaazacyclotetradecane ligand on C-steel at 30° C.

Equation (8) represents the relationship between free energy of adsorption ΔG°_{ads} and the modified adsorption equilibrium constant K_{ads}. $C_{solvent}$ is the molar concentration of the solvent, which, normally in the case of water, is 55.5mol L^{-1}.

$$k = \frac{1}{C_{solvent}} \exp\left[\frac{-\Delta G^{o}_{ads}}{RT}\right] \qquad (8)$$

where R is the universal gas constant and T is the thermodynamic temperature.

The free energy of adsorption ΔG°_{ads} is a very important thermodynamic tool that gives information about the type of adsorption process.

It is widely accepted that the standard adsorption free energy (ΔG°_{ads}) is related to the equilibrium constant of adsorption (K_{ads}), and ΔG°_{ads} can be calculated by the following equation (9):

$$\Delta G^{\circ}_{ads} = - RT \ln (55.5 K_{ads} \qquad (9)$$

Table 4.10 shows the calculated ΔG°_{ads} value, utilizing equation (10)

Table 4.10. Equilibrium constant of adsorption (K_{ads}) and $\Delta G^\circ_{ads.}$

Inhibitor	K_{ads} (L mol^{-1})	ΔG°_{ads} (kJmol^{-1})
1,8-dimethyl-1,3,6,8,10,13-hexaazacyclotetradecane ligand	5×10^4	-37.4

It is generally accepted that values for free energy of adsorption ΔG°_{ads} up to -20 kJ mol^{-1}, suggest the electrostatic interaction between the charged molecules and the charged metal surface (i.e. physisorption), whereas those around -40 kJ mol^{-1} or smaller involves charge sharing or transfer from organic molecules to the metal surface to form coordinate type of metal bond (chemisorption).[95,115-119]

The ΔG°_{ads} value obtained in this study is -37.4 kJ mol^{-1} and suggests that the adsorption mechanism of 1,8-dimethyl-1,3,6,8,10,13-hexaazacyclotetradecane ligand on mild steel surface in 1 M HCl medium involves chemisorption and it is spontaneous.[116]

4.6 MECHANISM OF CORROSION INHIBITION

The proposed mechanism of corrosion inhibition by the 1,8-dimethyl-1,3,6,8,10,13-hexaazacyclotetradecane is better understood on the basis of adsorption of the ligand on the metal surface. This adsorption is promoted by the presence of multiple N donor atoms of inhibitor, ring structure as well as the vacant d orbitals of the iron surface.[49,117] The ability of the molecules of this macrocyclic ligand to lie flat on the surface of mild steel thereby facilitating blockage of more surface area of the mild steel also contributed to its corrosion inhibitive property.[49]

Babić-Samardžija et al[50] suggested that the inhibition at metal surfaces usually involves the formation of some metal cluster complexes. This idea was supported by Quraishi et al[49] in their study suggesting that corrosion inhibition occurs by the adsorption of these macrocycles on to the surface of the metal through formation of a protective layer.[120,121] The mechanism of corrosion inhibition is therefore by chemisorption as indicated too by the ΔG°_{ads} value.

CHAPTER 5

CONCLUSION

5.1 CONCLUSION

- 1,8-dimethyl-1,3,6,8,10,13-hexaazacyclotetradecanenickel(II) was successfully synthesized via template condensation of ethylenediamine, formaldehyde, and methylamine in the presence of nickel(II) chloride.

- Demetallation of 1,8-dimethyl-1,3,6,8,10,13-hexaazacyclotetradecanenickel(II) complex was done under sodium hydroxide and sodium cyanide to obtain 1,8-dimethyl-1,3,6,8,10,13-hexaazacyclotetradecane ligand.

These compounds were characterised by spectrophotometric methods. Elemental analysis of C, H and N data obtained for the free ligand were in agreement with the predicted formula. Data of the infrared and ^{1}H-NMR spectroscopy represented that 1,8-dimethyl-1,3,6,8,10,13-hexaazacyclotetradecanenickel(II) complex is bound to the central nickel(II) ion via four N atoms to yield a square planar structure. Interpretation of EDX and UV-Vis data confirmed the removal of nickel(II) ion from the 1,8-dimethyl-1,3,6,8,10,13-hexaazacyclotetradecanenickel(II) complex.

- The comparison of inhibition zones for the novel ligand showed that antibacterial activity was significant against *Enterococcus* species than *Staphylococcus aureus*. Such finding could be an indication to generate useful information that may contribute to the differentiation of new biomedical branches.

- 1,8-dimethyl-1,3,6,8,10,13-hexaazacyclotetradecane studied is an effective inhibitor for mild steel corrosion in 1.0 M HCl solutions using electrochemical technique. This suggests the ligand can be employed as corrosion inhibitor for mild steel. The large molecular size and square planar structure of the ligand could have played a role in blocking the surface area of the mild steel thereby acting as an efficient inhibitor.

- The adsorption process of 1,8-dimethyl-1,3,6,8,10,13-hexaazacyclotetradecane ligand on mild steel in 1.0 M HCl solution was found to obey the Langmuir adsorption isotherm. The mechanism of corrosion inhibition is by chemisorption.

REFERENCES

6.0   REFERENCES

[1]   N.V. Gerbelue, V.B. Arion, J. Burges, second ed., Template synthesis of macrocyclic compounds. Wiley-VCH Weinleim, Germany (1999) 1-80.

[2]   K. Bowman-James, third ed., Macrocyclic ligands. John Wiley & Sons Ltd, USA (2006) 15-120.

[3]   S. Sujatha, S. Balasubramanian, B. Varghese, Synthesis, structural, spectral, electrochemical and spin equilibrium studies of hexaaza macrotricyclic complexes. *Polyhedron* 28 (17) (2009) 3723-3730.

[4]   E.R. Krishna, P.M. Reddy, M. Sarangapi, G. Hanmanthu, B. Geeta, K.S. Rani, V. Ravinder, Synthesis of N_4 donor macrocyclic Schiff base ligands and their Ru(II), Pd(II), Pt(II) metal complexes for biological studies and catalytic oxidation of didanosine in pharmaceuticals. *Spectrochimica Acta Part A: Molecular and Biomolecular Spectroscopy* 97 (2012) 189-196.

[5]   S. Sarkar, K. Dey, A series of transition and non-transition metal complexes from a N_4O_2 hexadentate Schiff base ligand: Synthesis, spectroscopic characterization and efficient antimicrobial activities. *Spectrochimica Acta* Part A 77 (2010) 740-748.

[6]   C.S. Velazquez, W.E. Broderick, M. Sabat , A.G. M. Barrett , B.M. Hoffman, metal-encapsulated porphyrazines: synthesis, x-ray crystal structure and spectroscopy of a tetratin-star-nickel(porphyrazine) S8 complex. *J. Am. Chem. Soc.*112 (20) (1990)7408–7410.

[7]   M.P. Suh, S.G. Kang, Synthesis and properties of Nickel (II) and Copper (II) Complexes of 14-Membered Hexaaza Macrocycles, 1,8-Dimethyl- and 1,8-Diethyl-1,3.6,8,10,13-hexaazacyclotetradecane. *Inorg. Chem.* 27 (1988) 2544-2546.

[8]   R.M. Ahmed, E.I. Yousif, H.A. Hasan, M.J. Al-Jeboori, Metal complexes of macrocyclic Schiff base ligand: preparation, characterization and biological activity. *The Scientific World J.* 2013 (2013) 1-7.

[9]   K. Singh, Y. Kumar, P. Puri, M. Kumar, C. Sharma, Cobalt, nickel, copper and zinc complexes with 1,3-diphenyl-1H-pyrazole-4-carboxaldehyde Schiff bases: Antimicrobial, spectroscopic, thermal and fluorescence studies. *Eu. J. Med. Chem.* 52 (2012) 313-321.

[10]   K.A.H.M. El-Bayouki, W.M. Basyouni, Y.A.F. Mohamed, M.M. Aly, S.Y. Abbas, Novel 4 (3H)-quinazolinones containing biologically active thiazole, pyridinone and chromene of expected antitumor and antifungal activities. *Eu. J. Chem.* 2 (4) (2011) 455-462.

[11]   W. Samee, O. Vajragupta, Antifungal, cytotoxic activities and docking studies of 2,5-dimercapto-1,3,4-thiaduazole derivatives. *African J. Pharmacy and Pharmacology* 5 (4) (2011) 477-485.

[12]   N.B. Patel, J.C. Patel, S.D. Patel, G.G. Barat, Synthesis, antibacterial and antifungal activity of pyrazolyl-quinazolin-4(3H)-one derivatives. *Orbital Elec. J. Chem.* 2 (3) (2010) 248-262.

[13]   S. Shujah, Zia-ur-Rehman, N. Muhammad, S. Ali, N. Khalid, M.N. Tahir, New dimeric and supramolecular organotin(IV) complexes with tridentate Schiff base as potential biocidal agents. *J. Organometallic Chem.* 696 (2011) 2772-2781.

[14]   Y. Kurogi, Y. Inoue, K. Tsutsuni, S. Nakamura, K. Nagao, H. Yoshisugu, Y. Tsuda, Synthesis and hypolipidemic activities of novel 2-[4-(diethoxyphosphoryl)methyl]phenyl] quinazolines and 4 (3H)-Quinazolinones. *J. Med. Chem.* 39 (1996) 1433-1437.

[15]   A.Y.H. Helali, M.T.M. Sarg, M.M.S. Koraa, M.S.F. El-Zoghbi, Utility of 2-methyl-quinazolin-4(3*H*)-one in the synthesis of heterocyclic compounds with anticancer activity. *Open J. Med. Chem.* 4 (2014) 12-37.

[16]   V. Alagarsamy, V.R. Solomon, M. Murugan, Synthesis and pharmacological investigation of novel 4-benzyl-1-substituted-4H-[1,2,4]triazolo[4,3-a]quinazolin-5-ones as new class of H_1-antihistaminic agents. *Bioorganic and Medicinal Chemistry* 15 (2007) 4009-4015.

[17]   V. Alagarsamy, S. Meena, K.V. Ramseshu, V.R. Solomon, K. Thirumurugan, K. Dhanabal, M. Murugan, Synthesis, analgesic, anti-inflammatory, ulcerogenic index and antibacterial activities of novel 2-methythio-3-substituted-5,6,7,8-tetrahydrobenzo (*b*) thieno[2,3-*d*]pyrmidin-4(3H)-ones. *Eu. J. Med. Chem.* 41 (2006) 1293-1300.

[18]   V. Alagarsamy, V.R. Solomon, K. Dhanabal, Synthesis and pharmacological evaluation of some 3-phenyl-2-substituted-3H-quinazolin-4-one as analgesic, anti-inflammatory agents. *Bioorg. Med. Chem.* 15 (2007) 235-241.

[19]   S.M. Mosaad, K.I. Mohammed, M.A. Ahmed, S.G. Abdel-Hamide, Synthesis of certain new 6-iodoquinazolines as potential antitubercular agents. *J. Applied Sciences* 4 (2) (2004) 302-307.

[20]   S. George, R.T. Kochupappy, Design, synthesis and antitubercular screening of certain novel thiadiazolyl pyrrolidine carboxamides as enoyl ACP reductase inhibitors. *Int. J. of Pharmacy and Pharmaceutical Sciences* 3 (2011) 280-284.

[21]   H. Georgey, N. Abdel-Gawad, S. Abbas, Synthesis and anticonvulsant activity of some quinazolin-4-(3H)-one derivatives. *Molecules* 13 (2008) 2557-2569.

[22]   P.R. Kumar, S. Raju, P.S. Goud, M. Sailaja, M.R. Sarma, G. Om Reddy, M. Prem Kumar, V,V.R.M. Krishna Reddy, T. Suresh, P. Hedge, Synthesis and biological evaluation of thiophene [3,2-*b*] pyrrol derivatives as potential anti-inflammatory agents. *Bioorg. & Med. Chem.* 12 (2004) 1221-1230.

[23]   R.K. Rawal, V.R. Solomon, Y.S. Prabhakar, S.B. Katti, E. De Clercq, Synthesis and QSAR studies on thiazolidinones as anti-HIV agents. *Combinatorial Chem. & High Throughput Screening* 8 (2005) 439-443.

[24]   M. Salavati-Niasari, F. Davar, Synthesis, characterization and catalytic activity of copper (II) complexes of 14-membered macrocyclic ligand;3,10-dialkyl-dibenzo-1,3,5,8,12-hexaazacyclotetradecanel/zeolite encapsulated nanocomposite materials. *Inorg. Chem. Comm.* 9 (2006) 304-309.

[25]   A. Jana, S. Mohanta, Syntheses, crystal structures, magnetochemistry and electrochemistry of macrocyclic dicopper(II) complexes: Monodentate behaviour of a potentially chelating ligand. *Inorg. Chim. Ac.* 405 (2013) 265-273.

[26]   G.A. Nelson, ed., Coordination Chemistry of Macrocyclic Compounds. Plenum, New York, USA (1979) 46-186.

[27]   M.S. Niasari, Synthesis and properties of 16-membered hexaaza macrocycles molecules of copper(II) produced by one-pot template. *Inorg. Chem. Comm.* 7 (2004) 698-700.

[28]   M.S. Niasari, H. Najafian, One-pot template synthesis and properties of Ni (II) complexes of 16- membered hexaaza macrocycles. *Polyhedron* 22 (2003) 2633-2638.

[29]   D.H. Busch, Transition metal complexes of the new synthetic macrocyclic ligands. *Helvetica Chim.* 50 (1967) 174-206.

[30]   N. McCallum, B. Berger-Bächi, M.M. Senn, Regulation of antibiotic resistance in *Staphylococcus aureus. Int. J. Medical Microbiology* 300 (2010) 118-129.

[31]   G.I. French, The continuing crisis in antibiotic resistance. *Int. J. Antimicrobial Agents* 36S3 (2010) S3- S7.

[32]   J. Hofmann, M.S. Cetron, M.M. Farley, W.S. Baughman, W.S. Facklam, R.R. Facklam, J.A. Elliott, K.A. Deaver, R.F. Breiman, The prevalence of drug-resistant

Streptococcus pneumoniae in Atlanta. *New England Journal of Medicine* 333 (8) (1995) 481-486.

[33]   G.H. Hitchings, Mechanism of action of trimethoprim-sulfamethoxazole-1. *J. Infectious Diseases* 128 (1973) S433-S436.

[34]   M.P. Mingeot-Leclercq, Y. Glupczynski, P.M. Tulkens, Aminoglycosides: activity and resistance. *Antimicrobial Agents and Chemotherapy* 43 (1999) 727-737.

[35]   B. Capitano, C.H. Nightingale, Optimizing antimicrobial therapy through use of pharmacokinetic/pharmacodynamics principles. Mediguide Infectious Diseases 21 (2001) 1-8.

[36]   D. Kernodle, second ed., Mechanisms of resistance to beta-lactam antibiotics, gram-positive Pathogens. ASM Press, Washington DC, USA (2000) 769-781.

[37]   S.R. Cornell, D.M. Tracz, K.H. Nierhaus, D.E. Taylor, Ribosomal protection proteins and their mechanism of tetracycline resistance. *Antimicrobial Agents and Chemotherapy* 47 (2003) 3675-3681.

[38]   T. Ahamad, N. Nishat, S. Parveen, Synthesis, characterization and anti-microbial studies of a newly developed polymeric Schiff base and its metal-polychelates. *J. Coord. Chem.* 61 (12) (2008) 1963-1972.

[39]   T. Arslan, F. Kandemirli, E.E. Ebenso, I. Love, H. Alemu, Quantum chemical studies on the corrosion inhibition of some sulphonamides on mild steel in acidic medium. *Corr. Sci. 51 (2009) 35-47.*

[40]   N. Nishat, T. Ahamad, S. M. Alshehri, S. Parveen, Synthesis, characterization, and biocide properties of semicarbazide—formaldehyde resin and its polymer metal complexes. *Eu. J. Medicinal Chem.* 45 (2010) 1287-1294.

[41]   T. Ito, K. Okuma, X.X. Ma, H. Yuzawa, K. Hiramatsu, Insights on antibiotic resistance of *S. aureus* from its whole genome: genomic island SCC. *Drug Resistance Updates* 6 (2003) 41-52.

[42]   D.M. Livermore, Antibiotic resistance in staphylococci. *Int. J. Antimicrobial Agents* 16 (2000) S3- S10.

[43]   H. Suzuki, T. Lefebure, P.P. Bitar, M.J. Stanhope, Comparative genomic analysis of the genus Staphylococcus including Staphylococcus aureus and its newly described sister species Staphylococcus simiae. *BMC Genomics* 13 (38) (2012) 1-8.

[44]   R.H. Deurenberg, E.E. Stobberingh, Infection, genetics and evolution. *Infection, Genetics and Evolution* 8 (2008) 747-763.

[45]   M.H. Reacher, A. Shah, D.M. Livermore, M.C.J. Wale, C. Graham, A.P. Johnson, H. Heine, M.A. Monnickemdam, K.F. Barker, D. James, R.C George, Bacteraemia and antibiotic resistance of its pathogens reported in England and Wales between 1990 and 1998: trend analysis. *BMJ* 320 (2000) 213-216.

[46]   L.M. Johnston, L.A. Jaykus, Antimicrobial resistance of Enterococcus species isolated from produce. *Applied and Environmental Microbiology* 70 (5) (2004) 3133-3137.

[47]   I. Kühn, A. Iversen, L.G. Burman, B. Olsson-Liljequist, A. Franklin, M. Finn, F. Aarestrup, A.M. Seyfarth, A.R. Blanch, X. Vilanova, H. Taylor, J. Caplin, M.A. Moreno, L. Dominguez, I.A. Herrero, R. Möllby, Comparison of Enterococcal populations in animals, humans, and the environment-a European study. *Int. J. Food Microbiology* 88 (2003) 133-145.

[48]   M.G Fontana, third Ed., Corrosion Engineering. McGraw-Hill, New York, USA (1986) 42-151.

[49]   M.A. Quraishi, K.R. Ansari, E.E. Ebenso, A new and effective macrocyclic compound as corrosion inhibitor for mild steel in hydrochloric acid solution. *Int. J. Electrochem. Sci.* 7 (2012) 13106-13120.

[50]   K. Babić-Samardžija, K.F. Khaled, N. Hackerman, Investigation of the inhibiting action of *O-*, *S-* and *N*-dithiocarbamato(1,4,8,11-tetraazacyclotetradecane)cobalt(III) complexes on the corrosion of iron in $HClO_4$ acid. *Applied Surface Science* 240 (2005) 327-340.

[51]   M.A. Quraishi, J. Rawat, Influence of iodide ions on inhibitive performance of tetraphenyl-dithia-octaaza-cyclotetradeca-hexaene (PTAT) during pickling of mild steel in hot sulphuric acid. *Materials Chemistry and Physics* 70 (2001) 95-99.

[52]   A.I. Onen, B.T, Nwufo, E.E Ebenso, R.M. Hlophe, Titanium (IV) oxide as corrosion inhibitor for aluminium and mild steel in acidic medium. *Int. J. Electrochem. Sci.* (2010) 1563-1573.

[53]   L. Dieter, first ed., Corrosion and surface chemistry of metals. EPFL press, Switzerland (2007) 2-121.

[54]   M.A. Quraishi, J. Rawat, Inhibition of mild steel corrosion by some macrocyclic compounds in hot and concentrated hydrochloric acid. *Mater. Chem. Phys.* 73 (2002) 118-122.

[55]   G.S.M. Costa, P.P. Corbi, C. Abbehausen, A.L.B. Formiga, W.R. Lustri, A. Cuin, Silver(I) and gold(I) complexes with penicillamine: synthesis, spectroscopic characterization and biological studies. *Polyhedron* 34 (2012) 210-214.

[56]   E.A. Wickenden, R.A. Krause, Complexes of nickel (II) with acetonitrile and coordination of perchlorate. The Inst. Gen. & Inoorg. Chem.,Univ. Florence, Italy, 4 (1964) 404-407.

[57] Z. Yan, T. Li, Crystal structure of 1,8-dimethyl-1,6,8,10,13-hexaazacyclotetradecane nickel(II) perchlorate, [Ni(C$_{10}$H$_{26}$N$_6$)][ClO$_4$]$_2$. *Z. Kristallogr. NCS* 224 (2009) 505-506.

[58] L. Ballester, A. Gutierrez, M.F. Perpinan, A.E. Sanchez, M. Fonari, M. Gdaniec, Hexaazamacrocyclic nickel and copper complexes and their reactivity with tetracyanoquinodimethane. *Inorg. Chem.* 46 (2007) 3946-3955.

[59] M. Salavati-Niasari, Zeolite-encapsulated nickel(II) complexes with 14-membered hexaaza macrocycle: synthesis and characterization. *Inorg. Chem. Comm.* 7 (2004) 963-966.

[60] Y.W. Park, S.S. Oh, Studies on reactions of a nickel complex of a new completely conjugated macrocyclic ligand. *Bull. Korean Chem. Soc.* 8 (6) (1987) 476-479.

[61] G.A. Bottomley, I.J. Clark, I.I. Creaser, L.M. Engelhardt, R.J. Geue, K.S. Hagen, J.M. Harrowfield, G.A. Lawrence, P.A. Lay, A.M. Sargeson, A.J. See, B.W. Skelton, A.H. White, F.R. Wilner, The synthesis and structure of encapsulating ligands: Properties of Bicyclic hexamines. *Aust. J. Chem.* 47 (1994) 143-179.

[62] M. Kumar, P. Neta, One-electron reduction and demetallation of copper porphyrins. *J. Phys. Chem.* 96 (1992) 9571-9575.

[63] L. Siegfried, T.A. Kaden, Kinetics and mechanism of the demetallation of macrocyclic Nickel(II) complexes by cyanide. *Helvetica Chimica Acta* 88 (2005) 380-390.

[64] C.D. Swor, D.R. Tyler, Synthesis and coordination chemistry of phosphine ligands. *Coord. Chem. Rev.* 255 (2011) 2860-2881.

[65] R.R. Zaky, T.A. Yousef, Spectral, magnetic, thermal, molecular modelling, ESR studies and antimicrobial activity of (*E*)-3-(2-(2-hydroxybenzylidene)hydrazinyl)-3-oxo-*n*(thiazole-2-yl)prpanamide complexes. *J. Molecular Structure* 1002 (2011) 76-85.

[66] N.T. Abdel-Ghani, M.F.A. El-Ghar, A.M. Mansour, Novel Ni(II) and Zn(II) complexes coordinated by 2-arylaminomethyl-1H-benzimidazole: Molecular structures,

spectral, DFT studies and evaluation of biological activity. *Spectrochimica Acta Part A: Molecular and Biomolecular Spectroscopy* 104 (2013) 134-142.

[67]   N. Nishat, M.M. Haq, T. Ahamad, V. Kumar, Synthesis, spectral and antimicrobial studies of a novel macrocyclic ligand containing a piperazine moiety and its binuclear metal complexes. *J. Coord. Chem.* 60 (1) (2007) 85-96.

[68]   A.A. El-sherif, T.M.A. Eldebss, Synthesis, spectra characterization, solution equilibria, in vitro antibacterial and cytotoxic activities of Cu(II), Ni(II), Mn(II), Co(II) and Zn(II) complexes with Schiff base derived from 5-bromosalicylaldehyde and 2-aminomethylthiophene. *Spectrochimica Acta Part* A 79 (2011) 1803- 1814.

[69]   Zia-ur-Rehman, N. Muhammad, S. Ali, I.S. Butler, A. Meetsma, Synthesis, spectroscopic properties, X-ray crystal analysis and antimicrobial activities of organotin(IV) 4-(4-methoxyphenyl)piperazine-1-carbodithioates. *Inorganica Chim. Ac.* 376 (2011) 381-388.

[70]   S.C. Ruchi, Synthesis, spectroscopic characterization, molecular modelling and antimicrobial activities of Mn(II), Co(II), Ni(II), Cu(II) complexes containing tetradentate aza Schiff base ligand. *Spectrochimica Acta Part A: Molecular and Biomolecular Spectroscopy* 103 (2013) 338-348.

[71]   N.A. El-Gamel, M.A. Zayed, Synthesis, structural characterization and antimicrobial activity evaluation of metal complexes of sparfloxacin. *Spectrochimica Acta* Part A 82 (2011) 414-423.

[72]   A.A. El-Sherif, M.R. Shehata, M.M. Shoukry, M.H. Barakat, Synthesis, characterization, equilibrium study and biological activity of Cu(II), Ni(II) and Co(II) complexes of polydentate Schiff base ligand. *Spectrochimica Acta* Part A 96 (2012) 889-897.

[73]   R.R. Zaky, K.M. Ibrahim, I.M. Gabr, Bivalent transition metal complexes of *o*-hydroxyacetophenone [N-(3-hydroxy-2-naphthoyl)] hydrazone: Spectroscopic, antibacterial,

antifungal activity and thermogravimetric studies. *Spectrochimica Acta* Part A 81 (2011) 28-34.

[74]   N.V. Loginova, T.V. Koval'chuk, Y.V. Faletrov, Y.S. Halauko, N.P. Osipovich, G.I. Polozov, R.A. Zheldakova, A.T. Gres, A.S. Halauko, I.I. Azarko, V.M. Shkumatov, O.I. Shadyro, Redox-active metal(II) complexes of sterically hindered phenolic ligands: Antibacterial activity and reduction of cytochrome c. Part II. Metal(II) complexes of o-diphenol derivatives of thioglycolic acid. *Polyhedron* 30 (2011) 2581-2591.

[75]   S. Manjunathan, C.N. Krishnan, synthesis and characterization of mono nuclear complexes of Mn^{2+}, Ni^{2+} and Cu^{2+} with tetradentate N_3O schiff base. *Asian J. Chem.* 19 (2) (2007) 861-866.

[76]   S.M. Saadeh, Synthesis, characterization and biological properties of Co(II), Ni(II), Cu(II) and Zn(II) complexes with an SNO functionalized ligand. *Arabian J. Chem.* 6 (2013) 191-196.

[77]   B. Spellberg, New antibiotic development: Barriers and opportunities in 2012, Alliance for the Prudent Use of Antibiotics Clinical Newsletter 30 (1) (2013) 8-10.

[78]   I.M. Gould, Antibiotic resistance: the perfect storm. *Int. J. Antimicrobial Agents* 34 (S3) (2009) S2-S5.

[79]   K. Hiramatsu, H. Hanaki, T. Ino, K. Yabuta, T. Oguri, F. Tenover, Methicillin-resistant staphylococcus aureus clinical strain with reduced vancomycin susceptibility. *Antimicrobial Agents and Chemotherapies* 40 (1997) 135-136.

[80]   G. Pesavento, B. Ducci, N. Comodo, A.L. Nostro, Antimicrobial resistance profile of staphylococcus aureus isolated from raw meat: A research for methicillin resistant staphylococcus aureus (MRSA). *Food control* 18 (2007) 196-200.

[81] M.T.J. Tajedor, M.M. Gonzalez, M.T.L. Pita, P.L. Gomez, J.L.B. Martin, Identification and antibiotic resistance of faecal enterococci isolated from water samples. *Int. J. Hygiene and Environmental Health* 203 (2001) 363-368.

[82] Standing Medical Advisory Committee of the UK Department of Health. The path of least resistance. London, Department of Health (1997).

[83] J.E. McGowan, Antimicrobial resistance in hospital organisms and its relation to antibiotic use. *Rev. Infect. Dis.* 5 (1983) 1033-1048.

[84] I.M. Gould, Coping with antibiotic resistance: the impending crisis. *Int. J. Antimicrobial Agents* 36S3 (2010) S1-S2.

[85] M.S. Butler, M.A. Cooper, Antibiotics in the clinical pipeline in 2011. *J. Antibiotics* 64 (6) (2011) 413-425.

[86] A. Fajdetić, A. Vinter, H.C. Paljetak, J. Pdovan, I.P. Jakopović, S. Kapić, S. Alihodžić, D. Filić, M. Modrić, N. Košutić-Hulta, R. Antolović, Z.I. Schoenfeld, S. Mutak, V.E. Haber, R. Spaventi, Synthesis, activity and pharmacokinetics of novel antibacterial 15-membered ring macrolones. *Eu. J. Medicinal Chem.* 46 (2011) 3388-3397.

[87] K. Outterson, J.H. Powers, I.M. Gould, A.S. Kesselheim, Questions about the 10 X '20 Initiative. *Clin. Infect. Dis.* 51 (2010) 751.

[88] H. Ashassi-Sorkhabi, M. Eshaghi, Corrosion inhibition of mild steel in acidic media by [BMIM]Br ionic liquid. *Mater. Chem. Phys.* 114 (2009) 267-271.

[89] H. Chen, Z. Zhang, R. Cai, W. Rao, F. Long, Molecularly imprinted electrochemical sensor based on nickel nanoparticles-graphene nanocomposites modified electrode for determination of tetrabromobisphenol A. *Electrochimica Acta* 117 (2014) 385-395.

[90] N.N. Likhanova, M.A. Dominguez-Aguilar, O. Olivares-Xometl, N. Nava-Entzana, E. Arce, H. Dorantes, The effect of ionic liquids with imidazolium and pyridinum cations on the corrosion inhibition of mild steel in acidic environment. *Corr. Sci.* 52 (2010) 2088-2097.

[91]   M.A. Quraishi, J. Rawat, Corrosion inhibiting action of tetramethyl-dithia-octaaza-cyclotetradeca-hexaene on corrosion of mild steel in hot 20% sulphuric acid. *Mater. Chem. Phys.* 77 (2002) 43-47.

[92]   V.V. Torres, V.A. Rayol, M. Magalhães, G.M. Viana, L.C.S. Aguiar, S.P. Machado, H. Orofino, E. D'Elia, Study of thioureas derivatives synthesized from a green route as corrosion inhibitors for mild steel in HCl solution. *Corr. Sci.* 79 (2014) 108-118.

[93]   A.K. Singh, Inhibition of mild steel corrosion in hydrochloric acid solution by 3-(4-((Z)-indolin-3-ylideneamino)phenylimino)indolin-2-one. *Ind. Eng. Res.* 51 (2012) 3215-3223.

[94]   M. Gopiraman, N. Selvakumaran, D. Kesavan, I.S. Kim, R. Karvembu, Chemical and physical interactions of 1-benzoyl-3,3-disubstituted thiourea derivatives on mild steel surface: corrosion inhibition in acidic media. *Ind. Chem. Res.* 51 (2012) 7910-7922.

[95]   K.C. Emregül, M. Hayyal, Studies on the effect of a newly synthesized Schiff base compound from phenazone and vanillin on the corrosion of steel in 2 M HCl. *Corr. Sci.* 48 (4) (2006) 796-812.

[96]   K. Nakamoto, fourth ed., Infrared and Raman Spectra of inorganic and coordination compound. John Wiley & Sons, New York, USA (1986) 203.

[97]   A.S. Adekunle, A.M. Farah, J. Pillay, K.I. Ozoemena, B.B. Mamba, B.O. Agboola, Electrocatalytic properties of Prussian blue nanoparticles supported on poly(*m*-aminobenzenesulphonic acid)-functionalised single-walled carbon nanotubes towards the detection of dopamine. *Colloids and Surfaces B: Biointerfaces* 95 (2012) 186-194.

[98]   A.S. Adekunle, K.I. Ozoemena, Electron transfer behaviour of single-walled carbon nanotubes electro-decorated with nickel and nickel oxide layers. *Electrochimica Acta* 53 (2008) 5774-5782.

[99]   J.E. Welton, SEM petrology atlas. The American Association of petroleum Geologists Pub., Tulsa, Oklahoma USA (1984) 5.

[100]   S. Chen, G. WU, D. Long, Y. Liu, Preparation, characterization and antibacterial activity of chitosan-$Ca_3V_{10}O_{28}$ complex membrane. *Carbohydrate Polymers* 64 (2006) 92-97.

[101]   S.A. Khan, N. Nishat, S. Parveen, R. Rasool, Preparation, spectral and biological investigation of formaldehyde-based ligand containing piperazine moiety and its various polymer metal complexes. *Spectrochimica Acta* Part A 81 (2011) 290-295.

[102]   H.M. Moghaddam, M. Malakootian, H. Beitollah, P. Biparva, Nanostructured base electrochemical sensor for determination of sulphite. *Int. J. Electrochem. Sc.* 9 (2014) 327-341.

[103]   T.A. Postlethwaite, J.E. Hutchison, K.W. Hathcock, R.W. Murray, Optical, electrochemical, and electrocatalytic properties of self-assembled thio-derivatized porphyrins on transparent gold films. *Langmuir* 11 (10) (1995) 4109-4116.

[104]   A.J. Bard, L.R. Faulkner, Second ed., Electrochemical Methods: Fundamentals and Applications. John Wiley & Sons, Hoboken, NJ, USA (2001) 44-156.

[105]   A.S. Adekunle, J. Pillay, K.I. Ozoemena, Probing the electrochemical behaviour of SWCNT-cobalt nanoparticles and their electrocatalytic activities towards the detection of nitrite at acidic and physiological pH conditions. *Electrochimica Acta* 55 (2010) 4319-4327.

[106]   J.N. Soderberg, A.C. Co, A.H.C. Sirk, V.I. Birss, Impact of porous electrode properties on the electrochemical transfer coefficient. *J. Phys. Chem.* B 110 (2006) 10401-10410.

[107]   E.S. Ferreira, C. Giancomelli, F.C. Giacomelli, A. Spinelli, Evaluation of the inhibitor effect of L-ascorbic acid on the corrosion of mild steel. *Mater. Chem. Phys.* 83 (2004) 129-134.

[108] W.H. Li, Q. He, S.T. Zhang, C.L. Pei, B.R. Hou, Some new triazole derivatives as inhibitors for mild steel corrosion in acidic medium. *J. Appl. Electrochem.* 38 (2008) 289-295.

[109] M. Mahdavian, M.M. Attar, Electrochemical behaviour of some transition metal acetylacetonate complexes as corrosion inhibitors for mild steel. *Corr. Sci.* 51 (2009) 409-414.

[110] A.M. Abdel-Gaber, M.S. Masoud, E.A. Khalil, E.E. Shehata, Electrochemical study on the effect of Schiff base and its cobalt complex on the acid corrosion of steel. *Corr. Sci.* 51 (2009) 3021-3024.

[111] A.S. Adekunle, O.A. Arotiba, B.B. Mamba, Electrochemical studies and sensing of iodate, periodate and sulphite ions at carbon nanotubes/ Prussian blue films modified platinum electrode. *Int. J. Electrochem. Sci.* 7 (2012) 8503-8521.

[112] L.C. Murulana, A.K. Singh, S.K. Shukla, M.M. Kabanda, E.E. Ebenso, Experimental and quantum chemical studies of some bis(trifluoromethyl-sulfonyl) imide imidazolium-based ionic liquids as corrosion inhibitors for mild steel in hydrochloric acid solution. *Ind. Eng. Chem. Res.* 51 (2012) 13282-13299.

[113] S.S.A.A. Pereira, M.M. Pegas, T.L. Fernandez, M. Magalhaes, T.G. Schontag, D.C. Lago, L.F.S.E. D'Elia, Inhibitory action of aqueous garlic peel extract on the corrosion of carbon steel in HCl solution. Corr. Sc. 65 (2012) 360-366.

[114] E.E. Oguzie, S.G. Wang, Y. Li, F.M. Wang, Corrosion and corrosion inhibition characteristics of bulk nanocrystalline ingot iron in sulphuric acid. J. Solid State Electrochem. 12 (2007) 721-728.

[115] G.K. Gomma, M.H. Wahdan, Effect of temperature on the acidic dissolution of copper in the presence of amino acids. *Mater. Chem. Phys.* 39 (1994) 142-148.

[116] K.Z. Mohammed, A. Hamdy, A. Abdel-Wahab, N.A. Farid, Temperature effect on corrosion inhibition of carbon steel in formation water by non-ionic inhibitor and synergistic influence of halide ions. *Life Sci. J.* 9 (2) (2012) 424-434.

[117] I. Ahamad, R. Prasa, M.A. Quaraishi, Experimental and theoretical investigation of adsorption of fexofenadine at mild steel/hydrochloric acid interface as corrosion. *J. Solid State Electrochem.* 14 (11) (2010) 2095-2105.

[118] R.A. Prabhu, T.V. Venkatesha, A.V. Shanbhag, G.M. Kulkarni, R.G. Kalkhambkar, Inhibition effects of some Schiff bases as the corrosion mild steel hydochloric acid solution. *Corr. Sci.* 50 (2008) 3356-3362.

[119] M. Behpour, S.M. Ghoreishi, N. Soltani, M. Salavati-Niasari, M. Hamadanian, A. Gandomi, Electrochemical and theoretical investigation on the corrosion inhibition of mild steel by thiosalicylaldehyde derivatives in hydrochloric acid solution. *Corr. Sci.* 50 (2008) 2172-2181.

[120] F. Bentiss, B. Mernari, M. Traisnel, H. Vezin, M. Lagrenée, On the relationship between corrosion inhibiting effect and molecular structure of 2,5-bis(*n*-pyridyl)-1,3,4-thiadiazole derivatives in acidic media: Ac impedance and DFT studies. *Corr. Sci.* 53 (2011) 487-495.

[121] D. Jope, J. Sell, H.W. Pickering, K.G. Weil, Application of a Quartz crystal microbalance to the study of copper corrosion in acid solution inhibited by triazole-iodine protective films. *J. Electrochem. Soc.* 142 (1995) 2170.